JOURNAL REVIEW

Azeotropic Distillation

Soemantri Widagdo
Polymer Processing Institute and Dept. of Chemistry & Chemical Engineering, Stevens Institute of Technology, Hoboken, NJ 07030

Warren D. Seider
Dept. of Chemical Engineering, University of Pennsylvania, Philadelphia, PA 19104

Recent and ongoing research in the distillation of nonideal mixtures is reviewed focusing on advances in the methodologies for the synthesis, design, analysis and control of separation sequences involving homogeneous and heterogeneous azeotropic towers. Maps of residue curves and distillation lines are examined, as well as geometric methods for the synthesis and design of separation sequences, trends in the steady-state and dynamic analysis of homogeneous and heterogeneous towers, the nonlinear behavior of these towers, and strategies for their control.

Emphasis is placed on the methods of computing all of the azeotropes associated with a multicomponent mixture, on the features that distinguish azeotropic distillations from their zeotropic counterparts, on the potential for steady-state multiplicity, and on the existence of maximum and minimum reflux bounds. Important considerations in the selection of entrainers are examined. For the synthesis of separation trains, when determining the feasible product compositions, the graphical methods are clarified, especially the conditions under which distillation boundaries can be crossed and bounding strategies under finite reflux. The application of geometric theory to locate the fixed points, at minimum reflux, is reviewed in connection with homotopy-continuation algorithms for this purpose. The use of homotopy-continuation algorithms, especially for the steady-state simulation of heterogeneous azeotropic distillations, is justified. Methods for phase stability analysis are reviewed in connection with the location of real bifurcation points at phase transitions, an important feature of algorithms for the dynamic simulation of heterogeneous azeotropic distillations.

Introduction

Virtually every chemical plant has a separation unit(s) to recover products, by-products, and unreacted raw materials. By and large, this is accomplished by multistage processes, with distillation dominant throughout the chemical industry. Although many new separation techniques are being developed, it seems clear that distillation will remain the method of choice, especially for the large-scale separation of nonideal mixtures. This view was presented convincingly by Fair (1987).

To our knowledge, Wang and Wang (1981) published the most recent review in an article that focuses on the analysis and simulation of multistage separation processes. Since then, the new developments have concentrated on the separation of nonideal mixtures, with emphasis on azeotropic distillation. Consequently, it has been our objective to present a comprehensive review of the methods for analysis, entrainer selection, column sequencing and design, and column control, while concentrating on azeotropic distillation, but considering the separation of nonideal mixtures in general. Many new concepts and computational tools are reviewed with suggestions provided for future research. An attempt is made to clarify the bounding strategies for the sequencing of azeotropic distillation towers, which involve complex graphical constructions that have been presented in several recent articles.

Azeotropy and polyazetropy

Azeotrope, an ancient Greek word that translates as "to

Correspondence concerning this article should be addressed to W. D. Seider.

boil unchanged," means that the vapor emitted has the same composition as the liquid (Swietoslawski, 1963). To classify the many azeotropic mixtures, Lecat (1918) examined their deviations from Raoult's law. For a multicomponent vapor–liquid system, the equilibrium constant for species i, K_i, is defined by

$$K_i \equiv \frac{y_i}{x_i} = \frac{\gamma_i^L f_i^L}{\phi_i^V P}, \tag{1}$$

where y_i and x_i are the mole fractions of species i in the vapor and liquid phases, respectively, at equilibrium. Herein, the degree of nonideality is expressed by the deviations from unity of the activity coefficient, γ_i^L, for the liquid phase and the fugacity coefficient, ϕ_i^V, for the vapor phase; f_i^L is the pure-liquid fagacity of species i. At low pressure, $\phi_i^V = 1$ and $f_i^L = P_i^S$, and Eq. 1 reduces to

$$K_i \equiv \frac{y_i}{x_i} = \gamma_i^L \frac{P_i^S}{P}, \tag{2}$$

where P_i^S is the vapor pressure of species i at the temperature T. A maximum-boiling azeotrope occurs for negative deviations from Raoult's law ($\gamma_i^L < 1.0$). For a minimum-boiling azeotrope, the deviations from Raoult's law are positive ($\gamma_i^L > 1.0$). When the deviations are sufficiently large ($\gamma_i^L \gg 1.0$), phase splitting may occur and a minimum-boiling heterogeneous azeotrope forms having a vapor phase in equilibrium with two liquid phases. A heterogeneous azeotrope occurs when the vapor–liquid envelope overlaps with the liquid–liquid envelope, as illustrated in Figure 1. For a homogeneous azeotrope, when $x_1 = x_{1,\text{azeo}} = y_1$, the mixture boils at this composition, as shown in Figure 1a. Whereas, for a heterogeneous azeotrope, when the overall liquid composition, $x_1 = x^o_{1,\text{azeo}} = y_1$, the mixture boils at this composition, as illustrated in Figure 1b, but the three coexisting phases have distinct compositions.

At an azeotropic point, the equilibrium constants for all of the species are unity. Hence, a simple distillation approaches this point, at which no further separation can occur. For this reason, in nonlinear dynamics, an azeotrope is called a *stationary* or *fixed point*. For the past two decades, several researchers, most notably Doherty and coworkers, have focused on the properties of fixed points to produce insights concerning the operation of azeotropic distillation towers, as well as to develop design methodologies. Although the analysis of nonlinear dynamics is highly mathematical, it is rapidly gaining acceptance by many practitioners in the field.

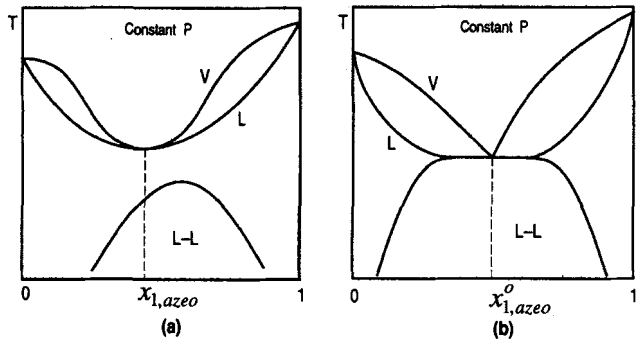

Figure 1. Binary phase diagram at a fixed pressure for a: (a) homogeneous azeotrope; (b) heterogeneous azeotrope.

Residue curves and distillation lines

In recent years, several of the mathematical and geometrical analyses in azeotropic distillation have utilized simple-distillation residue curves and distillation lines. Consequently, in this section, these constructs are derived, interpreted, and applied to the separation of homogeneous and heterogeneous mixtures in tray towers.

Residue Curves. Since the turn of this century, the *residue-curve map*, which represents the residue composition in simple distillation, has been used to characterize the behavior of binary azeotropic mixtures (Ostwald, 1900; Schreinemakers, 1901, 1903). Through the application of the residue-curve map, many years later, several Russian scientists analyzed the composition profiles in multicomponent distillation columns in the vicinity of azeotropes and pure species. Bushmakin and Kish (1957a,b) studied ternary mixtures, while Zharov (1967, 1968a,b) extended their analysis to quaternary mixtures and multicomponent systems, in general. Ten years later, Matsuyama and Nishimura (1977) and Doherty and Perkins (1978a,b; 1979) further developed and applied this analysis for the separation of multicomponent homogeneous mixtures. Recently, Pham and Doherty (1990a,b,c) extended the analysis to apply to heterogeneous mixtures.

A vapor–liquid residue-curve map is constructed by tracing the composition of the residue of a simple distillation in time. Consider L moles of liquid with mole fractions, x_i ($i = 1, \ldots, N_s$), in a simple distillation, as illustrated in Figure 2. A differential portion of this liquid, ΔL moles, is vaporized. The vapor phase has mole fractions, y_i ($i = 1, \ldots, N_s$), assumed to be in equilibrium with the remaining liquid. Since the residual liquid, $L - \Delta L$ moles, has mole fractions, $x_i + \Delta x_i$, the

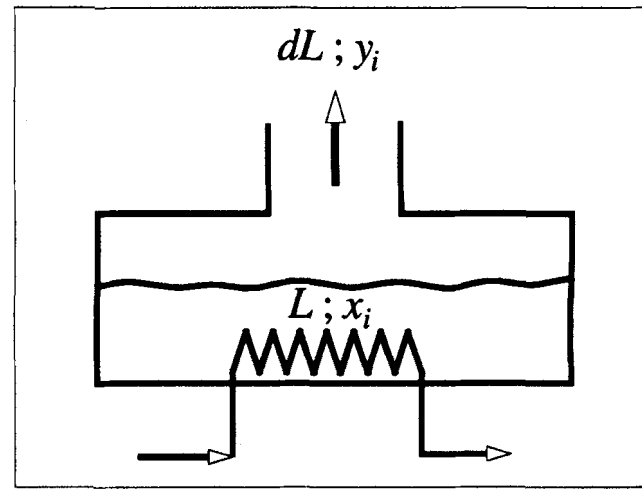

Figure 2. Simple-distillation still.

mass balance for species i is given by

$$Lx_i = (\Delta L)y_i + (L - \Delta L)(x_i + \Delta x_i) \qquad i = 1, \ldots, N_s - 1. \tag{3}$$

In the limit, as $\Delta L \to 0$,

$$\frac{dx_i}{dL/L} = x_i - y_i = x_i(1 - K_i\{T, P, \underline{x}, \underline{y}\}) \qquad i = 1, \ldots, N_s - 1, \tag{4}$$

and setting, $d\hat{t} = dL/L$,

$$\frac{dx_i}{d\hat{t}} = x_i - y_i \qquad i = 1, \ldots, N_s - 1, \tag{5}$$

where K_i is given by Eq. 1.

As discussed by Laroche et al. (1992b) and Fidkowski et al. (1993a), $\hat{t}$ can be interpreted as:

1. The dimensionless time, with the solutions of Eq. 5 defining a family of residue curves, as illustrated later in Figure 4. Note that each residue curve is the locus of the compositions of the residual liquid in time, as vapor is boiled off from a simple-distillation still. Often, an arrow is assigned in the direction of increasing time (and increasing temperature).

2. The dimensionless height of a packed column, with the solutions representing the liquid compositions, in equilibrium with the vapor compositions, in a packed column at *total reflux* (Van Dongen and Doherty, 1985).

When tray towers are modeled assuming vapor–liquid equilibrium, it is generally assumed that the residue curves are accurate representations of the liquid composition profiles at *total reflux* (Van Dongen and Doherty, 1985; Bekiaris et al., 1993). However, the residue curves are at best an approximation to the liquid composition profiles. In the discussion that follows, the approximation is considered first at total reflux, and then at finite reflux.

Consider a backward-difference approximation at tray $n+1$ in a distillation tower:

$$\left.\frac{d\underline{x}}{d\hat{t}}\right|_{n+1} = \frac{\underline{x}_{n+1} - \underline{x}_n}{\Delta\hat{t}} + \mathcal{O}\{(\Delta\hat{t})^2\}, \tag{6}$$

where n is the tray counter (counting downward). Substituting, Eq. 5 becomes

$$\frac{\underline{x}_{n+1} - \underline{x}_n}{\Delta\hat{t}} \approx \underline{x}_{n+1} - \underline{y}_{n+1}. \tag{7}$$

When $\Delta\hat{t}$ is set to unity, Eq. 7 becomes

$$\underline{x}_n \approx \underline{y}_{n+1}, \tag{8}$$

which is the equation for the operating line of a multistage tower at *total reflux*. Due to the approximation in Eq. 7, the residue curves, which are the solutions of Eq. 5, only *approximate* the liquid composition profiles at total reflux.

At finite reflux, the operating line in the rectifying section is given by the mass balance about the top n trays:

$$L_{n-1}\underline{x}_{n-1} = V_n\underline{y}_n - D\underline{y}_D \tag{9}$$

Expanding $\underline{x}_{n-1}$ about $\underline{x}_n$ using a Taylor series,

$$\underline{x}_{n-1} = \underline{x}_n + \frac{d\underline{x}_n}{dh}(\Delta h) + \mathcal{O}\{(\Delta h)^2\}, \tag{10}$$

where $\Delta h = h_{n-1} - h_n = -1$, Eq. 9 becomes

$$\frac{d\underline{x}_n}{dh} = \underline{x}_n - \frac{V_n}{L_{n-1}}\underline{y}_n + \frac{D}{L_{n-1}}\underline{y}_D + \mathcal{O}\{(\Delta h)^2\}. \tag{11}$$

Note that at total reflux, with $D = 0$ and $V_n = L_{n-1}$, Eq. 11 reduces to Eq. 5 with $\hat{t} = h$. However, the Taylor series expansion is only valid for $\Delta h \to 0$, and therefore, the solution of Eq. 5 approximates the liquid compositions at *total reflux*. Clearly, the solution of Eq. 11, at finite reflux, deviates even further from the residue curves.

The singular (fixed) points of the residue curves are points on the composition simplex where the driving force for change in the liquid composition is zero; that is, $d\underline{x}/d\hat{t} = 0$. Obviously, this condition is satisfied trivially at the azeotropes and pure-species vertices. For a ternary mixture with a binary azeotrope, there are four fixed points on a triangular diagram: the binary azeotrope and the three vertices. Furthermore, the behavior of the residue curves in the vicinity of singular (fixed) points depends on the eigenvalues of the Jacobian matrix of Eq. 5. For ternary mixtures, Eq. 5 is comprised of two nonlinear ordinary differential equations (ODEs). At each vertex, these ODEs have two identical eigenvalues and, at the azeotropic point, two distinct eigenvalues. In general, the solution at the highest-order singularity contains the most complex behavior, and hence, in this case, it is sufficient to study the behavior of the residue curves in the vicinity of the binary azeotrope. There are three behaviors, depending upon the two eigenvalues:

1. Two negative eigenvalues: $\lambda_{1,2} < 0$. In this case, as $\hat{t} \to \infty$, the residue curves approach the binary azeotrope, as illustrated in Figure 3a. Here, the azeotropic point is a *stable node*.

2. Two positive eigenvalues: $\lambda_{1,2} > 0$. In this case, the residue curves diverge from the binary azeotrope and the azeotropic point is an *unstable node*, from which all of the residue curves eminate, as illustrated in Figure 3b.

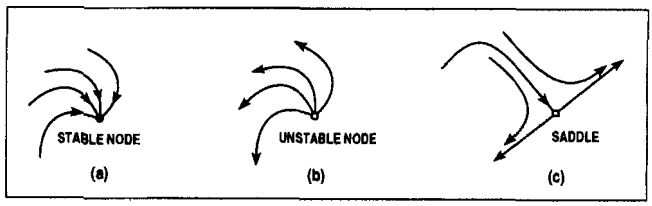

Figure 3. Stability of residue curves for a ternary system in the vicinity of a binary azeotrope.

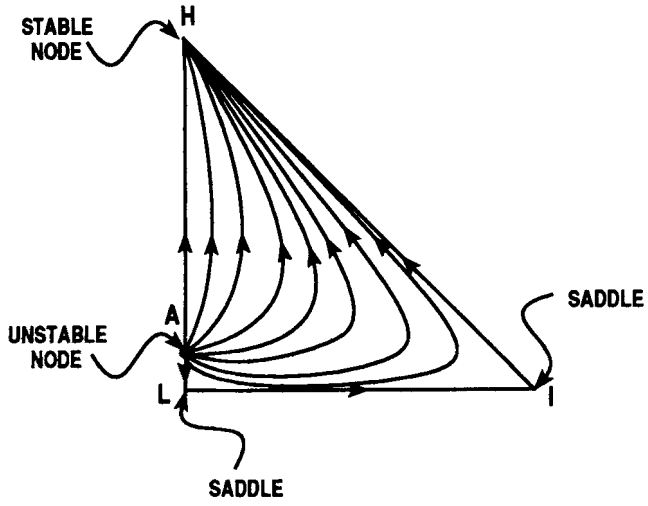

Figure 4. Residue curves of a ternary system with a minimum-boiling binary azeotrope.

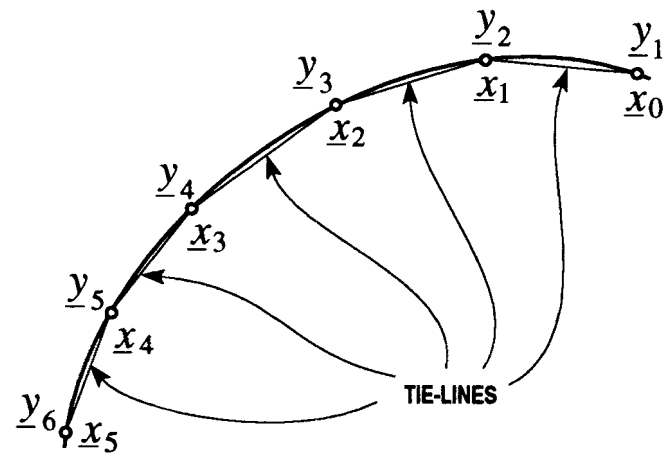

Figure 5. Distillation line and its tie-lines.

3. Positive and negative eigenvalues: $\lambda_1 < 0$, $\lambda_2 > 0$. In this case, the residue curves approach the binary azeotrope in the direction of the eigenvector associated with λ_1, and move away from it in the direction of the eigenvector associated with λ_2. Therefore, this azeotropic point is a *saddle*, as illustrated in Figure 3c.

As will be described later, in the subsection on the Geometric Interpretation, higher-order singularities often introduce one or more *simple-distillation boundaries* that separate two or more distillation regions. In each distillation region, a residue-curve map has one stable and one unstable node. For a ternary system with a minimum-boiling binary azeotrope of heavy (H) and light (L) species, no simple-distillation boundary is formed, and therefore, there are four fixed points: one unstable node at the binary azeotrope (A), one stable node at the heavy component (H), and two saddles at the vertices of the light (L) and intermediate (I) species, as illustrated in Figure 4. As the number of species increases, the residue curves in the vicinity of the azeotrope involving the most species become more complex. Zharov (1968a) studied a quaternary mixture and analyzed the eigenvalues of the residue curves in the neighborhood of a quaternary azeotrope. He discovered a three-dimensional saddle, which is absent in ternary systems.

Distillation Lines. Distillation lines, although similar to residue curves, have subtle differences, and consequently, care must be taken to use them in place of residue curves, when necessary, for the analysis of azeotropic towers. In this section, the distillation line is derived, and its behavior in the vicinity of its fixed points is discussed. In addition, and subsequently in the section on Feasible Product Composition, the relationship between the overall material balance line and the distillate line is considered.

Unlike the residue curve, the distillation line is the operating line at total reflux, where Eq. 9 reduces to Eq. 8, with the composition of the liquid stream leaving tray n, $\underline{x}_n$, identical to the composition of the vapor stream entering tray n, $\underline{y}_{n+1}$. The Gibbs phase rule implies that under isobaric (or isothermal) conditions, the vapor compositions at equilibrium on tray $n+1$ can be expressed as a function of the liquid compositions:

$$\underline{y}_{n+1} = \mathfrak{M}\{\underline{x}_{n+1}\}, \tag{12}$$

where $\mathfrak{M}$ is a function that maps $\underline{x}_{n+1}$ onto $\underline{y}_{n+1}$. At total reflux, Eq. 8 gives

$$\underline{x}_n = \mathfrak{M}\{\underline{x}_{n+1}\} \tag{13}$$

or

$$\underline{x}_{n+1} = \overline{\mathfrak{M}}\{\underline{x}_n\} = \overline{\mathfrak{M}}^2\{\underline{x}_{n-1}\} = \cdots = \overline{\mathfrak{M}}^{n+1}\{\underline{x}_0\}, \tag{14}$$

where $\overline{\mathfrak{M}}$ is the inverse of $\mathfrak{M}$. Equation 14 implies that $\underline{x}_{n+1}$ is obtained by applying the $\overline{\mathfrak{M}}$-mapping on $\underline{x}_0$ $(n+1)$ times, where each mapping corresponds to an additional stage. Thus, the distillation line is the locus of liquid compositions, $\underline{x}_0$, ..., $\underline{x}_n$, ..., that satisfy Eq. 14. Since Eq. 8 requires that the corresponding vapor compositions at equilibrium also lie on the same distillation line, Zharov (1968c) and Zharov and Serafimov (1975) define a distillation line as the locus of liquid compositions whose vapor compositions at equilibrium also lie on the same line. Geometrically, this requires that the vectors connecting $\underline{x}_n$ and $\underline{y}_n$ (tie lines) be the chords of the distillation line, as illustrated in Figure 5.

Let $\hat{\underline{x}}$ be the limiting composition of $\underline{x}_n$ as n approaches infinity, that is,

$$\hat{\underline{x}} = \lim_{n \to \infty} \overline{\mathfrak{M}}^n\{\underline{x}_0\}. \tag{15}$$

Equation 15 gives ultimate liquid composition as the number of trays approaches infinity. Therefore, $\hat{\underline{x}}$ is the so-called pinch, fixed, or singular point of a distillation line. Consequently, pure species and azeotropes are candidates for $\hat{\underline{x}}$, and furthermore, Zharov (1968c, 1969) shows that the distillation lines and residue curves have identical properties in the vicinity of singular points. By expanding Eq. 14 about a singular point, $\hat{\underline{x}}$, Zharov (1968c) studies the dynamics of the deviation variables, $\underline{x} - \hat{\underline{x}}$, and obtains stability properties identical to those illustrated in Figure 3.

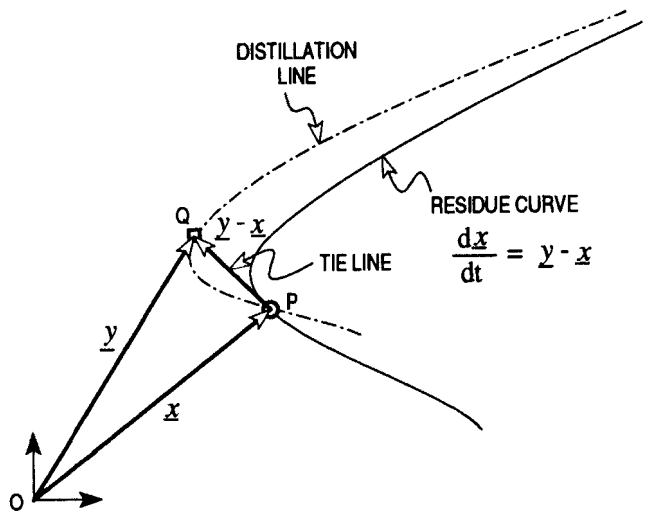

Figure 6. Residue curve and distillation line through *P*.

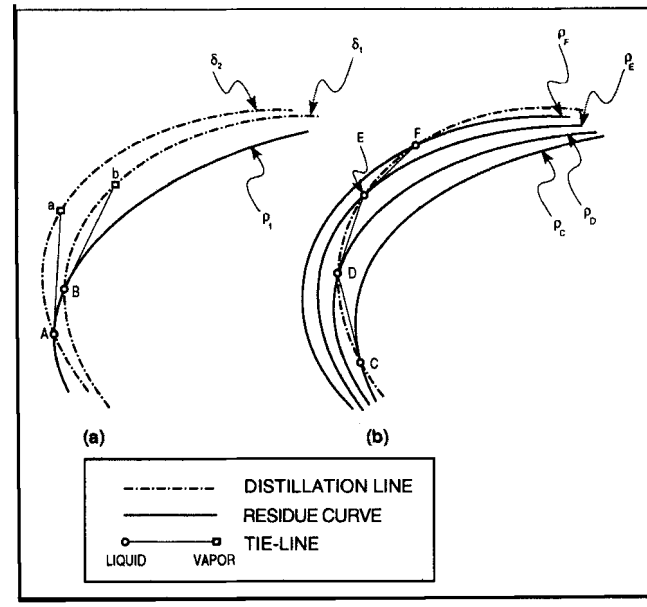

Figure 7. Geometric relationship between distillation lines and residue curves.

Geometric Interpretation. To utilize the residue curves and distillation lines properly in the geometrical methodologies for separation train synthesis and column design, to be covered in the section on Separation Train Synthesis and Column Design, it is important to understand their geometric properties. Let's begin with the observation that Eq. 5 requires the tie-line vectors, connecting liquid composition, $\underline{x}$, and vapor composition, $\underline{y}$, at equilibrium, to be tangent to the residue curves, as illustrated in Figure 6. Since these tie-line vectors must also be chords of the distillation line, the residue curves and the distillation lines must intersect at the liquid composition, $\underline{x}$. Note that when the residue curve is linear (as for binary mixtures), the tie-lines and the residue curve are colinear (i.e., the distillation lines coincide with the residue curves).

Figure 7a shows two distillation lines (δ_1 and δ_2) that intersect a residue curve at points A and B. As a consequence of Eq. 5, their corresponding vapor compositions at equilibrium, a and b, lie at the intersection of the tangents to the residue curves at A and B with the distillation lines δ_1 and δ_2. Clearly, the distillation lines do not coincide with the residue curves, as implied mistakenly in several articles. In Figure 7b, a single distillation line, connecting the composition on four adjacent trays (at C, D, E, F) and crossing four residue curves (ρ_C, ρ_D, ρ_E, ρ_F) at these points.

Residue-Curve and Distillation-Line Sketches. For a given mixture, the boiling points and the compositions of all of the azeotropes and polyazeotropes can be used to characterize the stability of every species and azeotrope therein. Given this stability information, the families of residue curves and distillation lines can be sketched in the composition simplex (a triangular diagram for ternary mixtures) (Petlyuk and Avetyan, 1971; Petlyuk et al., 1975a,b,c; Doherty and Perkins, 1979). This graphical representation can be extended to four species using tetrahedra (Zharov, 1968a,b,c, 1969; Rev et al. 1992, 1994), but not easily. Therefore, the graphical representations of Eqs. 5 and 13 are limited in practice to the separation of binary mixtures, using a mass separating agent, and ternary azeotropic mixtures, with no loss of generality.

To sketch the residue curves and distillation lines, first, the boiling points of the pure species are entered at the vertices. Then, the boiling points of the binary azeotropes are positioned at the azeotropic compositions along the edges, with the boiling points of the ternary azeotropes positioned at their compositions within the triangle. Then, arrows are assigned in the direction of increasing temperature, corresponding to the increasing temperature in a simple-distillation still or on the trays that approach the bottom of a distillation tower. Typical diagrams for mixtures involving binary and ternary azeotropes are illustrated in Figure 8. Figure 8a is for a simple system, without azeotropes, involving nitrogen, oxygen, and argon. In this mixture, nitrogen is the lowest-boiling species, argon is the middle boiler, and oxygen is the highest-boiling species. Thus, along the oxygen–argon edge the arrow is pointing to the oxygen vertex, and on the remaining edges the arrows points away from the nitrogen vertex. Since these arrows point away at the nitrogen vertex, all of the residue curves or distillation lines emanate from it. At the argon vertex, the arrows point to and away from it. Since the residue curves and distillation lines turn in the vicinity of this vertex, it is not a terminal point. Rather, it is referred to as a saddle point. All of the curves end at the oxygen vertex, which is a terminal point. For this ternary mixture, the map shows that pure argon cannot be obtained in a simple distillation. It is important to recognize that because the residue curves and distillation lines have the same properties at fixed points (vertices and azeotropes), both families of curves are sketched similarly. As discussed earlier, their differences are pronounced in regions that exhibit extensive curvature.

Simple-Distillation and Distillation-Line Boundaries. This graphical approach effectively locates the starting and terminal points and the qualitative locations of the residue curves and distillation lines. As illustrated in Figure 8b and 8c, it works well for binary and ternary azeotropes that exhibit multiple starting and terminal points. In these cases, one or more *simple-distillation or distillation-line boundaries* (lines *DE*

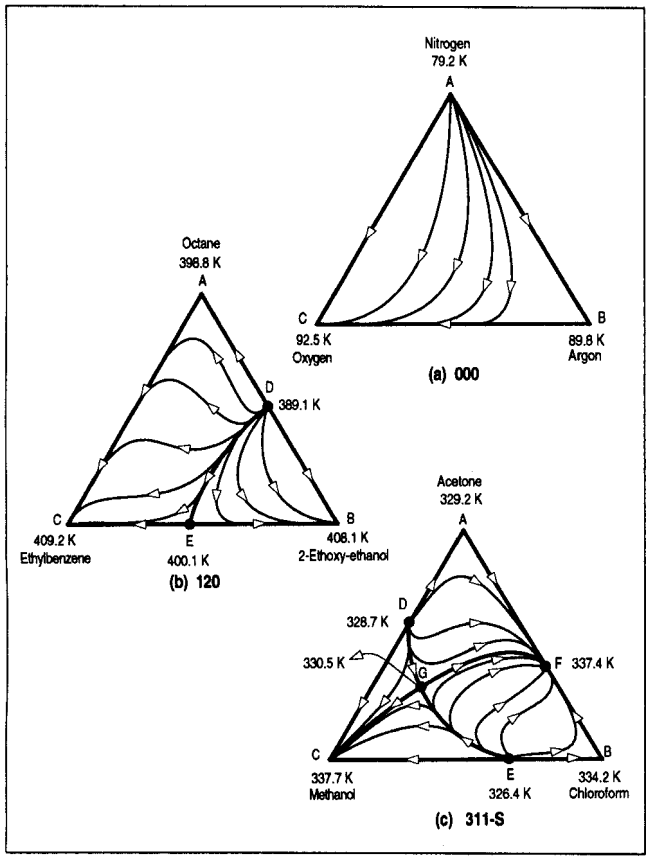

Figure 8. Maps of residue curves or distillation lines: (a) a system without azeotropes; (b) a system with two binary azeotropes; (c) a system with binary and ternary azeotropes (Stichlmair et al., 1989).

and *CF* in Figures 8b and 8c) divide these diagrams into regions with distinct pairs of starting and terminal points. It has been shown by Doherty and Perkins (1979) that, for the separation of homogeneous mixtures by *simple distillation*, these separatrices cannot be crossed. A feed located in region *ADECA* in Figure 8b has a starting point approaching the composition of the binary azeotrope of octane and 2-ethoxy-ethanol and a terminal point approaching pure ethylbenzene. Whereas, a feed located in region *DBED* has a starting point approaching the same binary azeotrope, but a terminal point approaching pure 2-ethoxy-ethanol. In this case, a pure octane product would not be possible.

Van Dongen and Doherty (1985) used the residue-curve maps for the design of multistage distillation processes. Their analysis implied that the compositions along the operating lines of a distillation tower cannot cross the simple-distillation boundaries (obtained using the simple-distillation still in Figure 2). In their analysis, with the assumption of constant molar overflow, species balances are written for the stages in the rectifying and stripping sections:

Rectifying Section:

$$\underline{y}^r_{m+1} = \frac{r}{r+1}\underline{x}^r_m + \frac{1}{r+1}\underline{x}_D \qquad m = 0, 1, \ldots, M \quad (16a)$$

$$\underline{x}^r_0 = \underline{x}_D \quad (16b)$$

Stripping Section:

$$\underline{x}^s_{n+1} = \frac{s}{s+1}\underline{y}^s_n + \frac{1}{s+1}\underline{x}_B \qquad n = 0, 1, \ldots, N, \quad (17a)$$

$$\underline{x}^s_0 = \underline{x}_B \quad (17b)$$

where the rectifying and stripping sections contain M and N stages, respectively, r and s are the reflux ratios in these sections, $\underline{y}^r_m$ is the vector of vapor mole fractions in the rectifying section on stage m, $\underline{x}^s_n$ is the vector of liquid mole fractions in the stripping section on stage n, $\underline{x}_D$ is the vector of distillate mole fractions, and $\underline{x}_B$ is the vector of bottoms-product mole fractions. Note that the stages are counted downward in the rectifying section and upward in the stripping section. These difference equations define the operating lines. When combined with Eq. 1, which relates the liquid and vapor compositions on a stage at equilibrium, the solution is a set of discrete points in the composition simplex, which are often connected to show their sequence. Alternatively, these difference equations can be approximated by ODEs expressed in the continuous variables, $\hat{\underline{x}}^r$, $\hat{\underline{x}}^s$, $\hat{\underline{y}}^r$, $\hat{\underline{y}}^s$:

Rectifying Section:

$$\frac{d\hat{\underline{x}}^r}{dh_r} \approx \hat{\underline{x}}^r - \frac{r}{r+1}\hat{\underline{y}}^r + \frac{1}{r}\underline{y}_D \quad (18a)$$

$$\hat{\underline{x}}^r\{h_r = 0\} = \underline{x}_D \quad (18b)$$

Stripping Section:

$$\frac{d\hat{\underline{x}}^s}{dh_s} \approx \frac{s}{s+1}\hat{\underline{y}}^s + \frac{1}{s+1}\underline{x}_B - \hat{\underline{x}}^s \quad (19a)$$

$$\hat{\underline{x}}^s\{h_s = 0\} = \underline{x}_B \quad (19b)$$

where h_r is the elevation in the rectifying section relative to the condenser ($h_r = 0$), and h_s is the elevation in the stripping section relative to the reboiler ($h_s = 0$). For infinitely large reflux and reboil ratios, corresponding to total reflux and total reboil in the continuous tower, Eqs. 18 and 19 reduce to

$$\frac{d\hat{\underline{x}}^r}{dh_r} \approx \hat{\underline{x}}^r - \hat{\underline{y}}^r \quad (20)$$

$$\frac{d\hat{\underline{x}}^s}{dh_s} \approx \hat{\underline{y}}^s - \hat{\underline{x}}^s, \quad (21)$$

which have the same form as the residue-curve equations, Eq. 5.

For this reason, many authors assume that the residue curves are a good approximation to the operating lines at total reflux. Rather, as discussed before, the distillation lines are equivalent to the operating lines at *total reflux*. It seems clear that the errors associated with the residue curves increase with the curvature of the operating lines. However, an analysis to quantify these errors has not been undertaken, to

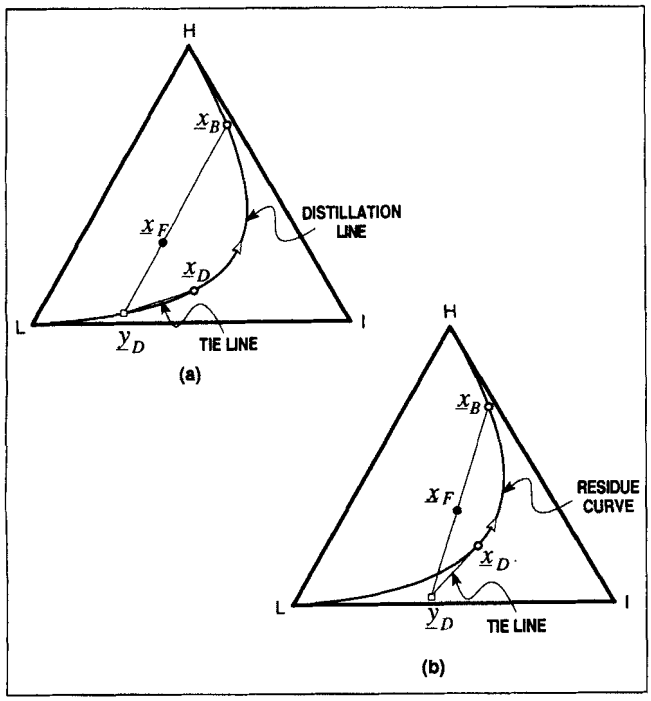

Figure 9. Overall mass-balance line with a partial/total condenser.

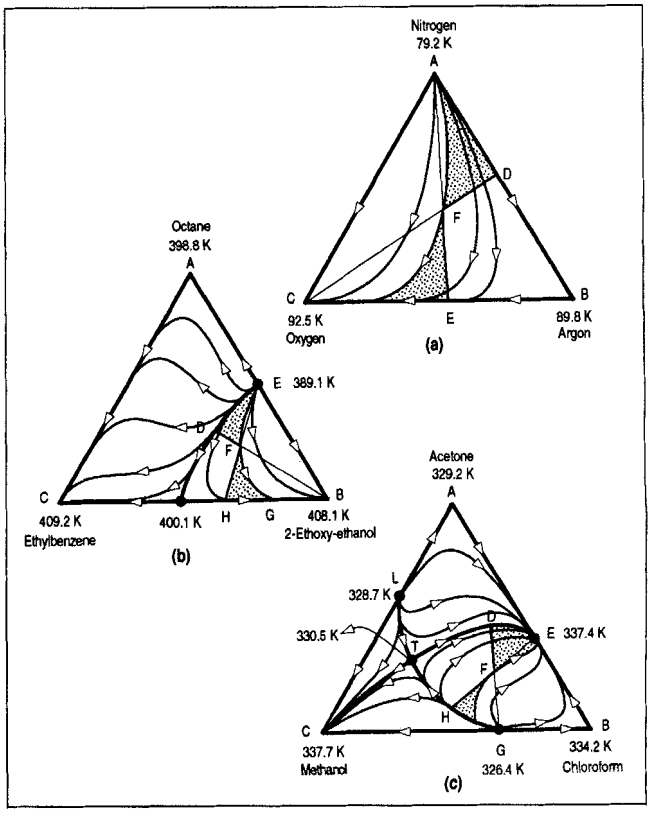

Figure 10. Regions of feasible distillate and bottoms-product compositions (shaded) for a ternary mixture: (a) a system without azeotropes; (b) a system with two binary azeotropes; (c) a system with binary and ternary azeotropes (Stichlmair et al., 1989).

our knowledge, and is recommended. Furthermore, although the fixed points of the maps of distillation lines and residue curves are identical, in general, the residue curves and distillation lines do not coincide. Yet, many of the strategies for the synthesis of separation trains, to be presented in the section on Separation Train Synthesis and Column Design, presume that the operating lines for distillation towers cannot cross the simple-distillation boundaries. As pointed out by Stichlmair et al. (1989), the appropriate boundaries are the separatrices on the maps of distillation lines; that is, the *distillation-line boundaries*. This raises a concern, which needs to be resolved, regarding the differences between the simple-distillation boundaries (associated with the residue curves) and the distillation-line boundaries. For the most part, particularly in the vicinity of a fixed point, small differences can be expected, although, to resolve this, more work on the theory and geometry of distillation lines is recommended.

Feasible Product Compositions at Total Reflux. In the design of azeotropic distillation towers and the synthesis of distillation trains, to be discussed in the section on Separation Train Synthesis and Column Design, it is desirable to bound the regions in which the compositions of the distillate and bottoms product reside. For this purpose, the limiting regimes of operation are examined; that is, total and minimum reflux. At total reflux, the product compositions reside on a distillation line, as shown in Figure 9a. Note that, for a partial/total condenser, the compositions of the bottoms product, $\underline{x}_B$, the feed, $\underline{x}_F$, and the distillate (vapor), $\underline{y}_D$, lie on the linear, overall material-balance line. A similar operating line at total reflux (minimum stages) is the curve *AFC* in Figure 10a. As the number of stages increases, the operating curve becomes more convex approaching *ABC*, where the number of stages approaches infinity (corresponding to minimum reflux). Furthermore, as a consequence of Eq. 15, the distillation line for a tower that contains an infinite number of stages has at least one fixed point. Hence, the operating line for a distillation tower that operates within these limiting regimes lies within the region *ABCFA*. Finally, in the limit of a pure nitrogen distillate, the line *AFE* represents a limiting overall material balance, with point *E* at the minimum concentration of oxygen in the bottoms product. Similarly, in the limit of a pure oxygen bottoms, the line *CFD* represents a limiting overall material balance, with point *D* at the minimum concentration of nitrogen in the distillate. Hence, the distillate composition is confined to the shaded region, *ADFA*, and the bottoms-product composition lies in the shaded region, *CEFC*. Operating lines that lie within the region *ABCFA* connect the distillate and bottoms-product compositions in these shaded regions. At best, only one pure species can be obtained. In addition, only those species located at the end points of the residue curves can be recovered in high purity, with the exception noted in the subsection on Feasible Product Compositions. Hence, the end points of the distillation lines determine the potential distillate and bottoms products for a given feed. This also applies to the complex mixtures in Figure 10b and 10c, it being noted that, under special circumstances, the distillation-line boundary can be crossed, as described in the subsection on Feasible Product Compositions.

The feed point determines the potential distillate and bottoms-product compositions. For example, in Figure 10b, for feed F, only pure 2-ethoxy-ethanol can be obtained. When the feed is moved across the distillation-line boundary, pure ethylbenzene can be obtained. In Figure 10c, only methanol can be recovered in high purity, for feeds in region *LTGCL*.

Since distillation lines are more difficult to construct, and less well understood, many authors approximate the operating lines at total reflux using the residue curves. When this is done, with a partial/total condenser, the composition of the distillate (vapor), y_D, is positioned as shown in Figure 9b (Fidkowski et al., 1993a).

When the distillation-line boundaries cannot be crossed, it should be pointed out that the experiments of Naka et al. (1976, 1983) do not contradict this restriction. Instead, they confirm experimentally and numerically that the composition profiles of a continuous azeotropic tower can cross the *valleys* and *ridges* of the boiling temperature surface projected onto the composition space. Van Dongen and Doherty (1984), Rev (1992), and Stichlmair (1991) have shown theoretically that, in general, the valleys and ridges do not start or end at the pure species or azeotropic points. These lines do not coincide with the distillation-line boundaries, and hence, the valleys and ridges can be crossed by the composition profiles.

Heterogeneous Distillation. It is often desirable to recover the entrainer using processes that are less energy intensive than distillation. This can be accomplished when the entrainer forms a heterogeneous azeotrope with one or more of the species in the feed. In heterogeneous azeotropic distillation towers, the overhead vapor is condensed into two liquid phases, with the entrainer phase easily decanted. Figure 11 shows the process flowsheet and its triangular diagram for the dehydration of ethanol using toluene as an entrainer. Ethanol and water form a low-boiling azeotrope. Although toluene is the heaviest species, it is an appropriate entrainer, since it forms minimum-boiling azeotropes with both water and ethanol. Hence, the arrows point toward both the ethanol and water vertices, allowing ethanol to be recovered in a high-purity bottoms product. Since toluene forms a ternary, minimum-boiling, heterogeneous azeotrope, the overhead vapor approaches this composition and condenses into two liquid phases, one rich in toluene and the other rich in water, which are separated in the decanter.

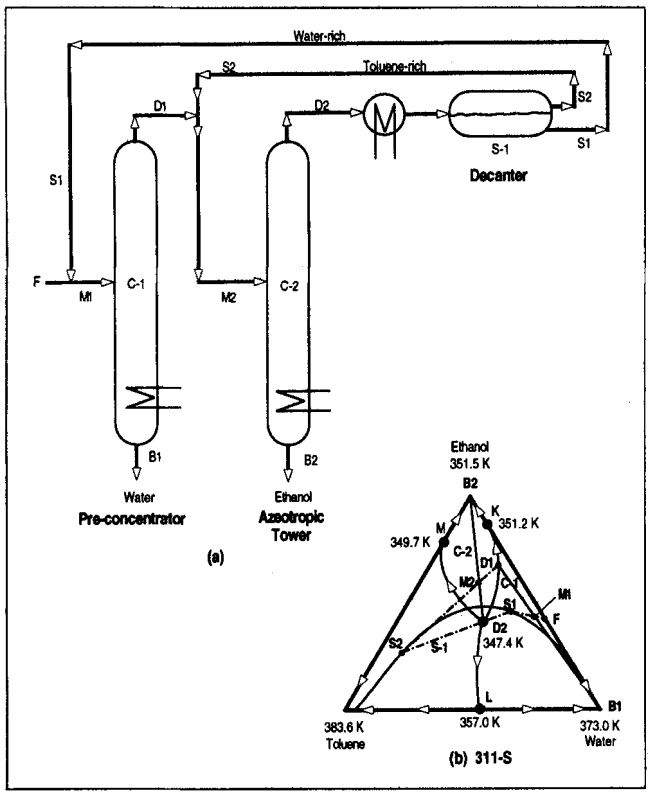

Figure 11. Dehydration of ethanol using toluene as an entrainer: (a) process flow diagram; (b) ternary composition diagram (Stichlmair et al., 1989).

Residue-curve maps have been constructed for heterogeneous systems by Matsuyama (1978) and Pham and Doherty (1990b), who show that Eq. 5 applies to heterogeneous mixtures. The liquid mole fractions, x_i, are replaced by the overall liquid mole fractions, x_i^o, and the equations for the heterogeneous residue-curve map are

$$\frac{dx_i^o}{d\hat{t}} = x_i^o - y_i \qquad i = 1, \ldots, N_s \qquad (22a)$$

$$y_i = x_i^I K_i^{VL}\left\{T, P, \underline{x}^I, \underline{y}\right\} \qquad i = 1, \ldots, N_s \qquad (22b)$$

$$x_i^{II} = x_i^I K_i^{LL}\{T, P, \underline{x}^I, \underline{x}^{II}\} \qquad i = 1, \ldots, N_s \qquad (22c)$$

$$x_i^o = \alpha x_i^I + (1-\alpha) x_i^{II} \qquad i = 1, \ldots, N_s \qquad (22d)$$

$$\sum_{i=1}^{N_s} x_i^I - \sum_{i=1}^{N_s} x_i^{II} = 0 \qquad (22e)$$

$$\sum_{i=1}^{N_s} y_i = 1 \qquad (22f)$$

and α is the fraction of the first liquid phase in the total liquid. Equations 22b–22f are solved to determine the compositions in vapor–liquid–liquid equilibrium as $\hat{t}$ is advanced in the integration.

Matsuyama (1978) showed that the residue-curve maps for homogeneous and heterogeneous systems are similar: that is, their composition spaces are divided into regions with simple-distillation boundaries. However, the residue-curve maps for systems containing heterogeneous azeotropes are far more restricted. Their azeotropes can only be saddles or *unstable* nodes (they cannot be maximum boiling). Further restrictions are given by Pham and Doherty (1990a,b). In addition, the compositions of the two liquid phases lie in different distillation regions. This unique property, which is not a characteristic of homogeneous systems, has been exploited to establish a methodology for the design and synthesis of heterogeneous azeotropic towers (Stichlmair et al., 1989; Pham and Doherty, 1990c), as illustrated in Figure 11a. The preconcentrator, C-1, removes water as the bottoms product. Its distillate, at D1, lies very close to the simple-distillation boundary, K(D2)L. The addition of entrainer, at S2, produces a stream that crosses this boundary into the region where high-purity ethanol is obtained as the bottoms product of the azeotropic tower, C-2. Its overhead vapor, D2, is in the vicinity of the

ternary azeotrope, and when condensed and subcooled forms two liquid phases that are decanted easily. The organic phase, at S2, lies in a different distillation region than the feed to column C-1, M1. When combined with D1, the feed M2, is on the other side of the simple-distillation boundary, in the distillation region M(D2)K(B2)M. The toluene-rich phase, S2, is recycled to column C-2 and the water-rich phase, S1, is combined with the fresh feed (F) to column C-1. The distillate and bottoms products of both towers and their overall mass-balance lines are shown in Figure 11b.

Note that most of the articles referred to earlier utilize residue-curve maps with their simple-distillation boundaries. Distillation-line maps, with their distillation-line boundaries, would provide more accurate bounds for the distillation regions, although often the distillation-line and simple-distillation boundaries do not differ appreciably.

Summary. In summary, the maps of residue curves and distillation lines are very useful for the preliminary design of separation sequences involving homogeneous and heterogeneous mixtures when minimal data are available. In the next few sections, the use of the residue curves and distillation lines for entrainer selection, to identify feasible regions of product compositions, and in column design and synthesis are discussed. First, however, two subsections provide additional background. Methods for computing the azeotropes associated with nonideal mixtures are covered to simplify the construction of maps of residue curves and distillation lines. Then the characteristics of azeotropic distillation towers are discussed, with emphasis on the properties that set them apart from distillation towers that do not involve azeotropic mixtures (so-called *zeotropic* distillations) and their impacts on the development of analysis tools, design methodologies and control strategies.

Computation of azeotropes

To construct maps of residue curves and distillation lines, *all* of the azeotropes in the mixture must be known and characterized as stable nodes, unstable nodes, or saddles. Although much binary, ternary, and polyazeotropic data are available (Horsley, 1973), and additional data are best obtained experimentally, the search for all of a mixture's azeotropes is often conducted using a phase-equilibrium model. Of course, the results depend on the ability of the model to accurately represent the phase-equilibrium data. Caution is warranted especially for heterogeneous systems, where it is difficult to find a model that represents both the vapor–liquid and liquid–liquid equilibrium data accurately. Furthermore, unstable saddle azeotropes are difficult to identify experimentally. In this section, the use of nonlinear analysis to locate all of the azeotropes associated with a nonideal mixture is described.

Using the principle of corresponding states and an equation of state, Teja and Rowlinson (1973) computed binary azeotropes at a constant temperature. Subsequently, Wang and Whiting (1986) extended their algorithm to apply to multicomponent systems at constant temperature or pressure. They note that for a pure species, as well as for mixtures at azeotropic compositions, the equality of the Gibbs free energies of the vapor and liquid phases ($G^V = G^L$) in phase equilibrium leads to an expression for the Helmholtz free energy of vaporization:

$$A^V - A^L = P(V^L - V^V), \tag{23}$$

where P is the pressure, and V^V and V^L are the molar volumes of the vapor and liquid phases, respectively (where Eq. 23 is a necessary, but not sufficient, condition for azeotropy), and furthermore, that at equilibrium, the chemical potentials of each of the species in the two phases are equal, giving:

$$\ln\{\phi_s^V/\phi_s^L\} = 0 \qquad s = 1, \ldots, N_s, \tag{24}$$

where ϕ_s^V and ϕ_s^L are the vapor and liquid fugacity coefficients of species s, respectively, and N_s is the number of species. Rather than solving Eq. 24 subject to the equality of the vapor and liquid mole fractions at the azeotropic point, Wang and Whiting solve Eqs. 23 and 24 to locate the azeotropic points. They solve Eq. 23 in an inner loop and Eq. 24 in an outer loop. This method has been tested successfully for several binary systems involving water and hydrocarbons and for one ternary system, while avoiding the spurious roots often encountered using the algorithm of Andersen and Prausnitz (1980). However, their algorithm does not locate all of the azeotropic compositions associated with a mixture. Recently, Fidkowski et al. (1993b) developed a homotopy-based method that efficiently locates all of the azeotropic compositions. Their algorithm is described next.

Beginning with the identity of liquid and vapor mole fractions at an azeotropic point,

$$f_i\{\underline{x}\} \equiv y_i\{\underline{x}\} - x_i = 0 \qquad i = 1, \ldots, N_s - 1, \tag{25}$$

Fidkowski et al. (1993b) developed a homotopy-continuation method to locate all of the azeotropes by finding all of the roots of this equation. They utilize the homotopy equations:

$$h_i\{\underline{x}; t\} = (1-t)g_i\{\underline{x}; t\} + tf_i\{\underline{x}; t\} \qquad i = 1, \ldots, N_s - 1 \tag{26}$$

with

$$g_i\{\underline{x}\} \equiv y_{\text{ideal},i}\{\underline{x}\} - x_i \qquad i = 1, \ldots, N_s - 1, \tag{27}$$

where $\underline{y}_{\text{ideal}}$ is the vector of vapor mole fractions in equilibrium with the liquid mole fractions, $\underline{x}$, for ideal liquid and vapor phases, where

$$y_{\text{ideal},i} = \frac{P_i^s}{P} x_i. \tag{28}$$

Substituting Eq. 28 into Eqs. 27 and Eq. 1 into Eqs. 25, and the resulting equations into Eqs. 26, gives

$$h_i\{\underline{x}; t\} = \left[(1-t) + t\frac{\gamma_i^L}{\phi_i^V}\right]\frac{P_i^s}{P} x_i - x_i \qquad i = 1, \ldots, N_s - 1, \tag{29}$$

subject to the constraint,

$$\sum_{i=1}^{N_s} x_i = 1. \tag{30}$$

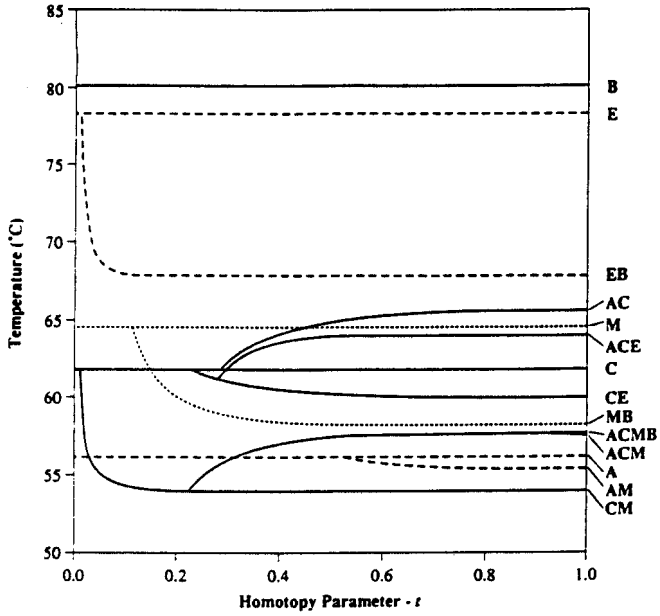

Figure 12. Cascade bifurcations associated with a mixture of acetone(A)–chloroform(C)–methanol(M)–ethanol(E)–benzene(B) at 1 atm (Fidkowski et al., 1993b).

Beginning with each pure species, which satisfy Eqs. 29 and 30 when the homotopy parameter, t, equals zero, all of the azeotropes are located as t varies from zero to unity. As t increases, cascade bifurcations occur. This is illustrated in Figure 12, for the acetone–chloroform–methanol–ethanol–benzene mixture at 1 atm (with the Wilson equation used to represent the liquid phase and an ideal vapor phase), where a new branch is born at each bifurcation point. For t near zero, N_s branches occur, each corresponding to one of the pure species. As t increases, the pure-species branches bifurcate to form branches with binary azeotropes. These, in turn, bifurcate to form branches with ternary azeotropes, and so on. When t reaches unity, all of the azeotropes are identified, with their temperatures and compositions determined.

Fidkowski et al. (1993b) also show that the stability of an azeotrope can be obtained by calculating the eigenvalues of the Jacobian matrix of the residue-curve map, which is equivalent to the negative of the Jacobian matrix of the homotopy equations (Eqs. 29) evaluated at $t = 1$. Knowing the eigenvalues of the residue-curve map, the topological consistency of the map is determined using the *topological index* theory (e.g., Zharov and Serafimov, 1975; Doherty, 1990) by examining the validity of the following relation:

$$\sum_{i=1}^{N_s} 2^i (N_i^+ + S_i^+ - N_i^- - S_i^-) = (-1)^{N_s - 1} + 1, \quad (31)$$

where N_i^+ and S_i^+ are the numbers of nodes and saddles involving i species, respectively, with topological indices of $+1$, while N_i^- and S_i^- are the numbers of nodes and saddles involving i species, respectively, with topological indices of -1. The topological indices are determined by counting the number of negative eigenvalues at each singular point, where singular points with an even or odd number of negative eigenvalues have topological indices of $+1$ and -1, respectively. The topological indices and the types of azeotropes for the acetone–chloroform–methanol–ethanol–benzene mixture at 1 atm are tabulated in Table 1. Note that the summation in Eq. 31 equals two, the righthand side of Eq. 31 with $N_s = 5$.

Table 1. Topological Indices and the Types of Azeotropes for the Acetone–Chloroform–Methanol–Ethanol–Benzene Mixture at 1 atm

Species/ Azeotropes	Boiling Point, °C	Type	Index
Acetone (A)	56.07	S	−1
Chloroform (C)	61.79	S	+1
Methanol (M)	64.54	S	−1
Ethanol (E)	78.29	SN	+1
Benzene (B)	80.10	SN	+1
AC	65.47	S	−1
AM	55.34	UN	+1
CM	53.91	UN	+1
CE	59.93	S	−1
MB	58.12	S	+1
EB	67.83	S	−1
ACM	57.58	S	+1
ACE	63.89	S	+1
ACMB	57.46	S	−1

Source: Fidkowski et al., 1993b.
Note: S = saddle, SN = stable node; and UN = unstable node.

To summarize, in the absence of reliable experimental data, Fidkowski et al. (1993b) have introduced a homotopy-continuation method to locate the real-bifurcation points at which branches of azeotropes are born. Although this methodology has been demonstrated to be very promising, it remains to perfect the methods of identifying the real bifurcation points and for initiating the new branches. Also, thus far, the methodology has been applied to mixtures in vapor–liquid equilibrium (VLE) and has not yet been extended to mixtures in vapor–liquid–liquid equilibrium (VLLE). Furthermore, it remains to examine how the phase-equilibrium models, their terms, and interaction coefficients, affect the solution diagrams; that is, the number of azeotropes and their compositions.

Azeotropic towers

Separations of azeotropic mixtures into nearly pure species are common in the chemical industries. When pressure-swing distillation is not viable because the azeotropic compositions are weak functions of pressure, two common alternatives are azeotropic and extractive distillation. These methods are also applied for the separation of mixtures that have unfavorable volatility differences (close-boiling species). In addition, they are applied in reactive distillation (e.g., esterification).

Heterogeneous azeotropic distillation is often preferred industrially over homogeneous azeotropic distillation due to the ease of recovery of the entrainer and the transition across a distillation boundary in the decanter. However, these towers can be difficult to operate because upsets can extend the liquid-phase split well into the stripping section (Kovach, 1986; Kovach and Seider, 1987a). Although this can severely limit the tray efficiencies (Goodliffe, 1934; Bolles, 1967; Van den

Meer, 1971; Van den Meer et al., 1971; Davies et al., 1987a,b), many studies report results to the contrary (Guinot and Clark, 1938; Shoenborn et al., 1941; Ashton et al., 1987; Herron et al., 1988; Davies et al., 1991). For this reason, it is necessary to characterize the dispersions that form on the distillation trays and their impact on the rates of mass transfer and the tray efficiencies. More research is needed in this area.

Heterogeneous azeotropic towers are often controlled by measuring the temperature difference between two trays and manipulating the reflux rates. When two liquid phases extend into the stripping section, the operators try to maintain the position of the temperature front associated with the interface between trays having one- and two-liquid phase(s). However, when this front is entirely within the tower, its movements do not significantly impact the product purities and recoveries (Widagdo et al., 1989), and hence, this strategy may result in unnecessary control actions. These complications have led several authors to promote the design of homogeneous azeotropic distillation towers (Jacobsen et al., 1991; Andersen et al., 1991a,b; Knapp and Doherty, 1992; Laroche et al., 1992a,b). Nevertheless, operation with two liquid phases on some of the trays can be the only viable choice. For example, when sec-butyl alcohol (SBA) is dehydrated using disec-butylether (DSBE), in the SBA-II tower of ARCO (Kovach and Seider, 1987a,b), low reflux rates can prevent phase splitting in the stripping section, but a high purity of SBA in the bottoms product cannot be obtained because the desired concentration of DSBE is exceeded.

Unlike in zeotropic towers, there exists a maximum reflux rate above which the separation deteriorates (Laroche et al., 1992b). This is because an increase in the reflux rate results in two competing effects. First, as in zeotropic towers, the orientation and position of the operating surface relative to the equilibrium surface is altered, thereby improving the separation. This is countered by a reduction in the entrainer concentration, due to dilution by the increased reflux, which results in a reduction of the relative volatility between the azeotropic species, and therefore, a poorer separation. Van Winkle (1967) and Laroche et al. (1992b) show that this is especially true when a heavy entrainer is used and no additional azeotrope is formed, as in extractive distillation. Furthermore, at infinite reflux no separation takes place. In the section on Column Performance, Homogeneous Azeotropic Distillation, this effect is explained for intermediate- and low-boiling entrainers, as well as for high-boiling entrainers.

For a heterogeneous tower (the SBA-II tower of ARCO), Widagdo et al. (1989) observe similar behavior. In addition to minimum and maximum reflux ratios, they show the existence of a critical reflux ratio above which the formation of two liquid phases is very sensitive to small changes in the reflux ratio. In addition to these competing effects, in a heterogeneous tower, the concentration front between trays having one- and two-liquid phase(s) travels down the tower as the reflux ratio increases, until it exits from the tower and the separation deteriorates drastically, as shown in Figure 13. Note that these effects are discussed more completely in the section on Column Performance, Heterogeneous Azeotropic Distillation.

Another peculiar behavior is that an increase in the number of trays does not necessarily improve the separation. This is illustrated by Laroche et al. (1992b) for the separation of

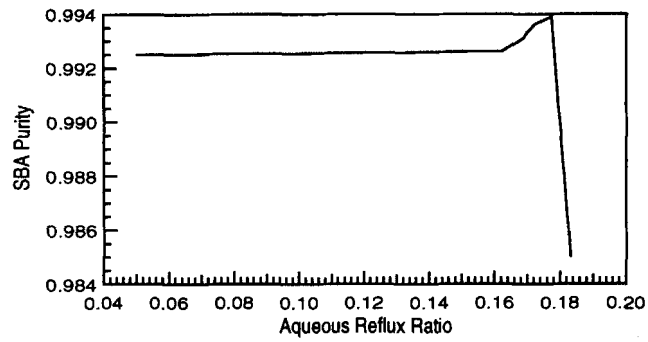

Figure 13. SBA purity as a function of the aqueous reflux ratio (Widagdo et al., 1989).

acetone and heptane using toluene as an entrainer (see Figure 14).

The multicomponent mixtures in azeotropic distillations usually contain two or more binary azeotropes. Hence, in sections of an azeotropic distillation tower, the compositions of binary azeotropes are often approached, with steep fronts in temperature and composition often separating these sections. For example, in Figure 15, for the dehydration of ethanol with benzene, the steep fronts in the stripping section separate the bottoms product from a section in which the composition of the ethanol-benzene azeotrope is approached near the feed tray. Robinson and Gilliland (1950) were the first to compute these composition and temperature profiles, and others have shown the extreme sensitivity of the composition and temperature fronts to small changes in the operating conditions, such as the reflux ratio, boilup rate, product recovery and purity, and the feed rate and composition (Magnussen et al., 1979; Prokopakis and Seider, 1983a). In connection with this sensitivity, Prokopakis and Seider (1983a) demonstrate the difficulty in identifying specifications that permit steady-state solutions having a single-liquid phase on all of the trays. Furthermore, Widagdo (1991) shows that as the temperature decreases, approaching the ternary azeotropic temperature of the benzene–ethanol–water mixture, toward the top trays, the envelope of vapor compositions shrinks. Yet another observation is that the models are

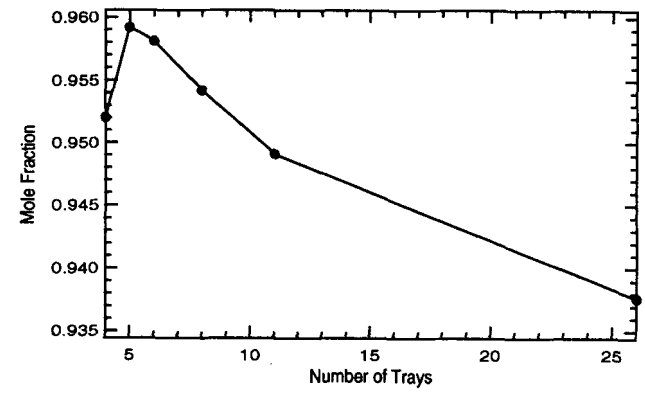

Figure 14. Effects of the number of trays on the mole fraction of acetone in the distillate for the acetone–heptane–toluene system (Laroche et al., 1992b).

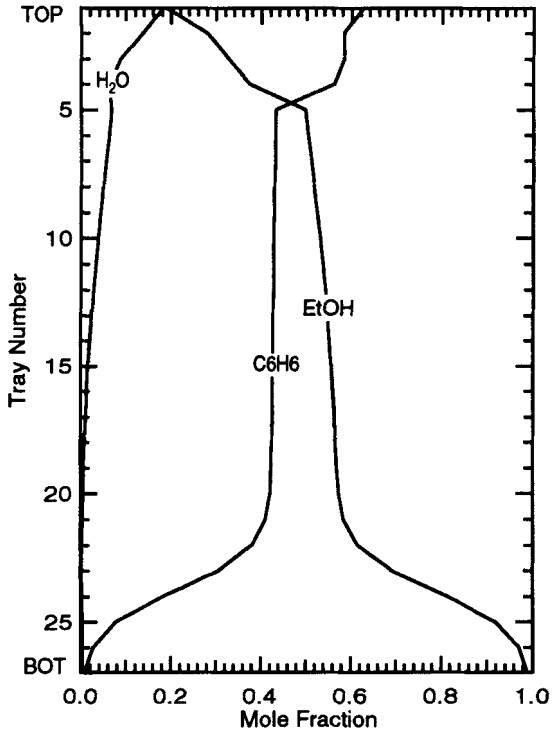

Figure 15. Profiles of liquid mole fractions for the dehydration of ethanol with benzene.

sufficiently nonlinear to include regions of the parameter space in which multiple steady states exist (Magnussen et al., 1979; Prokopakis et al., 1981; Prokopakis and Seider, 1983a). This sensitivity makes the efforts to simulate and control these towers more challenging. For simulation, Kovach and Seider (1987a) had to resort to Newton homotopy-continuation, a nearly global convergence method.

For hetereogeneous columns having two liquid phases on several trays, these problems are compounded by the need to accurately predict the formation of two liquid phases. In addition, at the interface between trays having one- and two-liquid phase(s), discontinuities may occur in the dynamic models. This observation and others associated with dynamic simulations have been reported only recently (Rovaglio and Doherty, 1990; Wong et al., 1991; Widagdo et al., 1992). Furthermore, although zeotropic and homogeneous azeotropic towers are controlled in similar ways, to our knowledge, only a few control studies have appeared for heterogeneous towers (Rovaglio et al., 1990a,b; 1992; 1993). These topics are considered further in the sections on Column Performance and Column Control.

Entrainer Selection

Although success in azeotropic distillation is largely determined by the choice of the entrainer, until recently, entrainers were selected using a trial and error procedure with much reliance on experimental data (Berg, 1969; Tassios, 1972). More recently, entrainers have been selected on the basis of their potential for producing feasible designs. In this section, simple rules using maps of distillation lines (operating lines at total reflux), in preference to residue curves (which approximate the operating lines at total reflux), are presented for screening the many possible entrainers. These were introduced by Doherty and Caldarola (1985), Stichlmair et al. (1989), and Stichlmair and Herguijuela (1992) and are useful in the early design stages, given specifications for the desired separations.

Unlike zeotropic distillations, the product compositions of azeotropic distillations depend on the feed composition and its position relative to the distillation-line boundaries. As noted earlier, many authors have used residue-curve maps with their simple-distillation boundaries. Since the simple-distillation and distillation-line boundaries are often in close proximity, their conclusions are often reasonable.

When selecting an entrainer, the principal concern is the structure of the maps of residue curves and distillation lines that are associated with the mixtures involving it. To facilitate the screening of potential entrainers, Matsuyama and Nishimura (1977) enumerate 113 different residue-curve maps that satisfy constraints imposed by *index* theory (Chap. 5 of Courant and Robbins, 1978; also, see the section on Computation of Azeotropes in the present article). Of these, eighty-seven residue-curve maps contain at least one minimum-boiling binary azeotrope (e.g., see figures 12 to 21, Doherty and Caldarola, 1985). Matsuyama and Nishimura classify the residue-curve maps for ternary mixtures by placing the lightest species (L) at the top vertex, the intermediate species (I) at the bottom-right vertex, and the heaviest species (H) at the bottom-left vertex, and assign three digits to identify the binary azeotrope on the $L-I$, $I-H$, and $H-L$ edges, using the following convention: 0—no azeotrope; 1—binary minimum-boiling azeotrope (unstable node); 2—binary minimum-boiling azeotrope (saddle); 3—binary maximum-boiling azeotrope (stable node); and 4—binary maximum-boiling azeotrope (saddle). A single letter, after the three digits, represents the type of ternary azeotrope: m—minimum-boiling ternary azeotrope (unstable node); M—maximum-boiling ternary azeotrope (stable node); and S—intermediate-boiling ternary azeotrope (saddle). Note that the residue-curve maps in Figures 8 and 11 have been classified using this convention.

As discussed in the section on Simple-Distillation and Distillation-Line Boundaries (following Eq. 21), the residue-curve maps approximate the liquid composition profiles through the feed point at total reflux. Because the residue curves cannot cross the distillation boundaries, both Van Dongen and Doherty (1985) and Stichlmair et al. (1989) suggest, as a first approximation, that the compositions of distillation towers operating at finite reflux cannot cross these boundaries. In practice, however, small excursions occur, but most operating lines are confined largely within a distillation region. On this basis, Doherty and Caldarola (1985), in their procedure for the synthesis of separation trains, assume that the overall mass-balance line, which connects the distillate, feed, and bottoms-product compositions, cannot cross the distillation boundaries. Based on this assumption, they propose that a good candidate for an entrainer is a compound that does not produce a distillation boundary between the species to be separated. For the hexane–methanol–methylacetate and the acetone–chloroform–benzene systems, Van Dongen and Doherty (1985) and Levy et al. (1985) observe that when the distillation boundary is nonlinear (curved), the steady-state

composition profile in a homogeneous distillation may cross from the convex side, and hence, the entrainer selection strategy of Doherty and Caldarola is conservative. More recently, Foucher et al. (1991) also used this assumption in a new methodology to automatically screen entrainers for the separation of azeotropic mixtures in homogeneous towers.

Stichlmair et al. (1989) proposed another strategy for entrainer selection, based on the concept that a homogeneous azeotropic mixture can be separated into nearly pure species only when a residue curve connects the desired products. To achieve this, they observe that, for high-boiling binary azeotropes, the entrainer should also be a high-boiling species or form a new high-boiling binary/ternary azeotrope. Similarly, for low-boiling, binary azeotropes, the entrainer should be a low boiler or form a new low-boiling binary/ternary azeotrope. As has been pointed out by Laroche et al. (1992b), the satisfaction of these criteria is necessary, but not sufficient, to produce a feasible design.

Laroche et al. (1992b) offer a critical analysis of these two criteria and discuss their impact on the design and synthesis of homogeneous azeotropic towers. In recent work, assuming curved distillation-line boundaries, Stichlmair and Herguijuela (1992) present rules for entrainer selection when the operating lines do and do not cross the distillation-line boundaries. The application of these rules, which are reproduced in Table 2, is discussed in the next section.

Table 2. Rules for Entrainer Selection

Mixtures with a minimum-boiling azeotrope:

- Low boiler (lower than the original azeotrope).
- Medium boiler that forms a minimum-boiling azeotrope with the low boiling species.
- High boiler that forms minimum-boiling azeotropes with both species. At least one of the new minimum-boiling azeotropes has a lower boiling temperature than the original azeotrope.

Mixtures with a maximum-boiling azeotrope:

- Low boiler (higher than the original azeotrope).
- Medium boiler that forms a minimum-boiling azeotrope with the high boiling species.
- High boiler that forms maximum-boiling azeotropes with both species. At least one of the new maximum-boiling azeotropes has a higher boiling temperature than the original azeotrope.

Source: Stichlmair and Herguijuela (1992).

Separation Train Synthesis and Column Design

In this section, methodologies for the synthesis and design of azeotropic distillations are discussed. Because the selection of the entrainer has a significant impact on the synthesis of the azeotropic distillation tower and the distillation train in which it resides, most synthesis strategies initially consider the entrainer, as described earlier. After the entrainer is selected, attention is directed to the sequence of the distillation towers, and then to the number of stages and reflux requirements for the individual towers. These are the subjects of the subsections that follow.

Feasible product compositions

When considering sequences of distillation towers, it is important to determine, for each potential tower, the feasible ranges of distillate and bottoms-product compositions. Traditionally, a sequence of columns has been proposed, with specifications for the number of equilibrium stages and the reflux ratio, and the ranges of the distillate and bottoms products have been studied by simulation. In recent years, several investigators (Stichlmair et al., 1989; Stichlmair, 1991; Stichlmair and Herguijuela, 1992; Fidkowski et al., 1993a; Wahnschafft et al., 1992a, 1993; Wahnschafft and Westerberg, 1993) have developed methods for determining the ranges of the distillate and bottoms-product compositions, given the feed composition. These techniques have resulted in much improved strategies for the synthesis of separation sequences. In the remainder of this subsection, these methods are described for operation at total-reflux and extended to normal operation at finite-reflux ratios.

Total-Reflux Bounding. The overall and species mass balances dictate that the feed, distillate, and bottoms-product compositions lie on a straight line, the so-called mass-balance line, with the distillate and bottoms-product compositions at the end points. Stichlmair and Herguijuela (1992) propose a method that bounds the compositions at total reflux, where the operating lines are the distillation lines. Note that the distillate and bottoms-product compositions lie on the same distillation line with the feed on a chord connecting these compositions, as illustrated for a ternary zeotropic mixture, in Figure 16a. To set the boundaries of the distillate and bottoms products, the distillation line through the feed composition (F in Figure 16b) is positioned. All compositions within the region bounded by the distillation line and the HL-axis are discarded. A mass-balance line is drawn through vertex L, pure distillate, and extended through F to B. A second mass-balance line is drawn through vertex H, pure bottoms product, and extends through F to D. These *extreme* mass-balance lines provide the remaining bounds for the distillate and bottoms-product compositions, as illustrated in Figure 16b, where the feasible compositions are displayed in the shaded regions, $LFDL$ and $HFBH$, respectively.

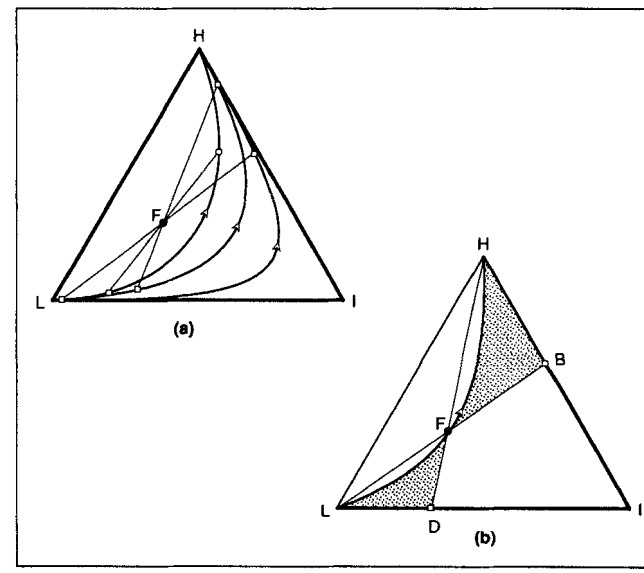

Figure 16. Potential distillate and bottoms-product compositions in a ternary zeotropic mixture.
The curves are distillation lines at total reflux.

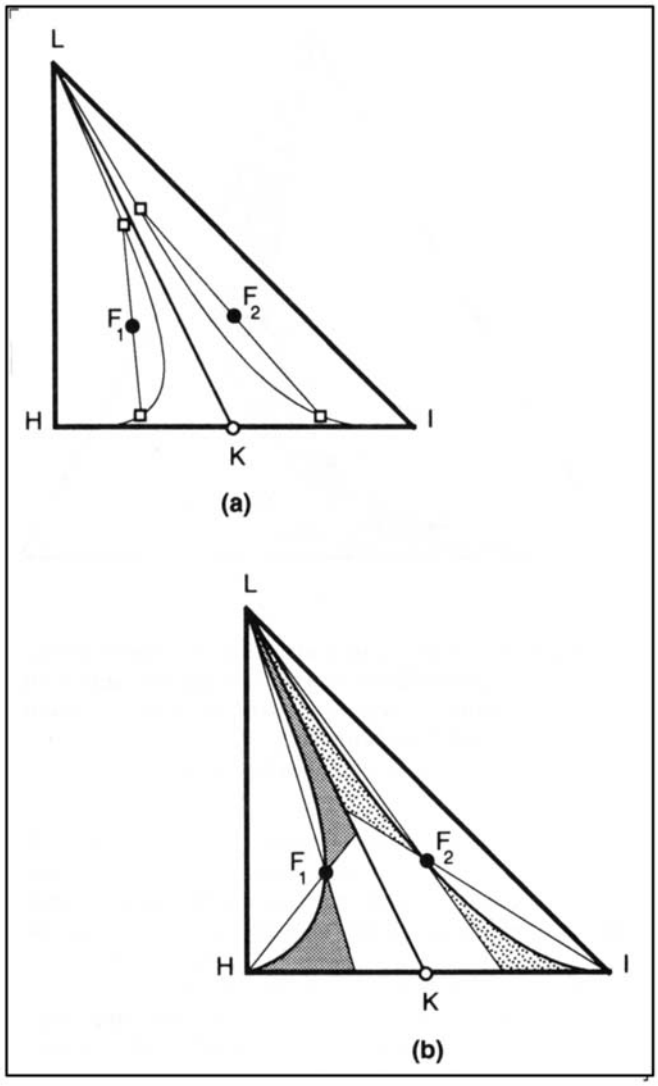

Figure 17. Potential distillate and bottoms-product compositions in a ternary system with a minimum-boiling *H–I* azeotrope and a linear, distillation boundary.

The curves are distillation lines at total reflux.

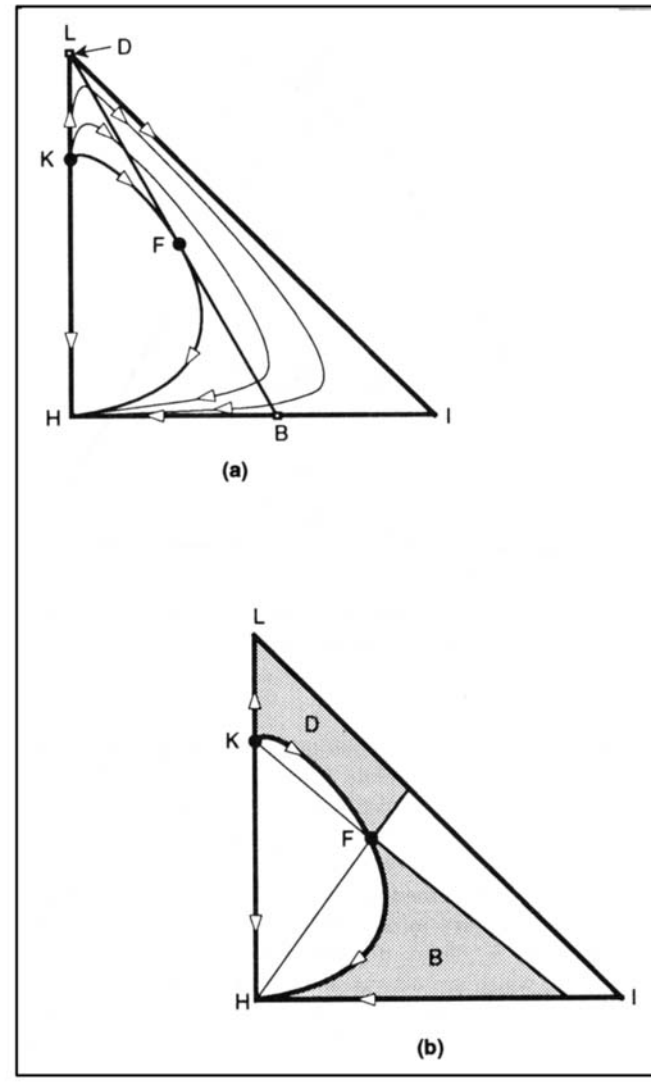

Figure 18. Potential distillate and bottoms-product compositions in a ternary system with a minimum *H–L* azeotrope.

The curves are distillation lines at total reflux.

Note that, as discussed in the section on Residue Curves and Distillation Lines, the distillation lines are the operating lines at total reflux, while the residue curves are approximations. For this reason, *distillation-line maps* are presented in this section, although several authors utilize residue-curve maps.

Having selected the entrainer, the regions of distillate and bottoms-product compositions are positioned. Consider a system with an azeotrope between the heavy and intermediate species (H and I), as illustrated in Figure 17. Using a low-boiling entrainer, L, two regions are separated by a *linear* distillation boundary that connects the azeotrope, K, and the low-boiling species, L. Figure 17a shows two feeds, F_1 and F_2, located in the two distillation regions ($HKLH$ and $IKLI$). Note that each mass-balance line is confined to the distillation region in which the feed is located. Figure 17b shows the regions of potential distillate and bottoms-product compositions for both feeds at total reflux. In region $HKLH$, a column can be constructed to collect H, as the bottoms product, or L, as the distillate. Similarly, for feeds in region $IKLI$, species L and I concentrate in the distillate and the bottoms product, respectively.

There are two situations that are noteworthy, as discussed in the paragraphs that follow. First, when the pure species are not at the end points of the distillation lines, they can be collected as products. Second, under certain circumstances, the distillate or bottoms products can lie in distillation regions other than that in which the feed resides.

The separation of a ternary mixture is illustrated in Figure 18a. This system does not have a distillation boundary and all of the distillation lines emanate from the minimum-boiling azeotrope, K, and end at H. One of the distillation lines traces the perimeter of the composition diagram along the $KLIH$ edges. For the feed, F, an overall mass-balance line can be drawn through the pure L vertex. Although species L

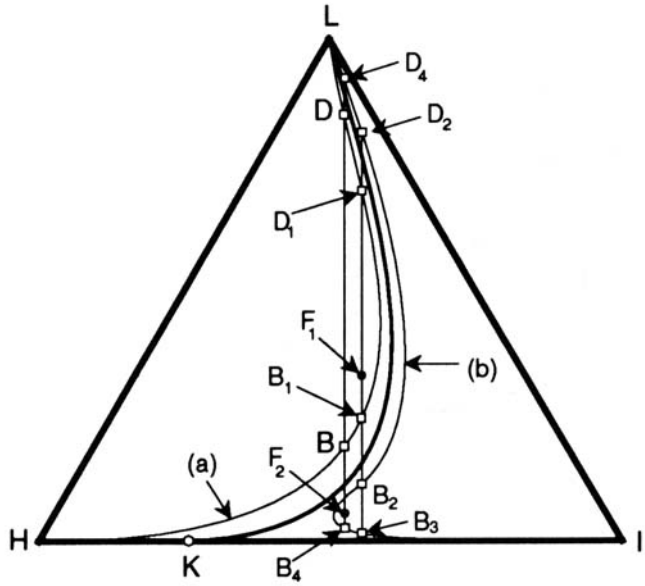

Figure 19. Feasible and infeasible crossings of a curved distillation-line boundary.

The curves are distillation lines at total reflux.

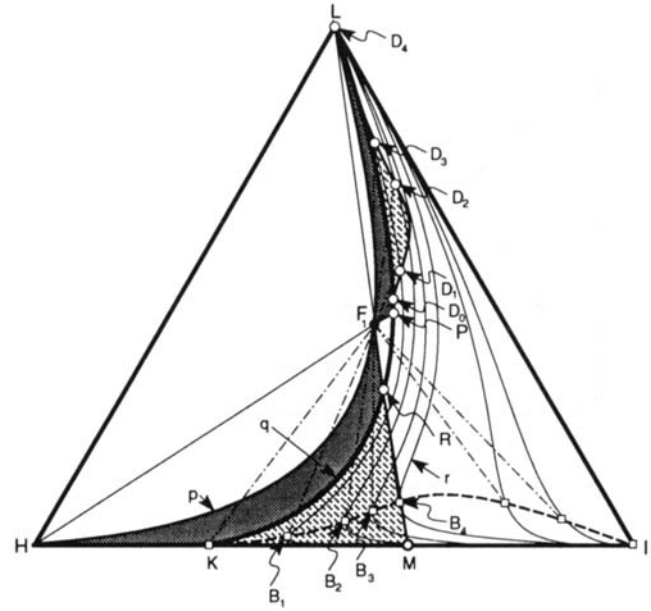

Figure 20. Potential distillate and bottoms-product compositions in a ternary system with a minimum-boiling *H–I* azeotrope and a curved distillation boundary.

The curves are distillation lines at total reflux.

is not the end point of the distillation line *KLIH*, pure *L* can be recovered in the distillate from this ternary mixture, and the region of potential distillate and bottoms products is illustrated in Figure 18b. Note that pure species *I* cannot be recovered for this feed composition.

To illustrate the crossing of a distillation boundary, Figure 19 shows a ternary mixture with a minimum-boiling *H–I* azeotrope at *K*. There are two distillation regions, *HLKH* and *IKLI*, which are convex and concave, respectively. Consider a feed, F_1, in the convex region *HLKH* located close to the distillation boundary. Figure 19 shows distillation lines *a* and *b* in the regions *HLKH* and *IKLI*, respectively. An overall mass-balance line can be drawn through F_1, which not only forms a chord to the distillation line *a* (B_1D_1) in the convex region but also to the distillation line *b* (B_3D_2) on the other side of the distillation boundary. The feed F_1 can have a distillate D_1 and a bottoms product B_1, with both located in the distillation region in which F_1 resides. It can also produce a distillate D_2, with either B_2 or B_3 as its bottoms product, located on the other side of the distillation boundary (on curve *b*). In this special situation, the three compositions do not lie within the same distillation region as F_1, and hence, the distillation boundary can be crossed. The overall mass-balance line through a feed, F_2, located in the concave region *IKLI*, also forms two chords to the distillation line *a* (*BD*) and to the distillation line *b* (B_4D_4). Note that the distillate, *D*, and the bottoms product, *B*, which are located on distillation line *a*, do not bracket the feed, F_2. Thus, the distillation boundary forms a barrier in this case. In general, because the feed composition must be bracketed by the distillate and bottoms-product compositions, a distillation boundary can be crossed only from the convex to the concave side. It follows that linear, distillation boundaries cannot be crossed.

The region of product compositions for feed F_1 is illustrated in Figure 20. Note that the potential product compositions lie in both distillation regions. The region of feasible compositions on the feed side is bounded by the distillation line *p* that passes through the feed, the distillation boundary (curve *q*), and the two overall mass-balance lines through pure species *H* and *L*. The bottoms products lie in the shaded portion of the F_1RKHF_1 region, and the distillates lie in the shaded portion of the F_1PLF_1 region. On the other side of the distillation boundary, the region of feasible bottoms-product compositions is bounded by the distillation boundary (curve *q*) and the overall mass-balance line that passes through pure species *L* (line LF_1M); that is, the lightly shaded region *RMKR*. The region of distillate compositions is also bounded by the distillation boundary (curve *q*). In addition, it is bounded by the end points of the chords (B_iD_i) that are tangent to the distillation lines at the tangent points (K, B_1, ..., B_4, ..., I) forming the dashed curve in Figure 20. Because the distillate and bottoms-product composition must lie on the same distillation line, for the feed composition at F_1, the distillate compositions must lie to the left of the overall mass-balance lines through the tangent points at B_i ($D_iF_1B_i$). It follows that, for the feed at F_1, the regions of feasible distillate and bottoms-product compositions, are the shaded portions of the union of F_1PLF_1 and $LD_0 \cdots D_3L$ regions, and the F_1MHF_1 regions, respectively.

Finite-Reflux Bounding. For binary mixtures, the highest purities are achieved at total reflux, while for multicomponent azeotropic mixtures, Van Dongen and Doherty (1985) and Laroche et al. (1992b) show that the best separation may not be achieved at total reflux. Consequently, care must be taken to determine whether the bounds on the distillate and bottoms-product compositions at total reflux are proper at finite reflux.

Recently, Wahnschafft et al. (1992a) and Fidkowski et al.

(1993a) proposed methodologies to better estimate the regions of feasible product compositions at finite reflux. Fidkowski et al. (1993a) introduce the *distillation limit*, which further limits the regions of feasible product compositions (otherwise bounded by the overall mass balance lines and the distillation line through the feed composition), and Wahnschafft et al. (1992a) use the *feed pinch-point trajectory*, to be defined below. In the subsequent discussion, the two approaches are described and contrasted.

Pinch-Point Trajectory. In examining the liquid composition profiles in the rectifying section of a single-feed distillation column, where the operating line is given by

$$\underline{y}_n = \frac{L_{n-1}}{L_{n-1}+D}\underline{x}_{n-1} + \frac{D}{L_{n-1}+D}\underline{y}_D \qquad (32)$$

Wahnschafft et al. (1992a) observe that the magnitude of the distillate, D (and, in turn, the reflux ratio), determines the difference between the compositions of the incoming vapor, $\underline{y}_n$, and the outgoing liquid, $\underline{x}_{n-1}$.

At finite reflux, the rectifying profile cannot be approximated by the residue curve through the distillate composition, $\underline{x}_D$, but crosses the residue curves from the concave side. This is contrary to the assumption that the rectifying profile coincides with the residue curve through $\underline{x}_D$ that appears, from time to time, in the articles referred to earlier. As shown in Figure 21, the tie line connecting the distillate composition, $\underline{y}_D$, and the liquid composition, $\underline{x}_D$, at equilibrium, is tangent to the residue curve ρ_1. Furthermore, Eq. 32 requires that the vapor composition leaving tray 1, $\underline{y}_1$, lies on this dotted tie line, with the magnitude of the distillate, D, determining the position of $\underline{y}_1$ with respect to $\underline{y}_D$. At total reflux, $\underline{y}_1 = \underline{x}_D$, and the liquid composition, $\underline{x}_1$, in equilibrium with $\underline{y}_1$, lies on the distillation line, δ_1, that passes through $\underline{x}_D$. At finite reflux, the liquid composition, $\underline{x}_1$, is located on the curve connecting a_1 and b_1, the liquid mole fractions at equilibrium with $\underline{x}_D$ and $\underline{y}_D$. Similarly, the vapor composition leaving tray 2, $\underline{y}_2$, lies on the dotted operating line connecting $\underline{x}_1$ and $\underline{y}_D$, and the liquid composition, $\underline{x}_2$, at equilibrium with $\underline{y}_2$, lies on ρ_5, bounded by a_2 and b_2. (Note that when $\underline{y}_2 = \underline{x}_1$, $\underline{x}_2$ is at a_2, and when $\underline{y}_2 = \underline{y}_D$, $\underline{x}_2$ is at b_2.) Thus, the rectifying column profiles are bounded by the locus of the so-called *distillate pinch points* $(b_0, b_1, b_2, \ldots)$ and the curve connecting $\underline{x}_D, a_1, \underline{x}_1, a_2, \underline{x}_2, \ldots$. The latter corresponds to the limit of operation at total reflux. Note that Wahnschafft et al. (1992a) mistakenly use the residue curve that passes through $\underline{x}_D$, ρ_1, as a bound instead of $\underline{x}_D$, a_1, $\underline{x}_1$, a_2, $\underline{x}_2$, ... Figure 21 shows that as $\underline{x}_n$ approach the pinch points $\underline{b}_n$, the operating lines connecting $\underline{x}_n$ and $\underline{y}_D$ approach the tie lines connecting $\underline{b}_n$ and $\underline{y}_D$. Note that when $\underline{x}_1 = b_1$ and $\underline{x}_2 = b_2$, the dotted operating lines and the dashed tie lines are colinear. In this circumstance, $\underline{x}_{n-1}$ and $\underline{y}_n$ approach equilibrium and the driving force for the separation becomes infinitesimal. This is equivalent to operation with an infinite number of stages, at a minimum reflux ratio, and hence, the points, b_1, ..., b_n, are referred to as distillate pinch-points. These are plotted on the so-called *distillate pinch-point curve* (dashed) in Figure 22, which is constructed by positioning the tangents to the residue curves that pass through the distillate composition, $\underline{x}_D$. Pinch-point curves for the bottoms-product and feed compositions are constructed similarly, as shown dashed, for the feed composition, in Figure 20. For systems with distillation boundaries, there are distinct pinch-point curves for each distillation region, as illustrated in Figure 23.

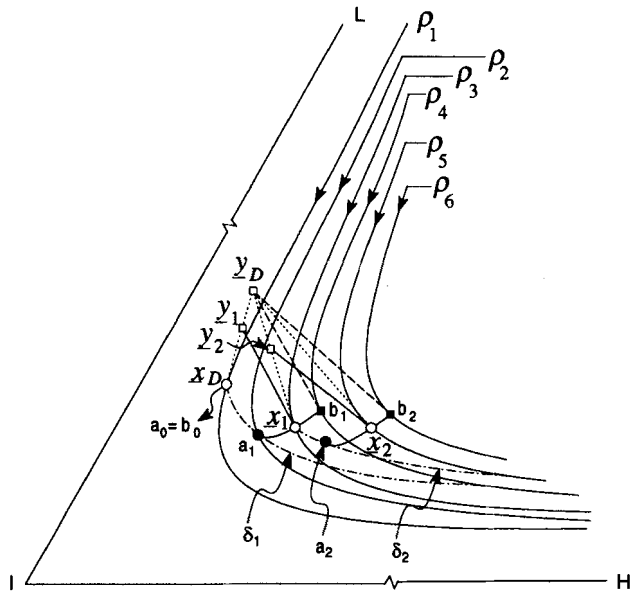

Figure 21. Liquid and vapor composition profiles in the rectifying section.

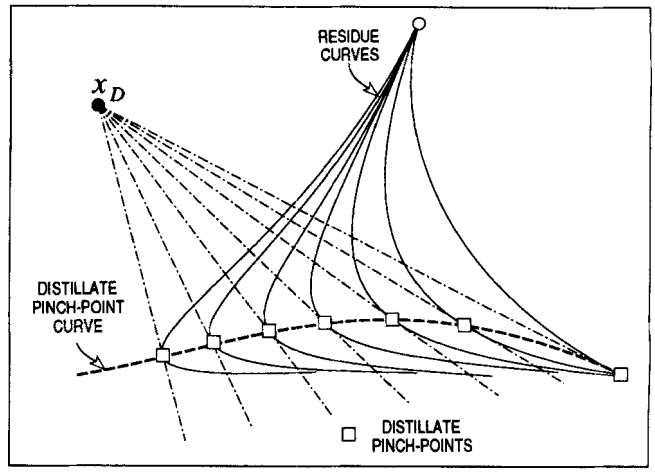

Figure 22. Distillate pinch-point curve.

Distillation Limit and Transition Line. A similar approach has been proposed by Fidkowski et al. (1993a), which also applies for single-feed distillation towers, with emphasis on the separation of ternary mixtures. Initially, the stripping and rectifying profiles are examined for the *direct* and *indirect* splits, as shown in Figure 24 for the ternary system $L-I-H$. For the direct split $(L-IH)$, the stripping profile meets the rectifying profile at $\hat{x}^s$, and hence, there are an infinite number of stages in the stripping section. For the indirect split $(LI-H)$, the rectifying profile meets the stripping profile at $\hat{x}^r$, and the rectifying section has an infinite number of stages. Levy and Doherty (1986) show that there is a unique transition between the direct and indirect splits. This

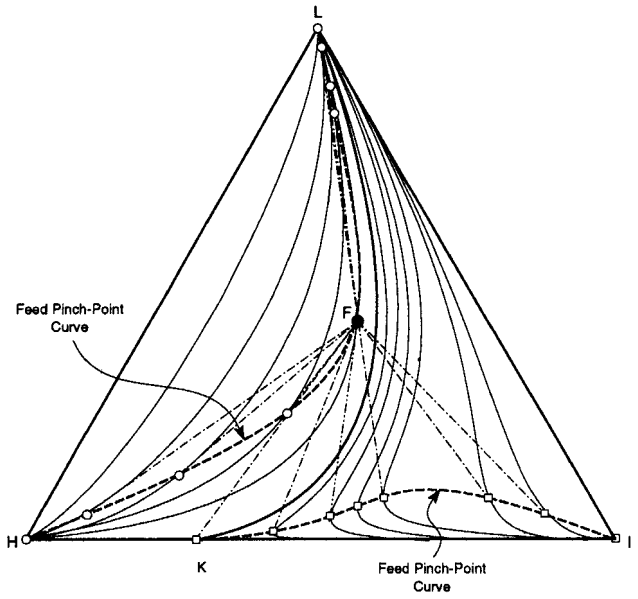

Figure 23. Feed pinch-point curves for mixtures with distillation boundaries.

is referred to as the *transition* split ($LI-IH$), with the *transition line* shown in Figure 25. Here, an infinite number of stages exists in both sections and the pinch points (stable nodes) of both profiles coincide at the feed stage:

$$\underline{\hat{x}}^r = \underline{\hat{x}}^s = \underline{\hat{x}}^f \tag{33}$$

Both tie lines coalesce with the overall mass-balance line joining $\underline{x}_D$, $\underline{z}_F$, and $\underline{x}_B$:

$$\frac{z_1^F - \hat{x}_1^f}{\hat{y}_1^f - \hat{x}_2^f} = \frac{z_2^F - \hat{x}_2^f}{\hat{y}_2^f - \hat{x}_2^f} \tag{34}$$

Equation 34 implies that the transition line joins the tie line of the feed pinch-point compositions, $\underline{\hat{x}}^f$ and $\underline{\hat{y}}^f$. Note that Eq. 34 is identical to the equation of the tangent that defines the feed pinch-points, as utilized by Wahnschafft et al. (1992a). Levy and Doherty refer to the locus of the feed pinch-points as the *distillation limit*.

Product Composition Bounds. As in the analysis at total reflux, the overall mass-balance lines through the vertices and the azeotropes bound the regions of feasible product compositions.

For a single-feed tower, the other bounds are located by finding the product compositions associated with the limiting cases when (1) the distillate composition equals the feed composition (stripping tower), and (2) the bottoms-product composition equals the feed composition (rectifying tower). The former implies that the bottoms-product composition is bounded by the liquid-feed pinch-point curve. While the latter requires that the distillate composition is bounded by the vapor-feed pinch-point curve, passing through the composition of the vapor at equilibrium with the feed composition, $\underline{y}_F$. These bounds give the regions of feasible product compositions proposed by Fidkowski et al. (1993a), as illustrated in

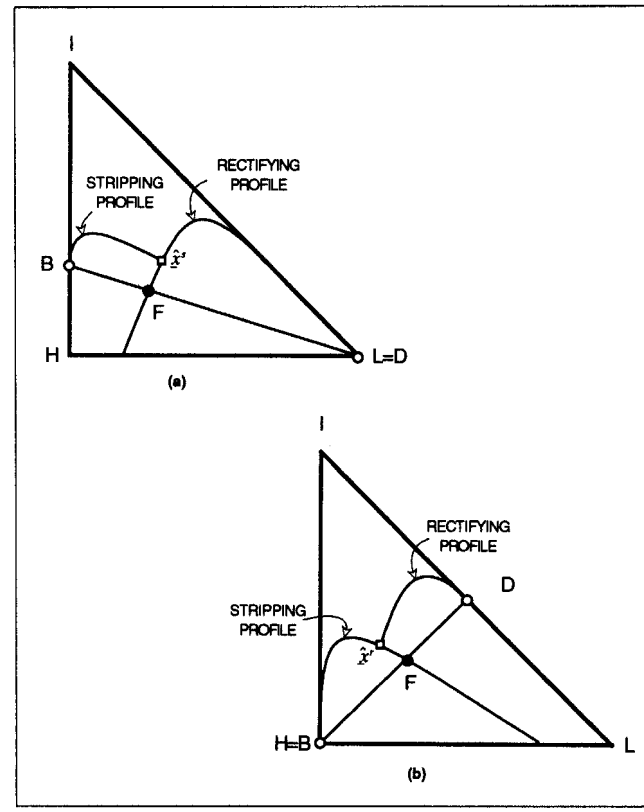

Figure 24. Column profiles for direct and indirect splits: (a) direct; (b) indirect.

Figure 26a. The bounding procedure of Wahnschafft et al. (1992a), shown in Figure 26b, which does not utilize the vapor-feed pinch-point curve, does not properly bound the distillate compositions. As illustrated in Figure 27, Fidkowski et al. (1993a) further divide the feasible product compositions into separate regions for *direct* and *indirect* splits; D_D and B_D, D_I and B_I, respectively.

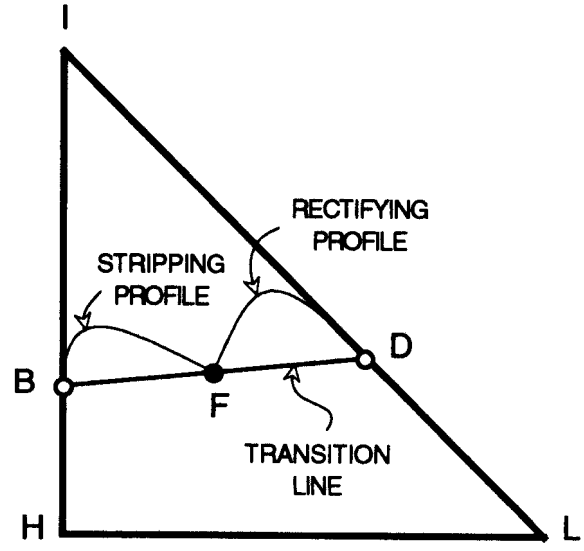

Figure 25. Transition split.

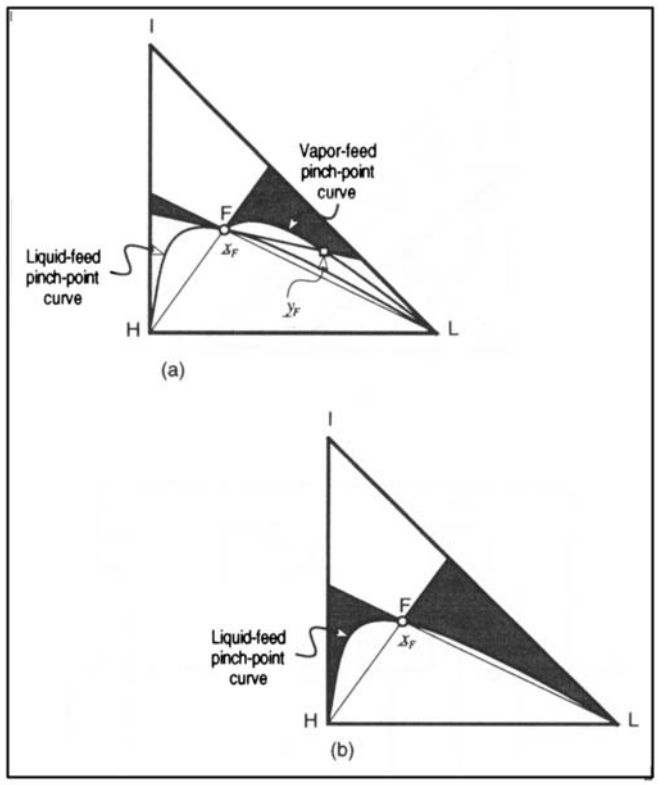

Figure 26. Regions of feasible product compositions for ideal mixtures: (a) Fidkowski et al. (1993a); Wahnschaft et al. (1992a).

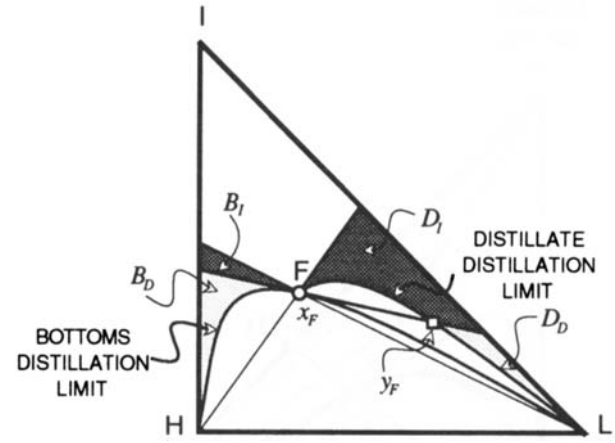

Figure 27. Feasible product compositions for an ideal mixture.

Summary. Fidkowski et al. (1993a) provide the proper bounds for the product compositions at finite reflux. For the limit at total reflux, the distillation-line map should be used instead of the residue-curve map. When the distillation boundaries are curved and the feed is located on the convex side, the feasible product compositions may extend into the adjacent distillation region. In future work, extensions to multicomponent mixtures in multifeed towers can be expected.

Separation train synthesis

Most of the sequencing algorithms for distillation columns, in general, have focused on homogeneous, multicomponent, ideal mixtures to be separated into nearly pure products (Thompson and King, 1972; Hendry and Hughes, 1972; Rathore and Powers, 1974a,b; Westerberg and Stephanopoulos, 1975; Rodrigo and Seader, 1975; Tedder and Rudd, 1978a,b,c; Tedder, 1980; Eliceche and Sargent, 1981; Nishida et al., 1981; Lu and Motard, 1982; Nadgir and Liu, 1983; Andrecovich and Westerberg, 1985a,b; Malone et al., 1985). With ideal mixtures, there are no special difficulties in selecting the species that concentrate in the distillate and bottoms products. Nevertheless, these efforts have helped to resolve many conflicting heuristics that have been in common usage.

Unfortunately, ideal separations are rarely encountered in practice. Motivated by the desire to establish a nonheuristic procedure for the sequencing of columns involving nonideal mixtures, Doherty and coworkers used residue-curve maps, first for homogeneous columns (Doherty and Caldarola, 1985), and later for heterogeneous azeotropic columns (Pham and Doherty, 1990c). As noted earlier, to establish the bounds between the distillation regions, distillation-line maps should be used rather than residue-curve maps, although often the distillation-line and simple-distillation boundaries do not differ appreciably. The basic difference between the design of sequences for ideal and nonideal mixtures is that the product distribution for the latter depends upon the distillation region in which the feed composition lies. Furthermore, as the number of species increases, the product compositions become more difficult to predict. However, when the maps of residue curves and distillation lines can be used, the feasible regions for the distillate and bottoms-product compositions are well defined and the strategy for synthesizing the distillation sequence is simplified considerably. This is illustrated for the separation of a binary, minimum-boiling azeotropic mixture (heptane and acetone) using an intermediate-boiling entrainer (benzene), as shown in Figure 28. For this mixture, which does not have a distillation boundary, Figure 29 shows the two distillation sequences that produce nearly pure heptane (A) and acetone (B). Note that the linear material balance lines, connecting the distillate, feed, and bottoms-product compositions, are illustrated for the two sequences in Figure 28.

Many entrainers, however, introduce new azeotropes and create one or more distillation boundaries. In constructing a distillation sequence, Doherty and Caldarola (1985) assume that the distillation boundaries are linear and neglect the effects of their curvature. Thus, the column profiles are confined to the region in which the feed composition is located and the sequencing problem is reduced to finding a way to cross these boundaries so as to achieve the prescribed products. Two alternatives are (1) to use an entrainer that does not produce a distillation boundary between the two species to be separated, and (2) to use an entrainer that induces liquid-phase splitting, as in *heterogeneous* azeotropic distillation. For an algorithm to sequence heterogeneous towers, see Pham and Doherty (1990c). In addition to these two alternatives, simple separations, such as membranes or adsorbers, can be used to cross a distillation boundary.

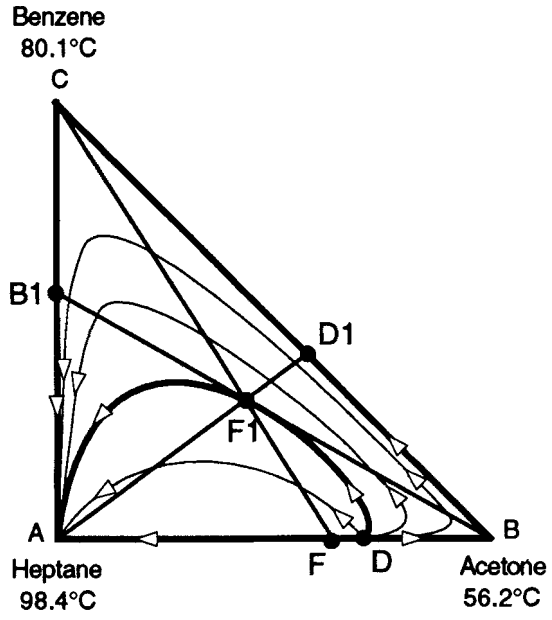

Figure 28. Distillation lines for the heptane–acetone–benzene system at 1 atm.

To avoid these alternatives, it would appear to be desirable to introduce a recycle loop as a means of crossing the distillation boundaries. In this approach, intermediate and/or product streams would be recycled. At the mixing point, the composition would be adjusted to lie in the desired region. As an illustration, consider the separation of A and B using an entrainer that forms a binary azeotrope with species A, as sketched in the distillation-line map in Figure 30a. The feed (F) contains mostly A, more concentrated than the $A-B$ azeotropic composition. A candidate column sequence is given in Figure 30b.

In this sequence, the fresh feed is mixed with the $A-C$ azeotrope to produce a combined feed, $F1$, to column $C1$. Species A is recovered as the bottoms product of $C1$ and the distillate, $D1$, lies close to the distillation boundary, DE. The distillate, $D1$, is mixed with the bottoms product, $B3$, of column $C3$ such that the combined mixture, $F2$, which is the feed to column $C2$, is located in the second distillation region, $BCEDB$. This accomplishes the task of crossing the distillation boundary. The second column, $C2$, is designed to produce pure B. The distillate, $D2$, is fed to the last column, which produces distillate, $D3$, and bottoms product, $B3$, which are both recycled to the first and second column, respectively. This configuration would produce pure A and B. However, Doherty and Caldarola (1985) show that this sequence is infeasible. They reason as follows—when a mass balance is prepared over columns $C2$ and $C3$ (see the dashed envelope in Figure 30), the compositions for the feed, $D1$, and products, B and $D3$, must lie on a straight line. Since the nearly pure bottoms product B is in the second distillation region, $D1$ cannot lie in the first distillation region. Stated differently, the sequence is infeasible since colinearity cannot be achieved with $D1$ in the first distillation region. In general, for systems with linear distillation boundaries, Doherty and Caldarola (1985) conclude that recycle loops cannot be used to cross these boundaries.

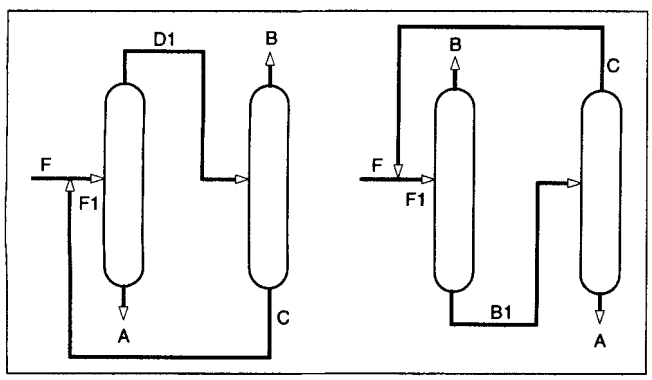

Figure 29. Alternate sequences for the separation of the heptane(A)–acetone(B)–benzene(C) system.

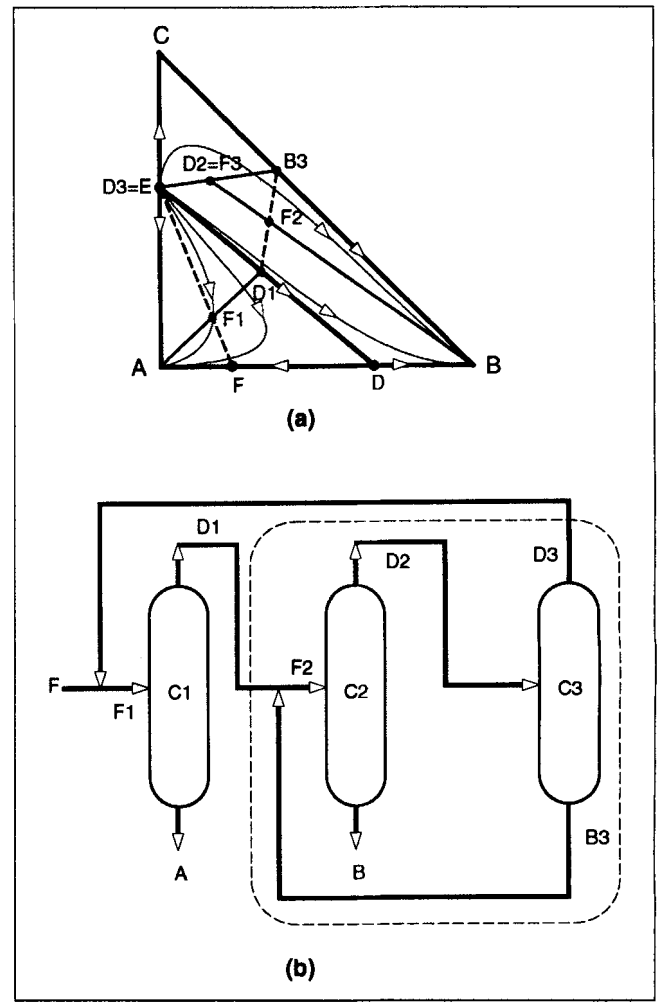

Figure 30. Distillation sequence for the separation of a binary azeotropic mixture with recycle.

Two more recent synthesis strategies have been proposed. In the first, which is implemented in a program called SPLIT, for each stream to be separated, the separation method is chosen before the feasible product compositions are considered and the operating conditions are selected (Wahnschafft

et al., 1991; Wahnschafft et al., 1992b; Wahnschafft et al., 1993). This approach is capable of introducing recycles. In the second, implemented in the MAYFLOWER system (Malone and Doherty, 1994), given the design specifications (pressure levels, product purities), residue-curve maps are constructed and feasible alternatives are created. Then, the internal flow rates and the number of theoretical stages are estimated (using the methods to be discussed in the next subsection), and cost estimates are computed. This approach is applied to synthesize a flowsheet for the dehydration of ethanol with diethoxymethane, which involves the addition of water (and a decanter) to cross the distillation boundary, and to synthesize flowsheets involving reactive distillation and liquid–liquid extraction.

Finally, in another recent paper, Siirola (1994) shows how to apply many of the techniques introduced 20 years earlier (Siirola, 1970; Siirola and Rudd, 1971) to synthesize processes for the manufacture of methyl acetate and the dehydration of acetic acid. For the first process, these steps lead to a flowsheet with a reactor, an extractor, a decanter, and eight distillation columns, involving two mass-separating agents. The flowsheet is modified using evolutionary strategies to eliminate four of the columns, before resynthesis into just two columns, one for reactive distillation and the other without reaction. At each stage in the synthesis, the residue curves and distillation boundaries are considered, the reflux rates and numbers of stages are estimated, steady-state simulations are performed, and opportunities are sought to reduce the differences between the intermediate streams and the desired products (using means-end analysis).

Column design

Having selected a potential column sequence, for each distillation column, the number of stages and the operating conditions are determined. Thus far, most of the design procedures for azeotropic columns have been developed for the separation of binary mixtures, with extensions to multicomponent systems through the use of the pseudobinary concept. In recent work, Doherty and coworkers have applied geometric theory, which is based upon topological concepts, as discussed by Lefschetz (1962) and Arnold (1973).

Before presenting the application of geometric theory, the work of Levy et al. (1985) is reviewed. These authors introduced a boundary-value design procedure (BVDP) to determine the minimum reflux ratio, given N_s of the distillate and bottoms mole fractions, $\underline{x}_D$ and $\underline{x}_B$, for ternary azeotropic mixtures with negligible heat effects, where N_s is the number of chemical species. Assuming constant molal overflow, species mass balances are written for stages in the rectifying and stripping sections:

Rectifying Section:

$$\underline{y}^r_{m+1} = \frac{r}{r+1}\underline{x}^r_m + \frac{1}{r+1}\underline{x}_D \qquad m = 0, 1, \ldots, M \tag{35a}$$

$$\underline{x}^r_0 = \underline{x}_D \tag{35b}$$

Stripping Section:

$$\underline{x}^s_{n+1} = \frac{s}{s+1}\underline{y}^s_n + \frac{1}{s+1}\underline{x}_B \qquad n = 0, 1, \ldots, N, \tag{36a}$$

$$\underline{x}^s_0 = \underline{x}_B \tag{36b}$$

where the rectifying and stripping sections contain M and N stages, r and s are the reflux ratios in these sections, $\underline{y}^r_m$ is the vector of vapor mole fractions in the rectifying section on stage m, and $\underline{x}^s_n$ is the vector of liquid mole fractions in the stripping section on stage n. These difference equations define the operating lines. At the feed stage, additional equations apply:

Overall Material Balance:

$$\frac{x_{F,i} - x_{B,i}}{x_{F,1} - x_{B,1}} = \frac{x_{F,i} - x_{D,i}}{x_{F,1} - x_{D,1}} \qquad i = 2, \ldots, N_s - 1 \tag{37}$$

Overall Energy Balance:

$$s = (r+q)\frac{x_{B,1} - x_{F,1}}{x_{F,1} - x_{D,1}} + q - 1 \tag{38}$$

Feed Stage Continuity:

$$\underline{x}^r_M = \underline{x}^s_N \tag{39}$$

where $\underline{x}_F$ is a vector of feed mole fractions and q is the feed quality.

To determine the minimum reflux ratio, the difference equations (Eqs. 35 and 36) are expressed as ODEs in the continuous variables: $\hat{\underline{x}}^r$, $\hat{\underline{x}}^s$, $\hat{\underline{y}}^r$, $\hat{\underline{y}}^s$.

$$\frac{d\hat{\underline{y}}^r}{dh} = \frac{r}{r+1}\hat{\underline{x}}^r + \frac{1}{r+1}\underline{y}_D - \hat{\underline{y}}^r = 0 \tag{40}$$

$$\frac{d\hat{\underline{x}}^s}{dh} = \frac{s}{s+1}\hat{\underline{y}}^s + \frac{1}{s+1}\underline{x}_B - \hat{\underline{x}}^s = 0 \tag{41}$$

where h is the elevation in the tower. When $d\hat{\underline{x}}^r/dh = d\hat{\underline{x}}^s/dh = 0$, Eqs. 40 and 41 apply to locate the two fixed (pinch) points (for a ternary system). First, Eq. 37 is solved for the unknown $\underline{x}_D$ and $\underline{x}_B$. Then, r is assumed, Eq. 38 is solved for s, and Eqs. 40 and 41 are solved for the fixed points: $\hat{\underline{x}}^r$, $\hat{\underline{x}}^s$. When $\hat{\underline{x}}^r = \hat{\underline{x}}^s$, r and s are minimized, corresponding to N, $M \to \infty$. This analysis has been extended by Knight and Doherty (1986) to include heat effects.

Furthermore, Julka and Doherty (1990) extended this methodology to apply for multicomponent systems ($N_s \geq 4$). For a quaternary system, four fixed points ($\hat{\underline{x}}^r_1$, $\hat{\underline{x}}^r_2$, $\hat{\underline{x}}^r_3$, $\hat{\underline{x}}^s_1$) are computed, all of which lie in the same plane, as illustrated in Figure 31. The curve between $\underline{x}_B$ and $\hat{\underline{x}}^s_1$ is the operating line in the stripping section. Vectors can be defined between $\underline{x}_F$ and the four fixed points:

$$\underline{d}_1 = \hat{\underline{x}}^r_1 - \underline{x}_F$$

$$\underline{d}_2 = \hat{\underline{x}}^r_2 - \underline{x}_F$$

$$\underline{d}_3 = \hat{\underline{x}}^r_3 - \underline{x}_F$$

$$\underline{d}_4 = \hat{\underline{x}}^s_1 - \underline{x}_F \tag{42}$$

These authors show that at minimum reflux these vectors lie

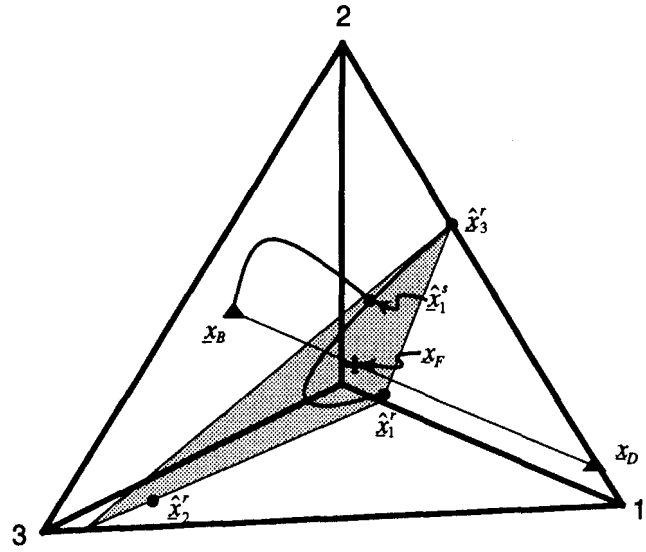

Figure 31. Isometric view of the fixed (pinch) points and operating lines for a quaternary distillation tower (Julka and Doherty, 1990).

in the same plane (shaded in Figure 31):

$$\det[\underline{d}_i, \underline{d}_j, \underline{d}_k] = 0 \qquad i, j, k \in \{1, 2, 3, 4\} \qquad (43)$$

and the volume spanned by $\underline{d}_i$, $\underline{d}_j$, and $\underline{d}_k$ is zero. Thus, at the minimum reflux ratio, the fixed points satisfy the zero-volume formula, and Eq. 43 replaces Eq. 39. In this manner, geometric theory is applied to determine the minimum reflux ratio. In addition, it is shown that this generalizes the Underwood equation to apply for multicomponent systems. To be reliable this method requires that all of the fixed points be located. Julka and Doherty (1993) present a continuation strategy, using the AUTO program (Doedel, 1986) for this purpose. Their design methodology has been further refined by Fidkowski et al. (1991).

The zero-volume formulas, although mathematically compact, are difficult to implement. In addition, they provide an exact solution only when the relative volatilities of the species are constant throughout the column, which is not the case for azeotropic towers. Nonetheless, industrial practitioners (Martin and Reynolds, 1988; Partin, 1993) have found this methodology to be very useful and practical for preliminary designs. In recognition of these limitations, Koehler et al. (1991) have developed a method for the calculation of the minimum reflux that uses the reversible distillation concept and eliminates the assumptions of constant relative volatilities and constant molar overflow. These authors show that their method gives comparable results to those obtained using the RADFRAC program (for solution of the material balance, equilibrium, summation of mole fractions, and heat balance (MESH) equations in ASPEN PLUS), and yet consumes significantly less computation time. More recently, Stichlmair et al. (1993) developed an alternative method, based on the pinch-point geometry, to estimate minimum reflux and reboiler ratios. These authors claim that their method is faster and more reliable than the zero-volume method of Julka and Doherty (1990) and the reversible method of Koehler et al. (1991). Although applied to ternary mixtures, the authors contend that their method can easily be extended to multicomponent mixtures.

Column Performance

Much of the literature on azeotropic distillation has been devoted to the analysis of operations. The early articles, which focused on steady-state operation, were reviewed by Haas (1992) in chap. 4 of *Distillation Design* by Kister (1992). Recently, the literature has concentrated on nonlinear effects, such as the occurrence of multiple steady states, and the analysis of heterogeneous azeotropic towers, with emphasis on the prediction of liquid-phase splitting. The most recent articles extend the analysis to the dynamics of heterogeneous columns (Rovaglio and Doherty, 1990; Wong et al., 1991; Widagdo et al., 1992). In this section, the nonlinear effects in homogeneous and heterogeneous towers, both steady state and transient, are examined.

Homogeneous azeotropic distillation

When operating homogeneous towers, it is important to consider both the maximum separation and the potential for steady-state multiplicity. These involve complex nonlinear effects that are addressed below.

Maximum Separation. The nonlinear relationship between the reflux rate and the extent of separation is illustrated thoroughly by Laroche et al. (1992b) for heavy, intermediate, and light entrainers that do not form new azeotropes with the species to be separated. Their work is best understood by examining the topology of the maps of distillation lines of the mixtures considered.

Heavy Entrainer. Consider the separation of the acetone–*n*-heptane mixture using toluene as the entrainer. Note that acetone and *n*-heptane form a minimum-boiling azeotrope and that toluene does not introduce azeotropes with these species. Using CHEMSIM (Andersen et al., 1989), Laroche et al. (1992b) show that at low reflux rates the separation increases as the reflux rate increases, reaches a maximum, and decreases to the composition of the binary azeotrope at infinite reflux, as illustrates in Figure 32. This is typical of extractive distillations that must be operated at moderate reflux rates to avoid dilution of the heavy entrainer

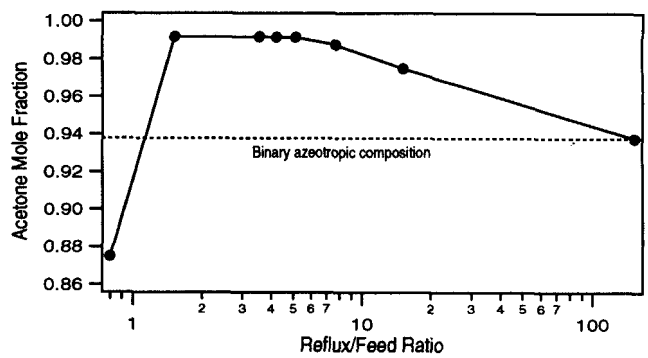

Figure 32. Acetone mole fraction in the bottoms product as a function of the reflux/feed ratio for the acetone–*n*-heptane–toluene system (Laroche et al., 1992b).

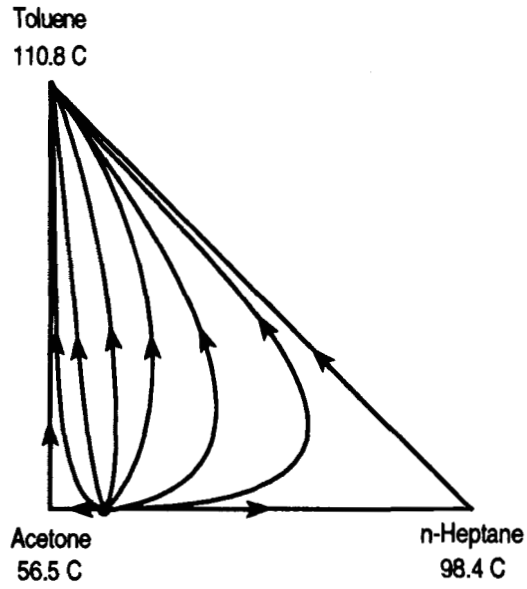

Figure 33. Map of distillation lines for the acetone–*n*-heptane–toluene system.

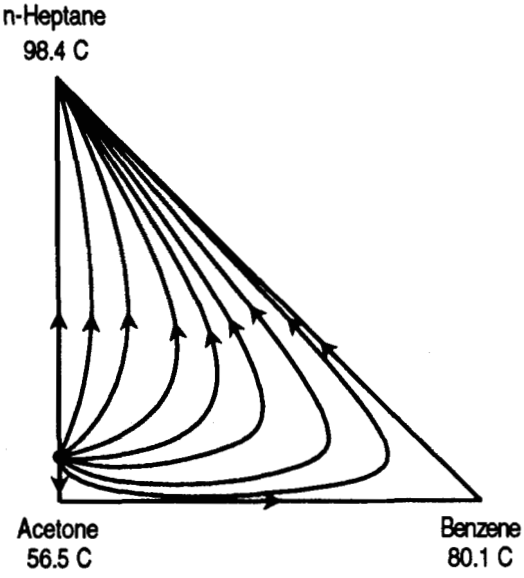

Figure 35. Map of distillation lines for the acetone–*n*-heptane–benzene system.

that hinders the separation at high reflux rates (Van Winkle, 1967). As shown in Figure 33, the distillation lines originate at the binary azeotrope and terminate at the toluene vertex in the absence of a distillation boundary. Hence, at infinite reflux, the bottoms product contains nearly pure toluene and the distillate approaches the composition of the binary azeotrope.

Intermediate Entrainer. Laroche et al. (1992b) also consider benzene, an intermediate-boiling entrainer, for the separation of acetone and *n*-heptane. As shown in Figure 34, the mole fraction of heptane in the bottoms product increases as the reflux/feed ratio increases and reaches a maximum at total reflux, which corresponds to the behavior of a zeotropic tower. Here the increased reflux does not dilute the intermediate entrainer in the column, and hence, the separation is improved. Since the map of distillation lines in Figure 35 has no distillation boundary, as the reflux approaches infinity, the tower yields a bottoms product that contains nearly pure heptane and a distillate that approaches the binary azeotropic composition.

Light Entrainer. Finally, Laroche et al. (1992b) consider the use of the light entrainer, methanol, to dehydrate ethanol. Note that the boiling point of methanol is lower than the temperature of the minimum-boiling azeotrope. As illustrated in Figure 36, the separation first improves with the reflux/feed ratio, reaches a maximum, and deteriorates at high reflux rates. Here, the separation does not deteriorate entirely at infinite reflux because the distillation boundary limits the product compositions at total reflux, as illustrated in Figure 37a. In Figure 37b, the ethanol–water feed, F, to the first column, C-1, has a composition just below the binary azeotropic composition. Point M represents the feed composition after it is mixed with the entrainer, methanol. The bottoms product of C-1, $B1$, contains mostly water and $D1$ represents the distillate composition, which lies close to the distillation boundary. This mixture is fed to the second column C-2. Since the distillation boundary is curved and the feed,

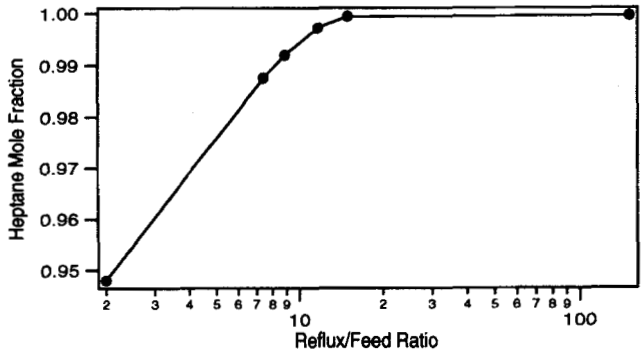

Figure 34. Heptane mole fraction in the bottoms product as a function of the reflux/feed ratio for the acetone–*n*-heptane–benzene system (Laroche et al., 1992b).

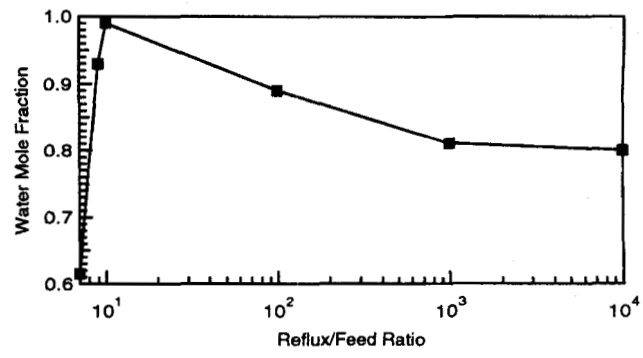

Figure 36. Water mole fraction in the bottoms product of column C-1 as a function of the reflux/feed ratio for the ethanol–water–methanol system (Laroche et al., 1992b).

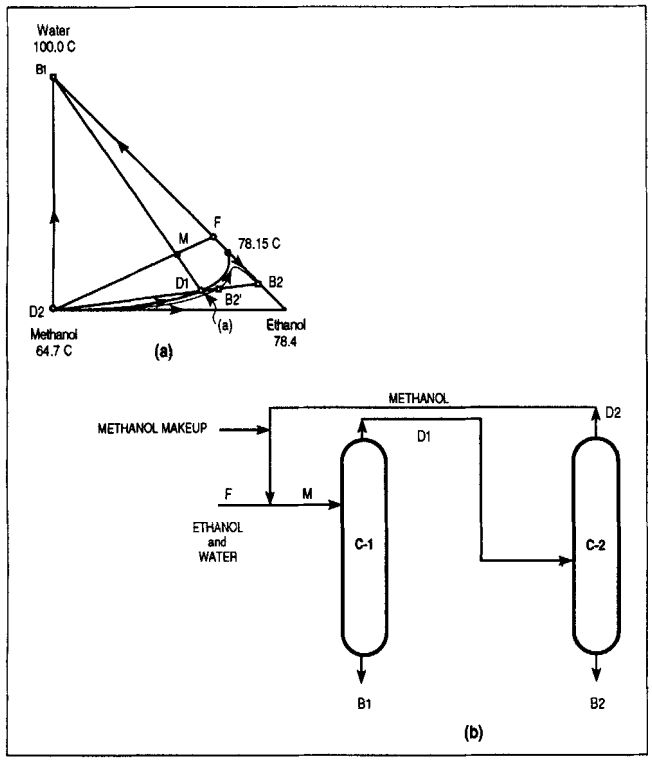

Figure 37. Dehydration of ethanol using methanol as an entrainer: (a) map of distillation lines; (b) separation sequence (Laroche et al., 1992b).

$D1$, lies in the concave region, it can cross the distillation boundary and produces nearly pure methanol, $D2$, in the distillate and $B2$ as the bottoms product.

As the entrainer/feed ratio increases, the feed, M, and the distillate, $D1$ move closer to the methanol vertex. Consequently, the water content in the bottoms product, $B2$, decreases. Due to the shape of the distillation line a, the overall mass balance line intersects as $B2$ and $B2'$. When the bottoms product of column C-2 corresponds to $B2$, the increasing entrainer/feed ratio improves the separation. On the other hand, when the bottoms-product composition of column C-2 corresponds to $B2'$, the increasing entrainer/feed ratio produces a poorer separation. This observation is a consequence of the analysis involving the crossing of distillation boundaries (see the section on Feasible Product Compositions) and is not addressed by Laroche et al. (1992b).

In summary, the steady-state behavior of azeotropic towers is explained largely through the examination of maps of distillation lines, which are gaining importance in operations. Additional research is needed to show their utility in the determination of operating strategies.

Steady-State Multiplicity. Although widely recognized in chemical reactors, for several decades, the existence of multiple steady-states in distillation towers has been considered for only fifteen years, principally in connection with azeotropic distillations. In this subsection, a few brief comments on bifurcation theory are provided, to introduce the discussion of steady-state multiplicity and to characterize the singularities observed in the models for azeotropic distillation towers. Then, theoretical analysis, principally to prove the existence of unique, steady-state solutions, and simulation results, to show the existence of multiple steady states, are reviewed. Emphasis is placed on homogeneous azeotropic distillations, although many of the nonideal solutions can split into two liquid phases. For the most part, the results presented herein pertain to towers that exhibit a single-liquid phase on the trays, with or without two liquid phases in a decanter.

Definition of Steady-State Multiplicity. To define steady-state multiplicity and understand its implications, it helps to consider bifurcation theory (Kubicek and Marek, 1983; Golubitsky and Schaeffer, 1985; Seydel, 1988), which deals with the dependence of the attractors (steady-state, periodic, quasi-periodic, and chaotic) of a system of nonlinear ordinary differential equations:

$$\frac{d\underline{x}}{dt} = \underline{\mathcal{F}}\{\underline{x}, t; p\} \qquad \underline{x}\{0\} = \underline{x}_o \tag{44}$$

$$\mathcal{F}: \Re^m \times \Re \times \Re^k \rightarrow \Re^m; \qquad \underline{x} \in \Re^m, \qquad t \in \Re, \qquad \text{and} \qquad \underline{p} \in \Re^k$$

on a parameter $p_j \in \underline{p}$, with new branches of solutions often introduced when the Jacobian of $\mathcal{F}$ is singular. Consider the dependence of $\underline{x}$ on a parameter p_j in a two-dimensional diagram, for which a scalar measure of the vector $\underline{x}$ is required. An element of $\underline{x}$, x_i, the maximum value of $\underline{x}$, $x_{\max} = \max\{|x_1|, |x_2|, \ldots, |x_m|\}$, or the Euclidian vector norm, $\|\underline{x}\| = (\sum_{i=1}^{m} x_i^2)^{1/2}$, are common measures. Such a two-dimensional diagram is often called a *branching* or *solution* diagram. It commonly contains branches of the steady-state solutions of Eq. 44 that form smooth curves, as shown in Figure 38. As the parameter p_j varies, the number of solutions often changes with the loss or gain of stability. New branches often emerge, end, or intersect at *limit* or *turning* points, *bifurcation* points, and *Hopf bifurcation* points. Figure 38 illustrates these points on a solution diagram. It contains

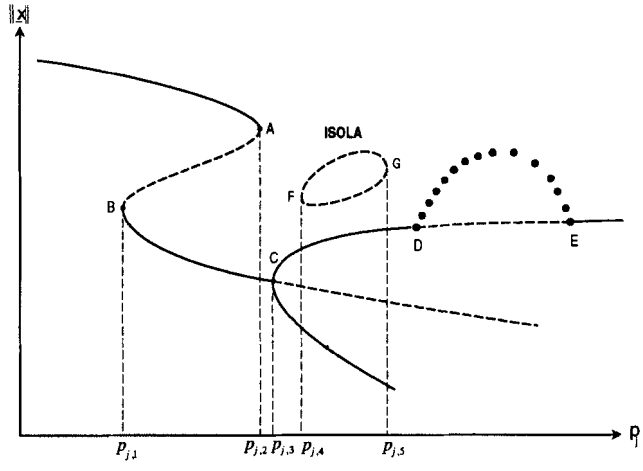

Figure 38. Typical solution diagram.

Points A, B, F, and G are limit points, point C is a real bifurcation point, and points D and E are Hopf bifurcation points. Steady-state solutions; stable (——) and unstable (– – –). Periodic branches (●●●●).

four turning points (A, B, F, and G), a real bifurcation point (C), two Hopf bifurcation points (D and E), and an isola. For parameter values $p_j < p_{j,1}$, a unique solution exists. As p_j increases between $p_{j,1} \le p_j \le p_{j,2}$, three solutions coexist. Between $p_{j,2} < p_j \le p_{j,3}$, the solution is unique. At the real bifurcation point, two new solutions are born. Then at $p_{j,4}$, two additional solutions accompany the isola and are retained until the isola disappears at $p_{j,5}$. Note the appearance and disappearance of the periodic branch at the Hopf bifurcation points (D and E).

In short, bifurcation analysis permits the characterization of the solutions of Eq. 44 as a parameter varies. Turning or real bifurcation points accompany multiple solutions, and Hopf bifurcation points are accompanied by periodic oscillations. In distillation, steady-state multiplicity is the principal concern. It occurs when, for a given set of parameters, $\underline{p}^*$, there exist two or more steady-state solutions of Eq. 44, $\underline{x}^*$. Real bifurcation points have been demonstrated but, to our knowledge, the instances of isolas and Hopf bifurcation points have not yet been associated with the models of distillation towers. Furthermore, in dealing with such physical systems, constraints often apply to assure nonnegative flow rates, to bound the mole fractions between zero and unity, and, perhaps less obvious, to satisfy the requirement that the phase distribution, at equilibrium, be *thermodynamically stable*. Therefore, it is important to check that the solutions are physically meaningful, especially when liquid-phase splitting is possible. Since physically unrealistic solutions must be discarded, they are disregarded in the discussion that follows.

Kienle and Marquardt (1991) and Gani and Jørgensen (1994) characterize two types of multiplicity: (1) output, and (2) input. Output multiplicity, the most commonly reported, occurs when multiple solutions exist for a given set of input variables (number of trays; feed rates, compositions, and locations; and heat duties). On the other hand, input multiplicity occurs when, for a given set of outputs, multiple values of the input variables exist. This is also referred to as *design* multiplicity. This type of multiplicity is most commonly reported in the literature.

Theoretical Analysis. The earliest analyses to determine the number and nature of steady-state solutions to multistage separation models involved binary mixtures under constant molar overflow [(CMO); Acrivos and Amundson, 1955; Rosenbrock, 1960, 1962]. More recently, during the past fifteen years, several attempts have been made to identify the conditions under which multiple solutions are not possible. In one of the first papers, Doherty and Perkins (1982) use residue-curve maps and linear-stability analysis to show that binary, homogeneous, multistage distillations have a unique steady-state solution under CMO. Then, using classic fixed-point theory, Sridhar and Lucia (1989) relaxed the CMO conditions and proved the uniqueness of solutions for binary distillations involving homogeneous mixtures at equilibrium, and at either specified temperature and pressure (T,P) profiles, or heat duty and pressure (Q,P) profiles, or reflux ratio, bottoms flow rate, and pressure (R,B,P) profiles. Subsequently, they extended their results to apply for homogeneous multicomponent mixtures (Sridhar and Lucia, 1990), but only for the (T,P) specification. Their analysis was extended for many other specifications by Lucia and Li (1992). Most recently, when examining several specifications, Li (1994) has shown that multiple solutions can exist when the (Q,P) profiles are specified even for ideal mixtures.

It is especially noteworthy that Sridhar and Lucia (1989) show liquid-phase homogeneity to be a *necessary* condition for solution uniqueness in binary and multicomponent, multistage separation processes for the specifications they studied. Thus far, the conditions under which heterogeneous columns have unique solutions have not been determined.

Simulation. To our knowledge, Magnussen et al. (1979) were the first to publish three steady-state profiles for a given set of specifications. Their simulations involve a tower to dehydrate ethanol using benzene as an entrainer. Since then, multiple steady states have been computed for the dehydration of several alcohol–water mixtures (Prokopakis et al., 1981; Kovach and Seider, 1987b; Venkataraman and Lucia, 1988; Kingsley and Lucia, 1988; Widagdo et al., 1989; Rovaglio and Doherty, 1990; Cairns and Furzer, 1990c; Laroche et al., 1992b; Bekiaris et al., 1993; Gani and Jørgensen, 1994). It is noteworthy that multiple steady states have also been computed for interlinked-distillation columns by Chavez et al. (1986) and Lin et al. (1987). In fact, multiple steady states have been computed for distillation towers involving ideal liquid phases and assuming CMO when the liquid reflux and vapor boilup (LV) are specified as mass, rather than molar, flow rates (Jacobsen and Skogestad, 1991). The latter effect is due to the nonlinear relationship between the mass and molar flow rates.

It is of special note that Laroche et al. (1992b) computed multiple steady states, assuming CMO, in homogeneous distillation columns that separate ternary, nonideal mixtures operated with large recirculation rates, because this led Bekiaris et al. (1994a) to investigate steady-state multiplicity in infinitely long columns at total reflux (∞/∞). The latter authors show how to identify the ranges of the distillate flow rate, for a fixed feed rate, in which multiple steady states exist without repeatedly solving the MESH equations. Instead, they use residue curves to approximate the limit of operation at total reflux, as described in the paragraphs that follow. Note that since the distillation lines are the operating lines at total reflux, distillation-line maps replace the residue-curve maps in this discussion.

For the other limit of infinite stages, it helps to recall that the operating lines can contain pinch points at the compositions of the azeotropes, the pure species, or the feed, as discussed in the section on Column Design. Consequently, there are just three types of distillation lines, as shown by Bekiaris et al. (1994a), for a ternary mixture with a minimum-boiling azeotrope between the light (L) and the heavy (H) species (Class 001). There are four pinch points, three at the pure-species vertices and one at the minimum-boiling azeotrope, as shown in Figure 39. Type I distillation lines have the distillate positioned at the composition of the minimum-boiling azeotrope ($\underline{x}_D = \underline{x}_A$, in Figure 39a–c), whereas Type II distillation lines have the bottoms product positioned at the heavy-species vertex ($\underline{x}_B = \underline{x}_H$, in Figure 39g–i). The remaining distillation lines, of Type III, follow the edges of the distillation-line map and include the intermediate-species vertex (I in Figure 38d–39f).

To locate the ranges of the distillate flow rate in which multiple steady states exist, Bekiaris et al. (1994a) *sketch* the distillate mole fraction as a function of the distillate flow rate,

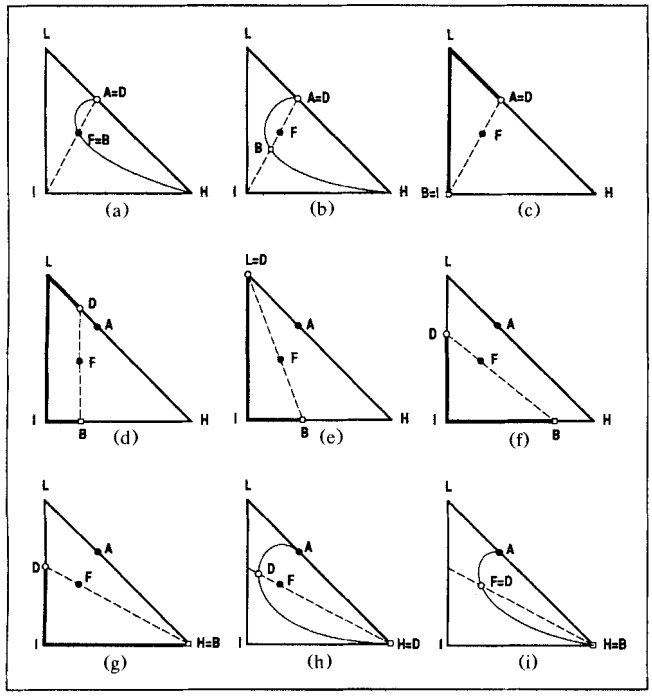

Figure 39. Concentration profiles for infinitely long columns at total reflux.

The solid curves are distillation lines and the dashed lines are overall mass-balance lines.

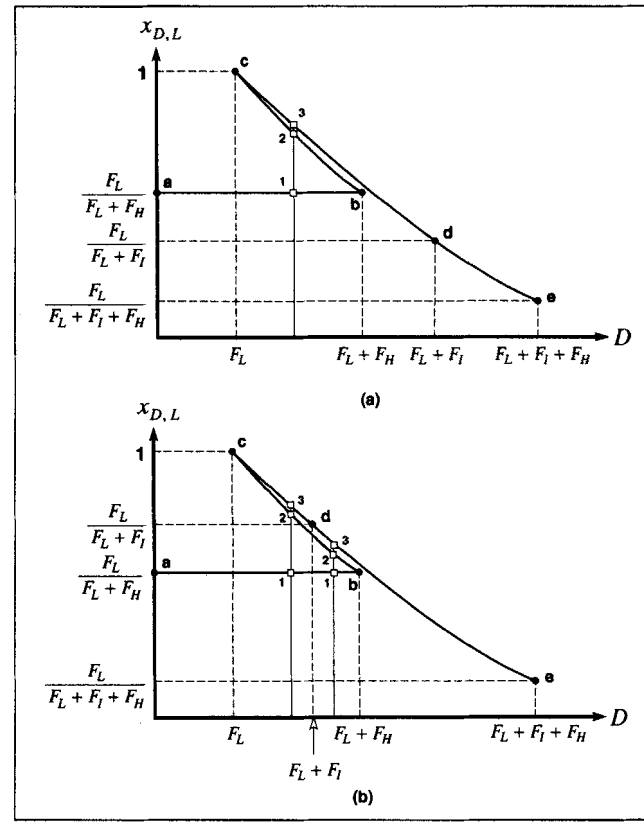

Figure 40. Mole fractions of the light species in the distillate as the distillate flow rate varies in an infinitely long column at total reflux for ternary mixtures of class 001: (a) $F_H < F_I$; (b) $F_H > F_I$.

using the distillation-line maps in Figure 39. When the feed composition is colinear with the azeotrope and species I, all of the diagrams in Figure 39 apply, and hence, such a feed composition is selected. Furthermore, F_L, F_I, F_H, and F are the flow rates of L, I, and H, in the feed and the total flow rate, respectively. The analysis begins with $\underline{x}_D = \underline{x}_A$ and $D = 0$, $B = F$ and $\underline{x}_B = \underline{x}_F$, as shown in Figure 39a, and $x_{D,L} = F_L/(F_L + F_H)$ at point a in Figure 40. As $\underline{x}_B$ moves toward I, on AI in Figure 39b, D increases to $F_L + F_H$, but $\underline{x}_D$ remains unchanged. This transition is shown as line ab on Figure 40. Note that at b, $D = F_L + F_H$ and the distillation line traces along the ALI edges of Figure 39c. As the overall mass-balance line rotates counterclockwise, $\underline{x}_D$ leaves $\underline{x}_A$ and approaches the vertex of species L, while $\underline{x}_B$ moves along the IH edge toward the vertex of species H, as shown in Figure 39d. As $x_{D,L}$ increases to unity along the curve bc in Figure 40, D decreases from $F_L + F_H$ to F_L. As $\underline{x}_D$ continues toward the vertex of species I, along the LI edge, D increases from F_L to $F_L + F_I$, and $x_{D,L}$ decreases from unity to $F_L/(F_L + F_I)$ along the curve cd in Figure 40. Note that curves bc and cde coincide, but are separated in the drawing to show that they coexist. At point d, the bottoms product is at the vertex of species H, as shown in Figure 39g. Next, $\underline{x}_D$ is moved toward $\underline{x}_F$ along DH, with D increasing to $F = F_L + F_I + F_H$, as illustrated in Figure 39h, and $x_{D,L}$ decreases to $x_{F,L}$ along the curve de in Figure 40.

In Figure 40, for $F_L < D < F_L + F_H$, three steady-state solutions of Types I, II, and III are shown. When $F_H < F_I$, d is lower than b, and one solution of Type I and two solutions of Type II exist, as illustrated in Figure 40a. Alternatively, when $F_H > F_I$, for $F_L < D < F_L + F_I$, similar steady-state solutions are obtained. However, for $F_L + F_I < D < F_L + F_H$, steady-state solutions of Types I, II, and III coexist, as illustrated in Figure 40b.

To validate these sketches, Bekiaris et al. (1994a) solved the MESH equations for a 44-tray column to separate acetone and heptane with benzene as the entrainer (Class 001). Three steady-state solutions were computed for reflux ratios as low as four when the distillate flow rate was varied. Hence, they conjecture that multiple solutions persist as the number of trays and the reflux rate are reduced, but this conjecture needs to be studied more carefully. It is also noted that they applied this methodology for ternary mixtures, capable of splitting into two liquid phases, with distillation boundaries (Bekiaris et al., 1994b).

For towers involving nonideal solutions, capable of splitting into two liquid phases, multiple steady states are difficult to compute and explain. In one study, Rovaglio et al. (1992) claim that the source of multiplicity is due to the extreme sensitivity of the temperature and concentration fronts to changes in the operating variables, such as the reflux and boilup rates, as well as convergence criteria that are not sufficiently tight. Gani and Jørgensen (1994) computed as many as ten solutions for a column to dehydrate ethanol with benzene as an entrainer, but they do not indicate their convergence tolerance and do not provide sufficient evidence that the solutions are fully converged. Because of this extreme

sensitivity, in a tower to dehydrate sec-butyl alcohol with disec butyl ether as the entrainer, Kovach (1986), Kovach and Seider (1987a,b; 1988) and Widagdo et al. (1989) used a very tight tolerance, 10^{-14}, on the L_2-norm of the residuals of the MESH equations. Similarly, Lucia et al. (1990) used a tolerance of 10^{-9}. In summary, to avoid spurious solutions, very tight convergence tolerances are required.

For homogeneous towers, it is important to check that multiple solutions are not due to the inadequacy of the phase stability test. In this regard, Kingsley and Lucia (1988) and Widagdo et al. (1989, 1992) show that in place of stable three-phase (VLL) solutions, multiple two-phase (VL) solutions are often computed, each of which is unstable. Furthermore, Cairns and Furzer (1990c) show, for the dehydration of ethanol with 2,2,4-trimethylpentane, that spurious solutions are computed when the second liquid phase is not modeled. In many towers, stability analysis must be performed very carefully to properly solve the MESH equations.

For mass-transfer models, Kienle and Marquardt (1991) consider either rectification or stripping sections in multicomponent distillation. Assuming an infinitely long section, with fixed boundary conditions at both ends, they show an infinite number of steady-state solutions. Using nonlinear wave theory (Hwang and Helfferich, 1989a,b; 1990), Helfferich (1993) studied the steady-state multiplicity in a column with fixed conditions at both ends. It is shown that steady-state multiplicity depends on the column length, from finite to infinite, and the mass-transfer rates. Multiplicity, involving an infinite number of steady states, is demonstrated for finite-length columns with infinite mass-transfer rates, as well as for infinitely long columns with infinite or finite mass-transfer rates, but not for columns of finite length with finite mass-transfer rates. Furthermore, it is conjectured that multiplicity requires rather unusual mass-transfer behavior. When the approach to a unique steady state is extremely slow, it could be interpreted mistakenly as a slow transition through an infinite number of steady-state solutions.

In summary, because the convergence tolerances are often not sufficiently well documented, the number of solutions to the models of multistage, multicomponent azeotropic distillation towers are often difficult to interpret. These need to be verified, preferably using a Newton-based method, with adequate precision (at least double precision) and sufficiently tight convergence tolerances. Additional research, combining experiments, theoretical analysis, and simulation results that are verified more carefully, can be expected to improve the design, control, and operation of these towers.

Dynamic Simulation. The rapid increase in computer power, coupled with the development of stiff integrators and methods for circumventing the singularities in high-index differential/algebraic systems, have stimulated more activity in the dynamic simulation of azeotropic distillation towers. These simulations are gaining importance in the startup and control of continuous towers and in the operation of batch distillations.

Prokopakis and Seider (1983b) were among the first to simulate the dynamics of azeotropic distillation towers. They used the Ballard and Brosilow (1978) formulation of the MESH equations and carried out the integration using a semi-implicit Runge-Kutta method. Far more comprehensive models were developed by Gani et al. (1986a,b), Cameron et al. (1986), and Gani and Cameron (1989) to represent the tray and downcomer hydraulics, flooding, entrainment, and weeping. The hydraulics effects, especially, are shown to be crucial in the development of models for the dynamics of startup and shut-down operations (Ruiz et al., 1988). To obtain steady-state solutions, when the MESH equations are difficult to solve (e.g., when simulating azeotropic distillations), Gani and Cameron (1989) integrate the dynamic models. This approach requires excessive computations, and in this respect, is similar to the homotopy-continuation methods (Allgower and Georg, 1980; Wayburn and Seader, 1984; Byrne and Baird, 1985) discussed previously.

Most of the dynamic models of distillation columns involve two assumptions: negligible vapor holdup and constant pressure. Choe and Luyben (1987) demonstrate that these assumptions lead to erroneous predictions of the dynamic responses for towers operated at high pressures (greater than 10 atm) and at low pressures (vacuum towers).

The inclusion of tray hydraulics in a dynamic model allows the tray pressure to be computed using the following relations:

$$U_j = f\{L_j, V_j, \text{tray geometry}\} \tag{45}$$

$$P_j = P_{j+1} + \Delta P_{j+1}\{L_j, V_j, \text{tray geometry}\} \tag{46}$$

where U_j is the holdup on tray j; L_j and V_j are the liquid and vapor flow rates leaving tray j; and P_j and P_{j+1} are the pressures on trays j and $j+1$, respectively. Recently, Flatby et al. (1994) proposed a model that incorporates these equations and a new algorithm to solve the phase equilibria on each tray, given the volume, composition, and internal energy of the holdup (i.e., performs a so-called UV-flash calculation). It is assumed that the liquid and vapor holdups are perfectly mixed, the two phases are at equilibrium, and heat losses through the column walls are negligible. In addition, flooding, weeping, and liquid–vapor entrainment are not considered. In this model, the MESH equations on tray j include:

Material Balances:

$$\frac{d}{dt}(u_{s,j}) = V_{j-1}y_{s,j-1} + L_{j+1}x_{s,j+1} - V_j y_{s,j} - L_j x_{s,j} + F_j z_{s,j}$$

$$s = 1, \ldots, N_s;\ j = 1, \ldots, N_t. \tag{47}$$

Energy Balance:

$$\frac{d}{dt}(E_j) = V_{j-1}h^V_{j-1} + L_{j+1}h^L_{j+1} - V_j h^V_j - L_j h^V_j + F_j h^F_j$$

$$j = 1, \ldots, N_t. \tag{48}$$

Vapor/Liquid Equilibria (UV-Flash):

$$(E_j, V_{tj}, u_{s,j}) \rightarrow (T_j, P_j, \nu, \underline{x}, \underline{y})$$

$$s = 1, \ldots, N_s;\ j = 1, \ldots, N_t. \tag{49}$$

Tray Hydraulics:

$$V_j = f_V\{P_j - P_{j+1}, U_{j+1}, \text{tray geometry}\} \qquad j = 1, \ldots, N_t \tag{50a}$$

$$L_j = f_L\{P_j - P_{j-1}, U_j, V_{j-1}, \text{tray geometry}\} \quad j = 1, \ldots, N_t. \tag{50b}$$

Given the initial conditions for the state variables (species molar holdups, $\underline{u}_j$, and the internal energy holdup, E_j), Eqs. 47 and 48 are integrated across a time step, Δt. Then, at $\underline{u}_j\{t + \Delta t\}$, $E_j\{t + \Delta t\}$, and tray volume, V_{tj}, the so-called flash equations, Eqs. 49, are solved for the tray temperature, T_j, tray pressure, P_j, vapor fraction, ν, and the mole fractions in the liquid and vapor phases, $\underline{x}_j$ and $\underline{y}_j$, respectively. Finally, Eqs. 50a and b are solved for V_j and L_j. Although promising, the sensitivity of V_j to $P_j - P_{j+1}$ causes the algorithm to slow, or even have difficulty converging, especially for towers that separate nonideal mixtures.

Heterogeneous azeotropic distillation

Many azeotropic mixtures of industrial importance are separated using entrainers that form heterogeneous azeotropes with the species to be separated; for example, in the dehydration of alcohols, benzene is introduced to dehydrate ethanol, isopropylether to dehydrate isopropanol, and disec-butylether (DSBE) to dehydrate sec-butyl-alcohol (SBA). Similarly, mesityl oxide (MSO) is introduced to dehydrate chloroform, toluene to dehydrate formic and acetic acids, and many others. In one study, Cairns and Furzer (1990a) present experimental concentration and temperature profiles, accompanied by theoretical results, for the dehydration of ethanol with an 11-component alkylate mixture at total reflux. Also, Herfurth et al. (1987) present experimental temperature profiles, at finite reflux, for a column to dehydrate ethanol with cyclohexane.

Tower Characteristics. The steady-state behavior of heterogeneous azeotropic distillations has been studied extensively. Many algorithms to solve the MESH equations, involving vapor–liquid–liquid equilibria, have been proposed (Block and Hegner, 1976; Ross and Seider, 1980; Ferraris and Morbidelli, 1981; Kovach and Seider, 1987a,b; Swartz and Stewart, 1987; Baden and Michelsen, 1987; Cairns and Furzer, 1990a,b). Most of these algorithms solve the MESH equations simultaneously using a modified Newton–Raphson method, with the exception of the algorithms by Kovach and Seider (1987b) and Swartz and Stewart (1987). The former use a homotopy-continuation method and the latter use a collocation method to integrate the MESH equations expressed in terms of a continuous distance coordinate (see Eqs. 18 and 19). Furthermore, it is noteworthy that most of these studies involve ternary mixtures with one partially miscible binary pair, usually ethanol, benzene, and water.

Since most entrainers are partially miscible with at least one of the species in the mixture, the overhead vapor, when cooled, condenses into two liquid phases. Normally, the heavy phase is decanted (withdrawn as product) and the lighter (entrainer) phase is returned to the tower as reflux. Often, a portion of the heavy phase is used to control the operation of these towers, and consequently, liquid-phase splitting is not limited to the decanter, but extends into the rectifying and even the stripping sections (Kovach and Seider, 1987a).

For these reasons, the models for heterogeneous towers must reliably and efficiently detect liquid-phase splitting. The tangent-plane distance criterion, formulated by Gibbs

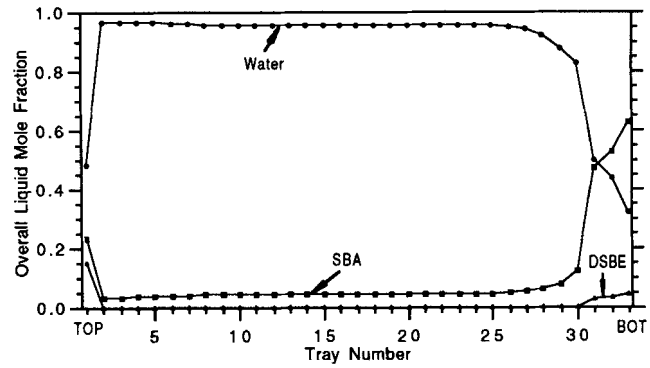

Figure 41. Profiles of overall liquid mole fractions at $R_{aqueous} = 0.2$.

(1873a,b), suggested by Baker et al. (1981), and implemented by Michelsen (1982a,b, 1984, 1986), is very reliable. However, for the simulation of heterogeneous towers, only Baden and Michelsen (1987), Cairns and Furzer (1990b), and Widagdo et al. (1992) employ this test.

Heterogeneous azeotropic towers have one or more steep temperature and concentration fronts, especially at the interfaces between trays having one and two liquid phase(s), whose positions are extremely sensitive to the reflux rates (Kovach and Seider, 1987a,b; Widagdo et al., 1989). Since this extreme sensitivity can lead to convergence problems, especially with the Newton-based methods, global convergence methods, such as the homotopy-continuation methods (Kovach and Seider, 1987b) have been more successful.

Like homogeneous azeotropic towers, heterogeneous towers exhibit a maximum separation. For a tower to dehydrate sec-butanol using disec-butyl ether, Widagdo et al. (1989) observed a sharp decrease in the purity of sec-butanol in the bottoms product as the aqueous reflux ratio exceeds a *critical* value, as shown in Figure 13. This occurs when the concentration fronts, at the interface between trays having one and two liquid phase(s), reach the bottom of the tower. Figure 41 shows the steep fronts at the bottom of the tower, when the reflux ratio exceeds the critical value.

Dynamic Simulation. For heterogeneous towers, several algorithms have been developed for dynamic simulation (Rovaglio and Doherty, 1990; Wong et al., 1991; Widagdo et al., 1992). As the *differential-algebraic* equations (DAEs) are integrated, the system index can exceed unity, with the Jacobian matrix of the algebraic equations becoming singular. This is especially a problem in heterogeneous towers as the interface between trays having one and two liquid phase(s) moves in response to disturbances. Hence, in the next subsection, the *index* is defined and examples are presented to show how higher-index DAEs arise.

Index of Differential-Algebraic Equations. Most dynamic models for distillation towers comprised ordinary differential and nonlinear equations (NLE), involving algebraic and transcendental terms:

$$\underline{F}\{\dot{\underline{x}}, \underline{x}, \underline{y}; t\} = 0 \qquad \underline{x}\{0\} = \underline{x}_0, \ \dot{\underline{x}}\{0\} = \dot{\underline{x}}_0 \tag{51a}$$

$$\underline{G}\{\underline{x}, \underline{y}; t\} = 0 \qquad \underline{y}\{0\} = \underline{y}_0, \ \dot{\underline{y}}\{0\} = \dot{\underline{y}}_0. \tag{51b}$$

The n ODEs are expressed as a function of n state variables,

$\underline{x}$, and the m NLEs involve m variables, $\underline{y}$, often referred to as *algebraic* variables. Equations 51a are typically the material and energy balances and Eqs. 51b are often the equations for phase equilibrium, tray hydraulics, and design specifications. For a system of DAEs, first derivatives of the state and algebraic variables are required; these are $\dot{\underline{x}}\{0\} = \dot{\underline{y}}\{0\} = 0$ when starting from a steady-state solution. The index of a system of DAEs is the number of differentiations of Eqs. 51, with respect to time, required to convert the system to ODEs. When $\underline{G}_{\underline{y}}$ is not invertible (singular), the index exceeds unity and Eqs. 51b cannot be solved. Note that the index of a system of DAEs can be viewed as a measure of the coupling between the ODEs and NLEs. The solution of Eqs. 51a lies on the manifold of Eqs. 51b (Rheinboldt, 1987), and the ODEs are often said to be constrained or on a manifold. When the index exceeds unity, consistent initialization is difficult to provide and errors in the algebraic variables are difficult to estimate. These topics, and many others, are covered by Pantelides et al. (1988), Gear (1988), Bachmann et al. (1989), Brennan et al. (1989), and Gani and Cameron (1992).

Pantelides et al. (1988) show that the index depends on the model formulation and the selection of the design specifications. For example, in a distillation tower, the index is two when the overhead pressure is specified. It becomes $N_t + 1$ when the bottoms pressure is specified, where N_t is the number of stages. Also, since the heat duty is an algebraic variable that appears only in the ODEs (energy balances), a higher-index system is obtained when the heat duties are not specified.

Model Formulation. To our knowledge, in all of the models for the dynamics of heterogeneous towers, phase equilibria have been assumed, with one recent exception; a mass-transfer model by Kooijman and Taylor (1995).

Consider first the work of Rovaglio and Doherty (1990) who studied the dynamics of towers to dehydrate ethanol with benzene as an entrainer. In their analysis, the pressure profile is computed using an equation to represent the tray hydraulics (Eq. 46) and the liquid phases are tested for instability, rather than the total holdup on each tray. Their results focus on the existence of three steady-state attractors. In response to a 10% increase in the feed flow rate, a shift from steady operation, through an intermediate, unstable steady state, to a third steady state, is shown.

Wong et al. (1991) extend the Ballard and Brosilow (1978) formulation, used by Prokopakis and Seider (1983b). They use the overall equilibrium constant, $\bar{K}$, introduced by Niedzwiecki et al. (1980) and employed by Schuil and Bool (1985), for the simulation of three-phase flash and distillation units:

$$\bar{K}^{-1} = \alpha(K')^{-1} + (1-\alpha)(K'')^{-1}, \tag{52}$$

where α is the fraction of the first liquid phase in the liquid holdup on each tray. In terms of $\bar{K}$, the material balances become

$$\frac{d\left(\bar{M}_j \bar{x}_{s,j}\right)}{dt} = \bar{L}_{j-1}\bar{x}_{s,j-1} - \left(\bar{L}_j + \bar{K}_{s,j}V_j\right)\bar{x}_{s,j} + \left(\bar{K}_{s,j+1}V_{j+1}\right)\bar{x}_{s,j+1} + F_j z_{s,j}, \tag{53}$$

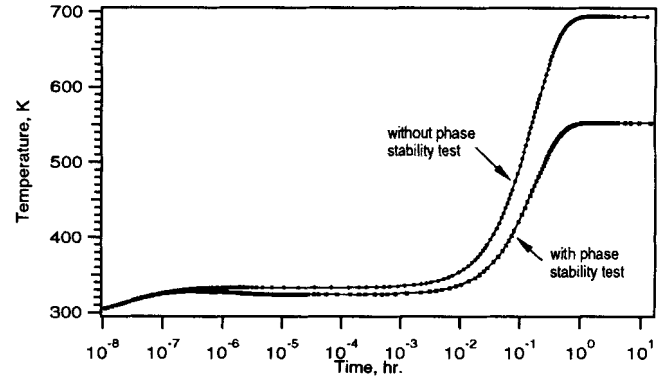

Figure 42. Effect of phase stability test on the dynamic response of a cooled VL-separator.

where $\bar{M}_j$ is the total liquid holdup, $\bar{L}_j$ is the total flow rate of the two liquid phases leaving tray j, and $\bar{x}_{s,j}$ is the total liquid mole fraction of species s on tray j. In their model, the pressure profile is specified and the Francis weir formula represents the tray hydraulics. Through the use of *overall* liquid properties, they easily adapt an algorithm for the simulation of homogeneous towers to simulate heterogeneous towers. Results are presented that show the dynamic responses to changes in the feed flow rate and composition, aqueous reflux ratio, reboiler duty, and entrainer makeup rate for towers to dehydrate ethanol with benzene. The purity of ethanol in the bottoms product is controlled by measuring the temperature on a tray in the stripping section and manipulating the aqueous reflux rate using a proportional-integral (PI) controller.

In an alternate approach, Widagdo et al. (1992) develop an index-one extension of the Naphtali-Sandholm (1971) formulation with a consistent initialization procedure. The tangent-plane distance criterion (Michelsen, 1982a) is implemented to test the stability of the phase distribution for the total holdup on each tray. The MESH equations are integrated using the backward-difference formulas (BDFs) (Gear, 1971) implemented in DASSL (Petzold, 1982a,b), an index-1 DAE solver. To permit the identification of the real bifurcation points at phase transitions, DASSL is modified, as discussed below.

Consider a vapor–liquid separator, subjected to a 50 kcal/h step decrease in heat duty. Figure 42 shows two responses, obtained with and without the phase stability test. When the phase stability test is off, although the MESH equations contain the variables and terms associated with two liquid phases, a VL branch is computed. However, when the phase stability test is implemented properly, a second liquid phase is born, as illustrated using a magnified scale in Figure 43. To track the proper branch, it is important to accurately test for phase instability as the integration progresses. In Figure 43, the VL phases are stable until point A is reached. As the temperature changes, the second liquid phase forms, with VLL phases along branch AB. The algorithm correctly locates the VL–VLL transition point A and the initialization algorithm computes the initial slope of the branch AB. At point B, the vapor is depleted, leaving stable LL phases. The phase stability algorithm detects this change, and the branch-switching algorithm locates point B and computes the initial slope of

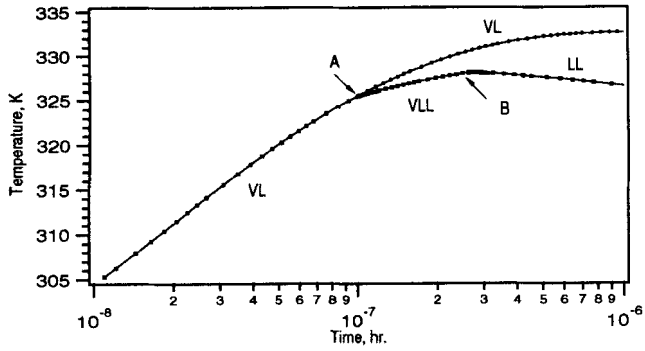

Figure 43. Phase changes in a cooled VL-separator.

the LL branch. The existence of real bifurcation points at phase transitions, such as A and B, was first observed by Kingsley and Lucia (1988) when finding the optimal operating conditions for three-phase distillation towers.

Widagdo et al. (1992) tested their model and algorithm for the dehydrations of ethanol using benzene and sec-butyl alcohol using disec-butyl ether. The latter system exhibits two partially miscible binary pairs and a minimum-boiling ternary azeotrope. Unlike for the ethanol–benzene–water system, the phase diagram at 363.2 K and 1.17 atm has two VLL regions, separated by a vapor envelope, as shown in Figure 44. These conditions are computed for tray 28 of a 33-tray tower. At the conditions of tray 2 (361.5 K and 1.14 atm), Figure 45 shows that, as the heterogeneous ternary azeotrope is approached, the vapor envelope becomes negligible, separating two thin VLL regions. Hence, to locate the second liquid phase on the top tray, the phase stability test must be implemented very carefully; that is, the transition between VL and VLL phase distributions must be located accurately to avoid cycling (instability of the VL phase distribution, introduction of a second liquid phase, and disappearance of the phase during integration of the MESH equations).

As an alternate approach, Lucia and Wang (1993) introduced complex variables when carrying out the integrations of process models in the vicinity of phase transitions. Although the advantages of their approach are presented for a flash vessel in the retrograde region, the extension to heterogeneous distillations remains to be demonstrated. In principle, the extension should be routine, although the number of elements in the Jacobian matrix increases by a factor of 4. It remains to compare the reliability and efficiency of these two approaches.

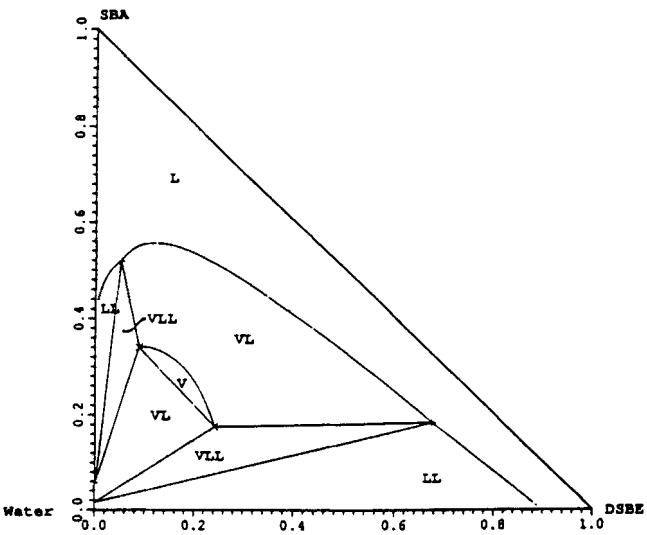

Figure 44. Phase diagram of the SBA–DSBE–water system at 363.2 K and 1.17 atm.

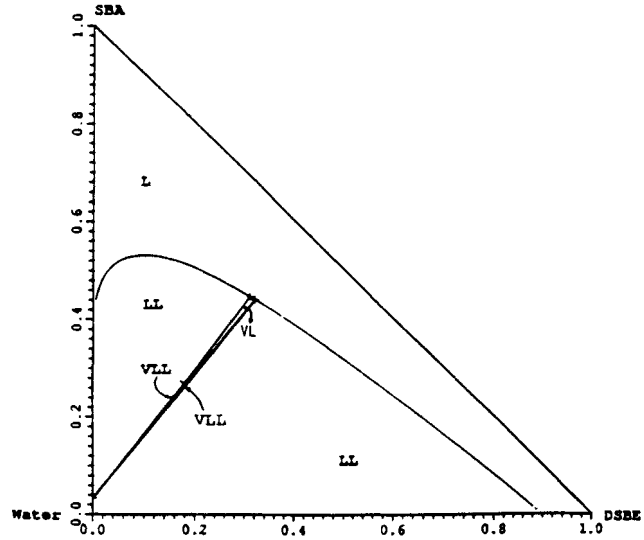

Figure 45. Phase diagram of the SBA–DSBE–water system at 361.5 K and 1.14 atm.

Finally, Widagdo et al. (1992) showed that a 12-tray tower to dehydrate sec-butanol exhibits a stable focus in response to a 2% decrease in the reboiler duty. The flow rates, temperatures, and compositions oscillate in their approach to the steady state, as illustrated in Figure 46. These correspond to oscillations in the phase distributions on trays 2 to 4, as illustrated in Figure 47.

In summary, it is important to accurately compute the phase distributions when performing dynamic simulations for heterogeneous azeotropic distillations. Although much progress has been made, these algorithms should be tested for the separation of additional mixtures of industrial importance. Furthermore, experimental data are sorely needed to verify the results of the simulations.

Column Control

A rich literature exists on the control of distillation towers. Two books (Shinskey, 1984; Luyben, 1992) are particularly noteworthy for the breadth and depth of their coverage. In addition, two articles are noteworthy for their emphasis on strategies for the selection of control configurations (Skogestad and Morari, 1987; Skogestad et al., 1990).

As mentioned earlier, azeotropic distillation towers present special control challenges due to the sensitive movements of their temperature and concentration fronts in response to small disturbances, such as in the feed rate and composition, reflux rate and boilup rate. These towers are characterized by multiple regimes of operation and, in some cases, their models exhibit multiple steady states. Hence, it

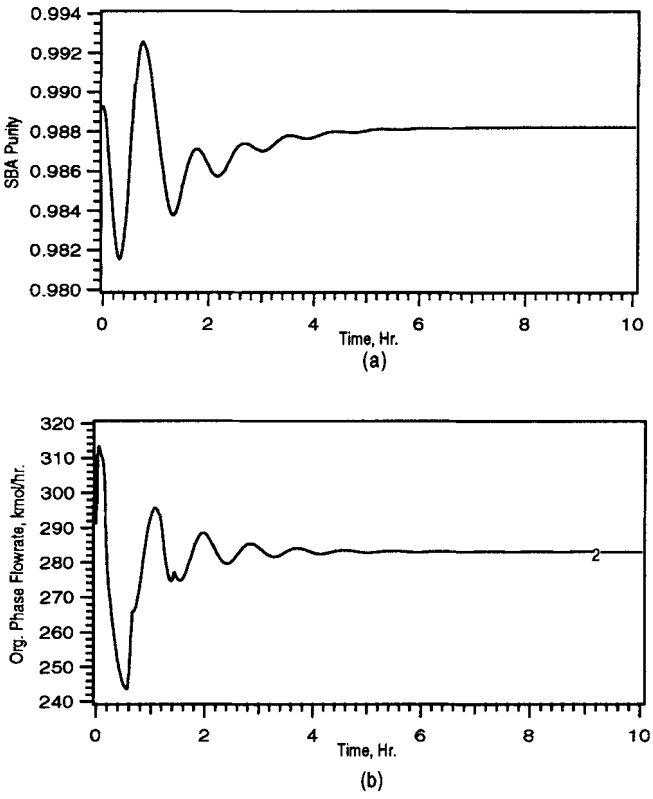

Figure 46. Dynamic response of a 12-tray tower to dehydrate sec-butanol to a 2% decrease in the reboiler duty: (a) mole fraction of SBA in the bottoms product; (b) flow rate of the organic phase on tray 2.

can be more difficult to maintain the desired product purities in response to these kinds of disturbances, many of which are unmeasured.

In this section, several chapters of books and articles devoted to the control of these more complex distillation operations are reviewed. One of the first, Chap. 10 of *Distillation Control for Productivity and Energy Conservation* by Shinskey (1984), concentrates on the operation of three common configurations for heterogeneous azeotropic distillations and a

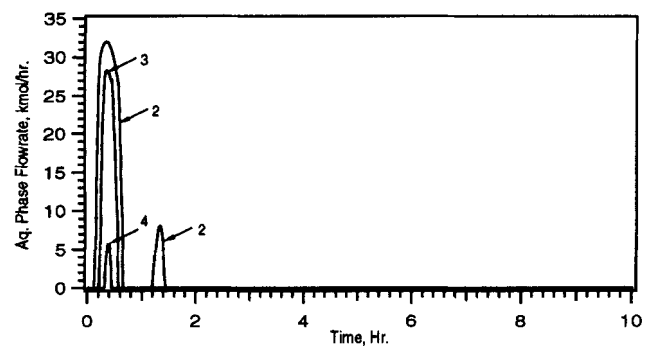

Figure 47. Aqueous phase flow rates on trays 2 to 4 after a 2% decrease in the reboiler duty; stage numbers are annotated.

common configuration for the separation of pressure-sensitive homogeneous azeotropes. Emphasis is placed on the open-loop relationships, principally the material and energy balances, between the desired outputs and the manipulated inputs. A key input is considered to be the ratio of the hydrocarbon reflux to the water reflux in a dehydration column.

Several articles by Gilles and coworkers were among the first to concentrate on the preparation of reduced-order models for the control of extractive distillations. The earliest, by Gilles et al. (1980), considers the dehydration of isopropanol using ethylene glycol. Emphasis is placed on the ability of a simplified dynamic model to track the movement of the steep temperature front in response to a step decrease in the feed rate. The article proposes the installation of additional thermocouples and an improved PI control algorithm that adjusts the steam flow rate due to deviations in the position of the temperature front from that at the desired set point. In addition, the deviations of two observed variables are monitored and utilized in the PI controller when the deviations in the position of temperature front are saturated; that is, when the temperature difference between adjacent trays become small. Subsequent articles extend this methodology for towers in which the alcohol and entrainer are removed in the distillate and bottoms product, respectively, and water vapor is removed as a sidedraw (Gilles and Retzbach, 1983; Retzbach, 1986). In a more recent article, step-response tests are used to linearize the process model, transfer functions are derived between the temperature outputs and the manipulated inputs, and various configurations are evaluated for multiple-input, multiple-output (MIMO) control (Lang and Gilles, 1989). Care is taken to select weighting coefficients and controller configurations that are effective even when the manipulated variables become saturated.

As discussed in the section on Column Performance, Laroche et al. (1992b) show highly nonlinear behavior in the region close to the minimum feed rate of the entrainer for homogeneous azeotropic distillations. In a related article, Jacobsen et al. (1991) show that, in the highly sensitive region, by concentrating on the high-frequency (initial response) of the process, it is possible to obtain tight and robust control with simple, single-loop PI controllers. Furthermore, they obtain controller performances that are comparable to those achieved for simple, zeotropic distillations. To avoid a reduction of the entrainer flow rate below the minimum, E_{min}, a feedforward controller is proposed.

For heterogeneous azeotropic distillations, Rovaglio and coworkers have prepared several articles that study the dynamics and control systems. First, as discussed in the section on Column Performance, Rovaglio and Doherty (1990) present a dynamic model and examine its performance for towers to dehydrate ethanol using benzene. Then, in closely related articles, Rovaglio et al. (1990a) present a feedforward control strategy, which is shown to be effective in an experimental tower, and Rovaglio et al. (1990b) describe the dynamic models and their implementation in the DYCODIS program. The latter provides facilities to examine the dynamic interactions between control loops, the dynamic responses with large time delays, and the stability of steady-state solutions, where multiple steady states exist. More recently, Rovaglio et al. (1993) demonstrated the importance of controlling the entrainer inventory for the smooth operation of

these towers, especially when multiple steady states exist. They show that, for the dehydration of ethanol with benzene, each steady state has a unique entrainer inventory. Different control schemes are compared and it is shown that, to control the ethanol purity in the bottoms product, it is preferable to adjust the benzene makeup rate to give a specified ratio of benzene/water in the tower inventory rather than to adjust the heat duty to give a specified tray temperature.

Concluding Remarks

Over the past two decades, we have witnessed a dramatic improvement in the methodologies for the synthesis, analysis, design, and control of azeotropic distillation processes. Much has been accomplished through the use of nonlinear analysis, such as bifurcation theory, to explain many of the nonlinear effects, and to produce new methodologies for the synthesis of sequences of azeotropic distillation towers and for the design of the individual towers. Despite progress in the development of less conventional separations, such as membrane and adsorption processes, distillation towers are likely to continue to be widely used for decades to come, taking advantage of many of the advances described herein. Many challenges remain to seek improvements in column performance through the development of new design, operation, and control strategies. In this article, an attempt has been made to review and clarify the important advances, over the past two decades. Emphasis is placed on the unresolved issues most likely to be addressed in the immediate future.

In the synthesis of separation trains, and their operation, key questions concern the role of the distillation boundaries, especially when the entrainer/feed ratio moves the operating lines closer to these boundaries. Strategies for bounding the product compositions, when operating at finite reflux ratios, need to be clarified and refined, especially for systems involving four or more species. Much remains to be resolved in the application of heuristics and algorithmic methods when synthesizing separation trains, especially those involving highly nonideal, azeotropic mixtures.

In the analysis and simulation of azeotropic towers, work is needed to clarify the sources of steady-state multiplicity and, especially, to show experimentally that it exists. Uniqueness conditions, comparable to those developed for homogeneous distillations, need to be developed for heterogeneous distillations. For the latter, especially during dynamic simulations, it may be possible to affect smoother phase transitions through the use of complex variables and operations. This procedure needs to be further developed and compared with recent strategies to locate real bifurcation points and to initiate new branches in the solution diagrams. In this regard, the homotopy-continuation method to locate all of the azeotropes in multicomponent mixtures needs to be evaluated to determine its effectiveness in locating all of the real bifurcation points and in initiating the new solution branches.

Acknowledgments

Professor Philip C. Wankat provided the impetus and recurring reminders throughout the five years over which this article was in preparation. His encouragement is very much appreciated. Partial funding providing by the Computer Integrated Engineering Program of the NSF under grant No. DDM-9114080 is gratefully acknowledged.

Programs and Sources

AUTO = bifurcation analysis of autonomous ODEs; E. Doedel, Concordia University
ASPEN PLUS = Advanced System for Process Engineering; Aspen Technology, Inc.
CHEMSIM = distillation column simulation; M. Morari, California Institute of Technology
DASSL = Differential/Algebraic Simulation System Language; L. Petzold, Lawrence Livermore Laboratory
DYCODIS = Dynamics and Control of Continuous Distillation System; M. Rovaglio, Politecnico di Milano
MAYFLOWER = program for synthesis of separation trains; M. F. Malone and M. F. Doherty, University of Massachusetts
RADFRAC = multicomponent distillation; Aspen Technology, Inc.

Literature Cited

Acrivos, A., and N. R. Amundson, "Applications of Matrix Mathematics to Chemical Engineering Problems," *Ind. Eng. Chem.*, **47**, 1533 (1955).

Allgower, E., and K. Georg, "Simplicial and Continuation Methods for Approximating Fixed Points and Solutions to Systems of Equations," *SIAM Rev.*, **22**, 28 (1980).

Andersen, H. W., L. Laroche, and M. Morari, "Effect of Design on the Control of Homogeneous Azeotropic Distillation Columns," *AIChE J.*, **30**, 1846 (1991a).

Andersen, H. W., L. Laroche, and M. Morari, "Dynamics of Homogeneous Azeotropic Distillation Columns," *Ind. Eng. Chem. Res.*, **30**, 1846 (1991b).

Andersen, H. W., L. Laroche, A. Skjellum, and M. Morari, "Distilla tion Column Simulation—Program Documentation: Version 0.3," Dept. of Chemical Engineering, California Institute of Technology, Pasadena (1989).

Andersen, T. F., and J. M. Prausnitz, "Computational Methods for High-Pressure Phase Equilibria and Other Fluid-Phase Properties Using a Partition Function: 2. Mixtures," *Ind. Eng. Chem. Proc. Des. Dev.*, **19**, 9 (1980).

Andrecovich, M. J., and A. W. Westerberg, "A Simple Synthesis Method Based on Utility Bounding for Heat-Integrated Distillation Sequence Synthesis," *AIChE J.*, **31**, 363 (1985a).

Andrecovich, M. J., and A. W. Westerberg, "A MILP Formulation for Heat-Integrated Distillation Sequence Synthesis," *AIChE J.*, **31**, 1461 (1985b).

Arnold, V. I., *Ordinary Differential Equations*, MIT Press, Cambridge, MA (1973).

Ashton, N. A., A. Arrowsmith, and C. J. Yu, "Distillation Hydraulics with Immiscible Liquids," *Inst. Chem. Eng. Symp. Ser.*, No. 104, B113 (1987).

Bachmann, R., L. Brull, and U. Pallaske, "A Contribution to the Numerical Treatment of Differential Algebraic Equations Arising in Chemical Engineering," DECHEMA Monograph, **118**, 343 (1989).

Baden, N., and M. L. Michelsen, "Computer Methods for Steady-State Simulation of Distillation Columns," *Inst. Chem. Eng. Symp. Ser.*, **104**, 425 (1987).

Baker, L. E., A. C. Pierce, and K. D. Luks, "Gibbs Energy Analysis of Phase Equilibria," SPE/DOE Second Joint Symp. on Enhanced Oil Recovery, Tulsa, OK (1981).

Ballard, D. M., and C. B. Brosilow, "Dynamic Simulation of Multicomponent Distillation Columns," AIChE Meeting, Miami (1978).

Bekiaris, N., G. A. Meski, C. M. Radu, and M. Morari, "Multiple Steady-States in Homogeneous Azeotropic Distillation," *Ind. Eng. Chem. Res.*, **32**, 2023 (1993).

Bekiaris, N., G. A. Meski, C. M. Radu, and M. Morari, "Design and Control of Homogeneous Azeotropic Distillation," *Comput. Chem. Eng.*, **18**, S15 (1994a).

Bekiaris, N., G. A. Meski, and M. Morari, "Multiple Steady States in Heterogeneous Azeotropic Distillation," Tech. Memo. No. CIT-CDS 94-012 (1994b).

Berg, L., "Selecting Agent for Distillation Processes," *Chem. Eng. Prog.*, **65**, 52 (1969).

Block, U., and B. Hegner, "Development and Application of a Simulation Model for Three-Phase Distillation," *AIChE J.*, **22**, 582 (1976).

Bolles, W. L., "The Solution of a Foam Problem," *Chem. Eng. Sci.*, **22**(9), 63 (1967).

Brenan, K. E., S. L. Campbell, and L. R. Petzold, *Numerical Solution of Initial-Value Problems in Differential-Algebraic Equations*, North-Holland, New York (1989).

Bushmakin, I. N., and I. N. Kish, "Rectification Investigations of a Ternary System Having an Azeotrope of the Saddle-Point Type," *J. Appl. Chem. USSR*, **30**, 401 (1957a).

Bushmakin, I. N., and I. N. Kish, "Separating Lines of Distillation and Rectification of Ternary Systems," *J. Appl. Chem. USSR*, **30**, 595 (1957b).

Byrne, G. D., and L. A. Baird, "Distillation Calculations Using a Locally Parameterized Continuation Method," *Comput. Chem. Eng.*, **9**, 593 (1985).

Cairns, B. P., and I. A. Furzer, "Multicomponent Three-Phase Azeotropic Distillation. 1. Extensive Experimental Data and Simulation Results," *Ind. Eng. Chem. Res.*, **29**, 1349 (1990a).

Cairns, B. P., and I. A. Furzer, "Multicomponent Three-Phase Azeotropic Distillation. 2. Phase-Stability and Phase-Splitting Algorithms," *Ind. Eng. Chem. Res.*, **29**, 1364 (1990b).

Cairns, B. P., and I. A. Furzer, "Multicomponent Three-Phase Azeotropic Distillation. 3. Modern Thermodynamic Models and Multiple Solutions," *Ind. Eng. Chem. Res.*, **29**, 1383 (1990c).

Cameron, I. T., C. A. Ruiz, and R. Gani, "A Generalized Model for Distillation Columns: II. Numerical and Computational Aspects," *Comput. Chem. Eng.*, **10**, 199 (1986).

Chavez, C. R., J. D. Seader, and T. L. Wayburn, "Multiple Steady-State Solutions for Interlinked Separation Systems," *Ind. Eng. Chem. Fund.*, **25**, 566 (1986).

Choe, Y.-S., and W. L. Luyben, "Rigorous Dynamic Models of Distillation Columns," *Ind. Eng. Chem. Res.*, **26**, 2158 (1987).

Courant, R., and H. Robbins, *What Is Mathematics?*, Oxford Univ. Press, Oxford (1978).

Davies, B., Z. Ali, and K. E. Porter, "Distillation of Systems Containing Two Liquid Phases," *AIChE J.*, **33**, 161 (1987a).

Davies, B., Z. Ali, and K. E. Porter, "Further Observations on the Transition Between the Spray and Bubbly Regimes," *Inst. Chem. Eng. Symp. Ser.*, No. 104, B541 (1987b).

Davies, B., Z. Ali, and K. E. Porter, "Spray-to-Bubbly Transition for Distillation Systems Containing Two Liquid Phases," *AIChE J.*, **37**(4), 597 (1991).

Doedel, E. J., *AUTO: Software for Continuation and Bifurcation Problems in Ordinary Differential Equations*, Computer Science Dept., Concordia Univ., Montreal, P.Q., Canada (1986).

Doherty, M. F., "A Topological Theory of Phase Diagrams for Multiphase Reacting Mixtures," *Proc. R. Soc. London A*, **430**, 669 (1990).

Doherty, M. F., and G. A. Caldarola, "Design and Synthesis of Homogeneous Azeotropic Distillation: III. The Sequencing of Columns for Azeotropic and Extractive Distillations," *Ind. Eng. Chem. Fundam.*, **24**, 474 (1985).

Doherty, M. F., and J. D. Perkins, "On the Dynamics of Distillation Processes: I. The Simple Distillation of Multicomponent Non-reacting, Homogeneous Liquid Mixtures," *Chem. Eng. Sci.*, **33**, 281 (1978a).

Doherty, M. F., and J. D. Perkins, "On the Dynamics of Distillation Processes: II. The Simple Distillation of Model Solutions," *Chem. Eng. Sci.*, **33**, 569 (1978b).

Doherty, M. F., and J. D. Perkins, "On the Dynamics of Distillation Processes: III. Topological Structure of Ternary Residue Curve Maps," *Chem. Eng. Sci.*, **34**, 1401 (1979).

Doherty, M. F., and J. D. Perkins, "On the Dynamics of Distillation Processes: VI. Uniqueness and Stability of the Steady State in Homogeneous Continuous Distillations," *Chem. Eng. Sci.*, **37**, 381 (1982).

Eliceche, A. M., and R. W. H. Sargent, "Synthesis and Design of Distillation Systems," *Inst. Chem. Eng. Symp. Ser.*, No. 61 (1981).

Fair, J. R., "Distillation: Whither, not Whether," *Inst. Chem. Eng. Symp. Ser.*, **104**, 613 (1987).

Ferraris, G. B., and M. Morbidelli, "Mathematical Modeling of Multistaged Separators with Mixtures Whose Components Have Largely Different Volatilities," *Comput. Chem. Eng.*, **6**(4), 303 (1981).

Fidkowski, Z. T., M. F. Malone, and M. F. Doherty, "Nonideal Multicomponent Distillation: Use of Bifurcation Theory for Design," *AIChE J.*, **37**, 1761 (1991).

Fidkowski, Z. T., M. F. Doherty, and M. F. Malone, "Feasibility of Separations for Distillation of Nonideal Ternary Mixtures," *AIChE J.*, **39**(8), 1303 (1993a).

Fidkowski, Z. T., M. F. Malone, and M. F. Doherty, "Computing Azeotropes in Multicomponent Mixtures," *Comput. Chem. Eng.*, **17**, 1141 (1993b).

Flatby, P., S. Skogestad, and P. Lundström, "Rigorous Dynamic Simulation of Distillation Columns Based on UV-Flash," *Proc. of ADCHEM'94, IFAC Symp.*, Kyoto, Japan (1994).

Foucher, E. R., M. F. Doherty, and M. F. Malone, "Automatic Screening of Entrainers for Homogeneous Azeotropic Distillation," *Ind. Eng. Chem. Res.*, **30**, 760 (1991).

Gani, R., and S. B. Jørgensen, "Multiplicity in Numerical Solution of Nonlinear Models: Separation Processes," *Comput. Chem. Eng.*, **18**, S55 (1994).

Gani, R., and I. T. Cameron, "Extension of Dynamic Models of Distillation Columns to Steady-State Simulation," *Comput. Chem. Eng.*, **13**, 271 (1989).

Gani, R., and I. T. Cameron, "Modeling for Dynamic Simulation of Chemical Processes: The Index Problem," *Chem. Eng. Sci.*, **47**, 1311 (1992).

Gani, R., C. A. Ruiz, and I. T. Cameron, "A Generalized Model for Distillation Columns: I. Model Description and Applications," *Comput. Chem. Eng.*, **10**, 181 (1986a).

Gani, R., C. A. Ruiz, and I. T. Cameron, "A Generalized Model for Distillation Columns: II. Numerical and Computational Aspects," *Comput. Chem. Eng.*, **10**, 199 (1986b).

Gear, C. W., "Simultaneous Numerical Solution of Differential/Algebraic Equations," *IEEE Trans. Circuit Theory*, **CT-18**, 89 (1971).

Gear, C. W, "DAE Index Transformations," *SIAM J. Sci. Stat. Comput.*, **9**(1), 39 (1988).

Gibbs, J. W., "Graphical Methods in the Thermodynamics of Fluids," *Trans. Conn. Acad.*, **2**, 309 (1873a).

Gibbs, J. W., "A Method of Geometrical Representation of the Thermodynamic Properties of Substances by Means of Surfaces," *Trans. Conn. Acad.*, **2**, 382 (1873b).

Gilles, E. D., B. Retzbach, and F. Silberberger, "Modeling, Simulation and Control of An Extractive Distillation Column," *Computer Applications to Chemical Engineering, ACS Symp. Ser. 124*, R. G. Squires and G. V. Reklaitis, eds. (1980).

Gilles, E. D., and B. Retzbach, "Reduced Models and Control of Distillation Columns and Sharp Temperature Profiles," *IEEE Trans. Automat. Contr.*, **AC-28**, 5 (1983).

Golubitsky, M., and D. G. Schaeffer, *Singularities and Groups in Bifurcation Theory*, Vol. 1, Springer-Verlag, New York (1985).

Goodliffe, A. H., "The Practical Testing of a Continuous Petroleum Still," *Trans. Inst. Chem. Engrs.*, **12**, 107 (1934).

Guinot, H., and F. W. Clark, "Azeotropic Distillation in Industry," *Trans. Inst. Chem. Engrs.*, **16**, 189 (1938).

Hass, J. R., "Rigorous Distillation Calculations," in Chap. 4 of *Distillation Design*, by H. Z. Kister, McGraw-Hill, New York (1992).

Helfferich, F. G., "Multiple Steady States in Multicomponent Countercurrent Mass-Transfer Processes," *Chem. Eng. Sci.*, **48**(4), 681 (1993).

Hendry, J. E., and R. R. Hughes, "Generating Separation Process Flowsheets," *Chem. Eng. Prog.*, **68**, 69 (1972).

Herfurth, H., A. Meirelles, S. Weiss, and H. Schubert, "Azeotropdestillation von Ethanol-Wasser mit Cyclohexan als Schleppmittel," *Chem. Tech.*, **39**, 331 (1987).

Herron, Jr., C. C., B. K. Kruelskie, and J. R. Fair, "Hydrodynamics and Mass Transfer on Three-Phase Distillation Trays," *AIChE J.*, **34**, 1267 (1988).

Horsley, L. H., *Azeotropic Data—III, Advances in Chemistry Series No. 116*, American Chemical Society, Washington, DC (1973).

Hwang, Y.-L., and F. G. Helfferich, "Dynamics of Continuous Countercurrent Mass Transfer Processes: III. Multicomponent Systems," *Chem. Eng. Sci.*, **44**, 1547 (1989a).

Hwang, Y.-L., and F. G. Helfferich, "Nonlinear Waves and Asym-

metric Dynamics of Countercurrent Separation Processes," *AIChE J.*, **35**, 690 (1989b).
Hwang, Y.-L., and F. G. Helfferich, "Dynamics of Continuous Countercurrent Mass Transfer Processes: IV. Multicomponent Waves and Asymmetric Dynamics," *Chem. Eng. Sci.*, **45**, 2907 (1990).
Jacobsen, E. W., L. Laroche, M. Morari, S. Skogestad, and H. W. Andersen, "Robust Control of Homogeneous Azeotropic Distillation Columns," *AIChE J.*, **37**, 1810 (1991).
Jacobsen, E. W., and S. Skogestad, "Multiple Steady States in Ideal Two-Product Distillation," *AIChE J.*, **37**, 499 (1991).
Julka, V., and M. F. Doherty, "Geometric Behavior and Minimum Flows for Nonideal Multicomponent Distillation," *Chem. Eng. Sci.*, **45**, 1801 (1990).
Julka, V., and M. F. Doherty, "Geometric Nonlinear Analysis of Multicomponent Nonideal Distillation: A Simple Computer-Aided Design Procedure," *Chem. Eng. Sci.*, **48**, 1367 (1993).
Kienle, A., and W. Marquardt, "Bifurcation Analysis of Multicomponent, Nonequilibrium Distillation Processes," *Chem. Eng. Sci.*, **46**, 1757 (1991).
Kingsley, J. P., and A. Lucia, "Simulation and Optimization of Three-Phase Distillation Processes," *Ind. Eng. Chem. Res.*, **27**, 1900 (1988).
Kister, H. Z., *Distillation Design*, McGraw-Hill, New York (1992).
Knapp, J. P., and M. F. Doherty, "A New Pressure-Swing Distillation Process for Separating Homogeneous Azeotropic Mixtures," *Ind. Eng. Chem. Res.*, **31**, 346 (1992).
Knight, J. R., and M. F. Doherty, "Design and Synthesis of Homogeneous Azeotropic Distillation: 5. Columns with Negligible Heat Effects," *Ind. Eng. Chem. Fundam.*, **25**, 279 (1986).
Koehler, J., P. Aguirre, and E. Blass, "Minimum Reflux Calculations for Nonideal Mixtures Using the Reversible Distillation Model," *Chem. Eng. Sci.*, **46**(12), 3007 (1991).
Kooijman, H. A., and R. Taylor, "A Nonequilibrium Model for Dynamic Simulation of Tray Distillation Columns," *AIChE J.*, **41**(8), 1852 (1995).
Kovach, J. W., III, "Heterogeneous Azeotropic Distillation—An Experimental and Theoretical Study," PhD Thesis, Univ. of Pennsylvania, Philadelphia (1986).
Kovach, J. W., III, and W. D. Seider, "Heterogeneous Azeotropic Distillation: Experimental and Simulation Results," *AIChE J.*, **33**(8), 1300 (1987a).
Kovach, J. W., III, and W. D. Seider, "Heterogeneous Azeotropic Distillation: Homotopy-Continuation Methods," *Comput. Chem. Eng.*, **11**, 6, 593 (1987b).
Kovach, J. W., III, and W. D. Seider, "Vapor-Liquid and Liquid-Liquid Equilibria for the System sec-Butyl Alcohol–Di-sec-Butyl-Ether-Water," *J. Chem. Eng. Data*, **32**, 16 (1988).
Kubicek, M., and M. Marek, *Computational Methods in Bifurcation Theory and Dissipative Structures*, Springer-Verlag, New York (1983).
Lang, L., and E. D. Gilles, "A Case Study of Multivariable Control for a Multicomponent Distillation Unit on a Pilot Plant Scale," *Proc. Amer. Contr. Conf.*, Pittsburgh (1989).
Laroche, L., N. Bekiaris, H. W. Andersen, and M. Morari, "Homogeneous Azeotropic Distillation: Separability and Flowsheet Synthesis," *Ind. Eng. Chem. Res.*, **31**, 2190 (1992a).
Laroche, L., N. Bekiaris, H. W. Andersen, and M. Morari, "The Curious Behavior of Homogeneous Azeotropic Distillation—Implications for Entrainer Selection," *AIChE J.*, **38**(9), 1309 (1992b).
Lecat, M., *L'azeotropisme, Donnees Experimentales, Bibliographie*, Bruxelles (1918).
Lefschetz, S., *Differential Equations: Geometric Theory*, Wiley, New York (1962).
Levy, S. G., D. B. Van Dongen, and M. F. Doherty, "Design and Synthesis of Homogeneous Azeotropic Distillation: 2. Minimum Reflux Calculations for Nonideal and Azeotropic Columns," *Ind. Eng. Chem. Fund.*, **24**, 463 (1985).
Levy, S. G., and M. F. Doherty, "A Design Procedure for Distillation Columns with Non-Sharp Splits," AIChE Meeting, Miami Beach (1986).
Li, H., "Analysis of Equilibrium-Staged Separation Processes," PhD thesis, Clarkson Univ., Potsdam, NY (1994).
Lin, W.-J., J. D. Seader, and T. L. Wayburn, "Computing Multiple Solutions to Systems of Interlinked Separation Columns," *AIChE J.*, **33**, 886 (1987).
Lu, M. D., and R. L. Motard, "A Strategy for the Synthesis of Separation Sequences," *Inst. Chem. Eng. Symp. Ser.*, No. 74 (1982).
Lucia, A., X. Guo, P. J. Richey, and R. Derebail, "Simple Process Equations, Fixed-Point Methods, and Chaos," *AIChE J.*, **36**(5), 641 (1990).
Lucia, A., and H. Li, "Constrained Separations and the Analysis of Binary Homogeneous Separators," *Ind. Eng. Chem. Res.*, **31**, 2579 (1992).
Lucia, A., and X. Wang, "Complex Domain Process Dynamics," AIChE Meeting, St. Louis, MO (1993).
Luyben, W. L., ed., *Practical Distillation Control*, Van Nostrand Reinhold, New York (1992).
Magnussen, T., M. L. Michelsen, and A. Fredenslund, "Azeotropic Distillation Using UNIFAC," *Inst. Chem. Eng. Symp. Ser. No. 56*, Intl. Symp. on Distillation, Rugby, England (1979).
Malone, M. F., and M. F. Doherty, "Separation System Synthesis for Nonideal Liquid Mixtures," FOCAPD'94 Conference, Snowmass, CO (July, 1994).
Malone, M. F., K. Glinos, F. E. Marquez, and J. M. Douglas, "Simple, Analytical Criteria for the Sequencing of Distillation Columns," *AIChE J.*, **31**(4), 683 (1985).
Martin, D. L., and P. W. Reynolds, "Process for the Purification of Diethoxymethane from a Mixture with Ethanol and Water," U.S. Patent No. 4,740,273 (1988).
Matsuyama, H., "Restrictions on Patterns of Residue Curves Around Heterogeneous Azeotropes," *J. Chem. Eng. Japan*, **11**(6), 427 (1978).
Matsuyama, H., and H. Nishimura, "Topological and Thermodynamic Classification of Ternary Vapor-Liquid Equilibria," *J. Chem. Eng. Japan*, **10**(3), 181 (1977).
Michelsen, M. L., "The Isothermal Flash Problem: I. Stability," *Fluid Phase Equil.*, **9**, 1 (1982a).
Michelsen, M. L., "The Isothermal Flash Problem: II. Phase Split Calculation," *Fluid Phase Equil.*, **9**, 21 (1982b).
Michelsen, M. L., "Calculation of Critical Points and Phase Boundaries in the Critical Region," *Fluid Phase Equil.*, **16**, 57 (1984).
Michelsen, M. L., "Some Aspects of Multiphase Calculations," *Fluid Phase Equil.*, **30**, 15 (1986).
Nadgir, V. M., and Y. A. Liu, "Studies in Chemical Process Design and Synthesis—V. A Simple Heuristic Method for Systematic Synthesis of Initial Sequences for Multicomponent Separations," *AIChE J.*, **29**(6), 926 (1983).
Naka, Y., T. Komatsu, I. Hashimoto, and T. Takamatsu, "Changes in Distillate Composition During Ternary Azeotropic Batch Distillations," *Int. Chem. Eng.*, **16**(2), 272 (1976).
Naka, Y., K. Kobayashi, H. Ochi, and T. Takamatsu, "The Effect of Valley and Ridge on Composition Profile in an Azeotropic Continuous Distillation Column," *J. Chem. Eng. Japan*, **16**(1), 36 (1983).
Naphtali, L. M., and D. P. Sandholm, "Multicomponent Separation Calculations by Linearization," *AIChE J.*, **17**, 148 (1971).
Niedzwiecki, J. L., R. D. Springer, and R. G. Wolfe, "Multicomponent Distillation in the Presence of Free Water," *Chem. Eng. Prog.*, **76**, 57 (1980).
Nishida, N., G. Stephanopoulos, and A. W. Westerberg, "A Review of Process Synthesis," *AIChE J.*, **27**, 321 (1981).
Ostwald, W., *Lehrbuch der Allgemeinen Chemie*, Engelmann, Leipzig (1900).
Pantelides, C. C., D. Gritsis, K. R. Morison, and R. W. H. Sargent, "The Mathematical Modeling of Transient Systems Using Differential-Algebraic Equations," *Comput. Chem. Eng.*, **12**, 449 (1988).
Partin, L. R., "Use Graphical Techniques to Improve Process Analysis," *Chem. Eng. Prog.*, **85**(1), 43 (1993).
Petlyuk, F. B., and V. S. Avetyan, "Investigation of Three Component Distillation at Infinite Reflux," *Theor. Found. Chem. Eng.*, **5**, 499 (1971).
Petlyuk, F. B., V. Y. Kievskii, and L. A. Serafimov, "Thermodynamic and Topological Analysis of the Phase Diagrams of Polyazeotropic Mixtures: I. Definition of Distillation Regions Using a Computer," *Russ. J. Phys. Chem.*, **49**, 1834 (1975a).
Petlyuk, F. B., V. Y. Kievskii, and L. A. Serafimov, "Thermodynamic and Topological Analysis of the Phase Diagrams of Polyazeotropic Mixtures: II. Algorithm for Construction of Structural Graphs for

Azeotropic Ternary Mixtures," *Russ. J. Phys. Chem.*, **49**, 1836 (1975b).

Petlyuk, F. B., V. Y. Kievskii, and L. A. Serafimov, "A Combined Thermodynamic and Topological Analysis of the Phase Diagrams of Polyazeotropic Mixtures—V: The Use of the Phase Equilibrium Model in Combined Thermodynamic and Topological Analysis," *Russ. J. Phys. Chem.*, **51**, 338 (1975c).

Petzold, L. R., "Differential/Algebraic Equations Are Not ODEs," *SIAM J. Sci. Stat. Comput.*, **3**(3), 367 (1982a).

Petzold, L. R., "A Description of DASSL: A Differential/Algebraic System Solver," Sandia Rep., SAND82-8637 (1982b).

Pham, H. N., and M. F. Doherty, "Design and Synthesis of Azeotropic Distillation: I. Heterogeneous Phase Diagram," *Chem. Eng. Sci.*, **45**(7), 1823 (1990a).

Pham, H. N., and M. F. Doherty, "Design and Synthesis of Azeotropic Distillation: II. Residue Curve Maps," *Chem. Eng. Sci.*, **45**(7), 1837 (1990b).

Pham, H. N., and M. F. Doherty, "Design and Synthesis of Azeotropic Distillation: III. Column Sequences," *Chem. Eng. Sci.*, **45**(7), 1845 (1990c).

Prokopakis, G. J., B. A. Ross, and W. D. Seider, "Azeotropic Distillation Towers with Two Liquid Phases," in *Foundations of Computer-Aided Chemical Process Design*, R. S. H. Mah and W. D. Seider, eds., AIChE, New York (1981).

Prokopakis, G. J., and W. D. Seider, "Feasible Specifications in Azeotropic Distillation," *AIChE J.*, **29**(1), 49 (1983a).

Prokopakis, G. J., and W. D. Seider, "Dynamic Simulation of Azeotropic Distillation Towers," *AIChE J.*, **29**(6), 1017 (1983b).

Rathore, R. N. S., and G. J. Powers, "Synthesis Strategies for Multi-Component Separation Systems with Energy Integration," *AIChE J.*, **20**(3), 491 (1974a).

Rathore, R. N. S., and G. J. Powers, "Synthesis of Distillation Systems with Energy Integration," *AIChE J.*, **20**(5), 940 (1974b).

Retzbach, B., "Control of an Extractive Distillation Plant," paper presented at the IFAC Symp.—DYCORD'86, Bournemouth, UK (Dec. 8–10, 1986).

Rev, E., "Crossing of Valleys, Ridges and Simple Boundaries by Distillation in Homogeneous Ternary Mixtures," *Ind. Eng. Chem. Res.*, **31**, 893 (1992).

Rev, E., P. Mizsey, and Z. Fonyo, "Framework for Designing Feasible Schemes in Quaternary Azeotropic Distillation," *Hung. J. Ind. Chem.*, **20**, 285 (1992).

Rev, E., P. Mizsey, and Z. Fonyo, "Framework for Designing Feasible Schemes of Multicomponent Azeotropic Distillation," *Comput. Chem. Eng.*, **18**, S43 (1994).

Rheinboldt, W. C., *Numerical Analysis of Parameterized Nonlinear Equations*, Wiley, New York (1987).

Robinson, C. S., and E. R. Gilliland, *Elements of Fractional Distillation*, McGraw-Hill, New York (1950).

Rodrigo, B. F. R., and J. D. Seader, "Synthesis of Separation Sequences by Ordered Branch Search," *AIChE J.*, **21**(5), 885 (1975).

Rosenbrock, H. H., "A Theorem of Dynamic Conservation for Distillation," *Trans. Inst. Chem. Eng.*, **38**, 279 (1960).

Rosenbrock, H. H., "A Lyapunov Function with Applications to Some Nonlinear Physical Problems," *Automatica*, **1**, 31 (1962).

Ross, B. A., and W. D. Seider, "Simulation of Three-Phase Distillation Towers," *Comput. Chem. Eng.*, **5**, 7 (1980).

Rovaglio, M., and M. F. Doherty, "Dynamics of Heterogeneous Distillation Columns," *AIChE J.*, **36**, 39 (1990).

Rovaglio, M., T. Faravelli, G. Biardi, P. Gaffuri, and S. Soccol, "Precise Composition Control of Heterogeneous Azeotropic Distillation Towers," *Comput. Chem. Eng.*, **16**, S181 (1992).

Rovaglio, M., T. Faravelli, G. Biardi, P. Gaffuri, and S. Soccol, "The Key Role of Entrainer Inventory for Operation and Control of Heterogeneous Azeotropic Distillation Towers," *Comput. Chem. Eng.*, **17**(5/6), 535 (1993).

Rovaglio, M., E. Ranzi, G. Biardi, M. Fontana, and R. Domenichini, "Rigorous Dynamics and Feedforward Control Design for Distillation Processes," *AIChE J.*, **36**(4), 576 (1990a).

Rovaglio, M., E. Ranzi, G. Biardi, and T. Faravelli, "Rigorous Dynamics and Control of Continuous Distillation Systems—Simulation and Experimental Results," *Comput. Chem. Eng.*, **14**(8), 871 (1990b).

Ruiz, C. A., I. T. Cameron, and R. Gani, "A Generalized Model for Distillation Columns: III. Study of Startup Operations," *Comput. Chem. Eng.*, **12**, 1 (1988).

Schreinemakers, F. A. H., "Dampfdrucke im System: Wasser, Aceton und Phenol," *Z. Phys. Chem.*, **39**, 440 (1901).

Schreinemakers, F. A. H., "Dampfdrucke im System: Benzol, Tetrachlorkolenstoff und Athylalkohol," *Z. Phys. Chem.*, **47**, 257 (1903).

Schuil, J. A., and K. K. Bool, "Three-Phase Flash and Distillation," *Comput. Chem. Eng.*, **9**, 295 (1985).

Seydel, R., *From Equilibrium to Chaos: Practical Bifurcation and Stability Analysis*, Elsevier, New York (1988).

Shinskey, F. G., *Distillation Control for Productivity and Energy Conservation*, 2nd ed., McGraw-Hill, New York (1984).

Shoenborn, E. M., J. H. Koffolt, and J. R. Withrow, "Rectification in the Presence of an Insoluble Component," *AIChE Trans.*, **37**, 957 (1941).

Siirola, J. J., "The Computer-Aided Synthesis of Chemical Process Designs," PhD Thesis, Univ. Wisconsin, Madison (1970).

Siirola, J. J., "An Industrial Perspective of Process Synthesis," FOCAPD'94 Conference, Snowmass, CO (July, 1994).

Siirola, J. J., and D. F. Rudd, "Computer-Aided Synthesis of Chemical Process Designs," *Ind. Eng. Chem. Fundam.*, **10**, 353 (1971).

Skogestad, S., and M. Morari, "Control Configuration Selection for Distillation Columns," *AIChE J.*, **33**(10), 1620 (1987).

Skogestad, S., P. Lundström, and E. W. Jacobsen, "Selecting the Best Distillation Control Configuration," *AIChE J.*, **36**(5), 753 (1990).

Sridhar, L. N., and A. Lucia, "Analysis and Algorithms for Multistage Separation Processes," *Ind. Eng. Chem. Res.*, **28**, 793 (1989).

Sridhar, L. N., and A. Lucia, "Analysis of Multicomponent, Multistage Separation Processes: Fixed Temperature and Pressure Profiles," *Ind. Eng. Chem. Res.*, **29**, 1668 (1990).

Stichlmair, J. G., "Separation of Ternary Mixtures by Rectification," *Int. Chem. Eng.*, **31**, 423 (1991).

Stichlmair, J. G., J. R. Fair, and J. L. Bravo, "Separation of Azeotropic Mixtures via Enhanced Distillation," *Chem. Eng. Prog.*, **85**, 63 (1989).

Stichlmair, J. G., and J. R. Herguijuela, "Separation Regions and Processes of Zeotropic and Azeotropic Ternary Distillation," *AIChE J.*, **38**, 1523 (1992).

Stichlmair, J. G., H. Offers, and R. W. Potthoff, "Minimum Reflux and Minimum Reboil in Ternary Distillation," *Ind. Eng. Chem. Res.*, **32**, 2438 (1993).

Swartz, C. L. E., and W. E. Stewart, "Finite-Element Steady State Simulation of Multiphase Distillation," *AIChE J.*, **33**, 1977 (1987).

Swietoslawski, W., *Azeotropy and Polyazeotropy*, Pergamon Press, New York (1963).

Tassios, D. F., ed., *Azeotropic and Extractive Distillation*, Adv. in Chemistry Ser., No. 115, Amer. Chem. Soc. (1972).

Tedder, D. W., "Optimization for Energy Conservation," *Chem. Eng. Prog.*, **76**, 63 (1980).

Tedder, D. W., and D. F. Rudd, "Parametric Studies in Industrial Distillation: I. Design Comparisons," *AIChE J.*, **24**, 303 (1978a).

Tedder, D. W., and D. F. Rudd, "Parametric Studies in Industrial Distillation: II. Heuristic Optimization," *AIChE J.*, **24**, 316 (1978b).

Tedder, D. W., and D. F. Rudd, "Parametric Studies in Industrial Distillation: III. Design Methods and Their Evaluation," *AIChE J.*, **24**, 323 (1978c).

Teja, A. S., and J. S. Rowlinson, "The Prediction of the Thermodynamic Properties of Fluids and Liquid Mixtures: IV. Critical and Azeotropic States," *Chem. Eng. Sci.*, **28**, 529 (1973).

Thompson, R. W., and C. J. King, "Systematic Synthesis of Separation Schemes," *AIChE J.*, **18**, 941 (1972).

Van Dongen, D. B., and M. F. Doherty, "On the Dynamics of Distillation Processes: V. The Topology of the Boiling Temperature Surface and Its Relation to Azeotropic Distillation," *Chem. Eng. Sci.*, **39**(5), 883 (1984).

Van Dongen, D. B., and M. F. Doherty, "Design and Synthesis of Homogeneous Azeotropic Distillations. 1. Problem Formulation for a Single Column," *Ind. Eng. Chem. Fundam.*, **24**, 454 (1985).

Van den Meer, D., "Foam Stabilisation in Small and Large Columns," *V.D.I. Proc., Inst. Chem. Eng., Berichte Nr. 182*, Nurenberg, West Germany (1971).

Van den Meer, D., F. J. Zuiderweg, and H. J. Scheffer, "Foam Suppression in Extract Purification and Recovery Trains," *Proc. Int. Solvent Extraction Conf.* No. 124, Hague, Holland (1971).
Van Winkle, M., *Distillation*, McGraw-Hill, New York (1967).
Venkataraman, S., and A. Lucia, "Solving Distillation Problems by Newton-Like Methods," *Comput. Chem. Eng.*, **12**, 55 (1988).
Wahnschafft, O. M., T. P. Jurian, and A. W. Westerberg, "SPLIT: A Separation Process Designer," *Comput. Chem. Eng.*, **15**, 565 (1991).
Wahnschafft, O. M., J. W. Koehler, E. Blass, and A. W. Westerberg, "The Product Composition Regions of Single-Feed Azeotropic Distillation Columns," *Ind. Eng. Chem. Res.*, **31**, 2345 (1992a).
Wahnschafft, O. M., J. P. L. Rudulier, P. Blania, and A. W. Westerberg, "SPLIT: II Automated Synthesis of Hybrid Liquid Separation Systems," *Comput. Chem. Eng.*, **16**, 305 (1992b).
Wahnschafft, O. M., J. P. L. Rudulier, and A. W. Westerberg, "A Problem Decomposition Approach for the Synthesis of Complex Separation Processes with Recycles," *Ind. Eng. Chem. Res.*, **32**, 1121 (1993).
Wahnschafft, O. M., and A. W. Westerberg, "The Product Composition Regions of Azeotropic Distillation Columns: II. Separability in Two-Feed Columns and Entrainer Selection," *Ind. Eng. Chem. Res.*, **32**, 1108 (1993).
Wang, J. C., and Y. L. Wang, "A Review of the Modeling and Simulation of Multistage Separation Processes," *Proc. Conf. on Foundations of Computer-aided Process Design*, Vol. II, R. S. H. Mah and W. D. Seider, eds., AIChE, New York, p. 121 (1981).
Wang, S. H., and W. B. Whiting, "New Algorithm for Calculation of Azeotropes from Equations of State," *Ind. Eng. Chem. Proc. Des. Dev.*, **25**, 547 (1986).
Wayburn, T. L., and J. D. Seader, "Solution of Systems of Interlinked Distillation Columns by Differential Homotopy-continuation Methods," in *Proc. of the Conf. on Foundations of Computer-aided Process Design*, A. W. Westerberg and H. H. Chien, eds., CACHE, Austin, TX, p. 765 (1984).
Westerberg, A. W., and G. Stephanopoulos, "Studies in Process Synthesis—I: Branch and Bound Strategy with List Techniques for the Synthesis of Separation Schemes," *Chem. Eng. Sci.*, **30**, 963 (1975).
Widagdo, S., *Dynamic Analysis of Heterogeneous Azeotropic Distillation*, PhD thesis, Stevens Inst. of Technol., Hoboken, NJ (1991).
Widagdo, S., W. D. Seider, and D. H. Sebastian, "Bifurcation Analysis in Heterogeneous Azeotropic Distillation," *AIChE J.*, **35**(9), 1457 (1989).
Widagdo, S., W. D. Seider, and D. H. Sebastian, "Dynamic Analysis of Heterogeneous Azeotropic Distillation," *AIChE J.*, **38**(9), 1457 (1992).
Wong, D. S. H., S. S. Jang, and C. F. Chang, "Simulation of Dynamics and Phase Pattern Changes for an Azeotropic Distillation Column," *Comput. Chem. Eng.*, **15**(5), 325 (1991).
Zharov, V. T., "Free Evaporation of Homogeneous Multicomponent Solutions," *Russ. J. Phys. Chem.*, **41**, 1539 (1967).
Zharov, V. T., "Free Evaporation of Homogeneous Multicomponent Solutions. II. Four Component Systems," *Russ. J. Phys. Chem.*, **42**, 58 (1968a).
Zharov, V. T., "Evaporation of Homogeneous Multicomponent Solutions: III. Behavior of Distillation Lines near Singular Points," *Russ. J. Phys. Chem.*, **42**, 195 (1968b).
Zharov, V. T., "Phase Representations and Rectification of Multicomponent Solutions," *J. Appl. Chem. USSR*, **41**, 2530 (1968c).
Zharov, V. T., "Phase Representations and Rectification of Many-component Solutions," *J. Appl. Chem. USSR*, **42**, 94 (1969).
Zharov, V. T., and L. A. Serafimov, *Physicochemical Fundamentals of Distillations and Rectifications* (in Russian), Khimiya, Leningrad (1975).

Manuscript received Aug. 17, 1994, and revision received Apr. 12, 1995.